DEVELOPMENT OF A SMALL ANIMAL MODEL TO STUDY TISSUE ENGINEERING STRATEGIES FOR GROWTH PLATE DEFECTS

A Dissertation
Presented to
The Academic Faculty

By

Rhima Coleman

In Partial Fulfillment
Of the Requirements for the Degree
Doctor of Philosophy in Bioengineering

Parker H. Petit Institute for Bioengineering and Bioscience
Georgia Institute of Technology

August, 2007

DEVELOPMENT OF A SMALL ANIMAL MODEL TO STUDY TISSUE ENGINEERING STRATEGIES FOR GROWTH PLATE DEFECTS

Approved by:

Dr. Robert E. Guldberg, Advisor
School of Mechanical Engineering
Georgia Institute of Technology

Dr. Ray Vito
School of Mechanical Engineering
Georgia Institute of Technology

Dr. Regis O'Keefe
Center for Musculoskeletal Research
University of Rochester Medical Center

Dr. Ravi Bellamkonda
Department of Biomedical Engineering
Georgia Institute of Technology

Dr. Barbara Boyan
Department of Biomedical Engineering
Georgia Institute of Technology

Date Approved: July 9, 2007

For my family.

To all those who have given, are giving, and will give me strength. I thank you. I have, am, and always will offer myself in return.

ACKNOWLEDGEMENTS

How does one thank those that have helped her though growth. Those that saw the resistance and persevered so that I may persevere. Note that these words are insufficient, but they are the tools I have. For now.

To my advisor. Who cared enough not to give up on me through it all. I thank Dr. Guldberg for his continuous belief in my abilities when I had given up on myself. There was no reason to continue to pour energy into me and my project.

To Dr. Natasha Case – my mentor and good friend. Her dedication to her project was an inspiration. Her willingness to take time out to discuss issues inside lab and out allowed me to shape my thoughts. Her patience with me was astounding. It took me a while to understand what it was I was lacking to finish, but that lesson will stay with me always. Natasha's willingness to take care of my *in vitro* work while I was figuring it all out kept me on track. The sacrifice is appreciated and will never be forgotten.

To Dr. Angel Duty. Always a smile. Always a positive attitude. Confidence and dedication defined her time with me. Her honesty and openness through good and bad was an inspiration.

I would like to thank Dr. Blaise Porter for his willingness to help in the lab and contributing many discussions on my research. Dr. Srinidhi Nagaraja and Angela Lin who always kept things lively and contributed a great deal to development of the micro-CT protocols presented here. When I wanted to do the impossible, they were always willing to help me hammer out a way. I cannot forget those who came after: Mela, Ken, Yash, Chris, and Joel. They put up with all of my performances and were great help with

tissue culture and surgery. I could not have done it without you guys. And last, but in no way of less importance, I would like to thank Dr. Alex Peister. She came rather late in my tenure, but through her I have learned more about the finer details of cell culture than in all the years before her arrival. She has been an important addition to our lab during her stay and she will be missed.

I thank the members of the Levenston Lab who were instrumental to developing many of the tissue culture techniques used throughout the course of my research. Dr. Marc Levenston, Dr. Chris Wilson, and John Connelly have contributed their time and knowledge to my research and far-fetched ideas. I would also like to thank Jen Phillips who started this project with me and, though she left me for another lab, has been a constant friend and source of support. I will miss her greatly.

Drs. Janna Kay Mouw and Stacy Marie Imler are the two greatest friends any person could have. Most people are lucky if they find one person in their entire lives that are willing to give of themselves as they have given to me. Without them this could not be possible. Without them I would not have found the strength to go on. What they have contributed to my life goes beyond the bounds of this work and with all my heart I thanks them.

Finally, I would like to thank my family. Their encouragement has been a beacon. The no-nonsense frankness of my twin sister, Khia, was always delivered with a side of love. I would not trade our bond for anything. Mom always supported all of my decisions, even if she though I was crazy. She always lent an ear, even when she had no idea of what I was talking about. Tasha and Yahna came through in a pinch. Kwei

talked some sense into me when he had to. Bill always made me smile. I love you all. I hope I can return the favor.

TABLE OF CONTENTS

LIST OF TABLES

LIST OF FIGURES

LIST OF ABBREVIATIONS

AGA	Agarose
ALG	Alginate
ALP	Alkaline phosphatase
BMP	Bone morphogenetic proteins
BMSC	Bone marrow derived stem cell
DMMB	Dimethylmethylene blue
EO	Endochondral ossification
FBS	Fetal bovine serum
FGF	Fibroblastic growth factor
IGF	Insulin-like growth factor
Ihh	Indian hedge hog
Micro-CT	Microcomputed tomography
PEG	Polyethylene glycol
PGA	Polyglycolic acid
PLLA	polyL-lactic acid
PTHrP	Parathyroid related protein
PTHrP-R	Parathyroid related protein – receptor
sGAG	Sulfated glycosaminoglycan
TGF-β	Transforming growth factor – beta

SUMMARY

The growth plate is a cartilaginous tissue responsible for the longitudinal growth of long bones. It is a complex tissue composed of chondrocytes whose maturation and proliferation is tightly regulated by a biochemical feedback loop. Injury to this tissue can result in a limb length discrepancy or angular deformity that may lead to life long disability. Given the recent rise in the number of growth plate injuries and the variability in success of current therapies, there is a significant need for a greater understanding of growth plate injury pathology and the development of improved treatment strategies.

Cartilage tissue engineering strategies offer an attractive alternative to regenerating growth plate tissue and restoring growth function. Bone marrow-derived stem cells (BMSCs) have been shown to be able to undergo chondrogenic differentiation and *in vitro* and *in vivo* and therefore offers an appealing and abundant cell resource for developing tissue engineering strategies for the treatment of growth plate defects. However, the dependence of chondrogenic differentiation and matrix accumulation on monolayer expansion protocols and three-dimensional (3D) culture environment has received little attention.

Prior to developing treatment strategies for growth plate injury repair, it is essential to first understand the interconnection between alterations in growth plate morphology and subsequent limb deformities. To that end, we have established a surgical defect model of growth plate injury in Sprague Dawley rats and developed a novel technique to quantitatively monitor growth plate morphology in health and disease

using microcomputed tomography (micro-CT) imaging. In an effort to develop a tissue engineering treatment strategy for growth plate injury, the role of monolayer expansion, 3D scaffold, and growth factor regimen in the chondrogenic differentiation of rat BMSCs was also examined. This research study has demonstrated the utility of micro-CT as a non-invasive imaging modality for assessing growth plate injury and repair. This work has also provided an improved understanding of the interrelationship of monolayer expansion, 3D culture environment, and growth factor regimen in BMSC chondrogenic differentiation. Finally, this work suggests that an injectable *in situ* gelling hydrogel is a feasible method for decreasing limb length discrepancies, however, neither implantation of agarose alone into the defect nor the inclusion of BMSCs fully corrects growth disruption.

Chapter 1

INTRODUCTION

In response to injury to the growth plate, an influx of vasculature and progenitor cells from the bone marrow cavity may stimulate the formation of a bone bridge (epiphysiodesis) through all or part of the growth plate. This often results in a loss in growth function and premature closure of the growth plate and, ultimately, limb length discrepancies or angular deformity. Current treatment includes excision of the bone bridge and interposition of a filler material, typically autologous fat. However, the clinical outcome of these procedures is highly variable, ranging from a 15-38% success rate [1]. Large transphyseal bone bridges cannot be treated by interposition of fat and eventually, once skeletal maturity occurs, treatment of the discrepancy in limb length may require highly invasive limb lengthening procedures.

Research in this area has focused on developing tissue engineering techniques to treat this type of injury. Before repair of the growth plate can be achieved, however, understanding the consequences of injury on growth plate and whole bone morphology must be determined. Previously, this has been accomplished using radiographic and histomorphometric analysis, which is semi-quantitative at best. The *objective* of the research was to develop a small animal growth plate defect model in Sprague Dawley rats to examine the efficacy of cartilage tissue engineering strategies in treating growth plate defects and to use microcomputed tomography (micro-CT) to *quantitatively* evaluate changes in growth plate and whole bone morphology. Our goal was to not only prevent bone bridge formation within growth plate defects, but also to restore growth function by

employing a combination of scaffold and pluripotent marrow-derived stromal cells. The specific aims were to:

I. To develop a small animal growth plate defect injury model in Sprague Dawley rats that exhibits clinical features of growth plate injury in humans.

Rats have been widely used to study the fracture healing, osteoporosis, radiation effects on growth plate morphology, and, more recently, to study the biomolecular events of growth plate defect healing. We used micro-CT and histological techniques to detect morphological changes in growth plate morphology and bone length over time in response to a centralized growth plate defect created in the distal femurs of Sprague Dawley rats. We *hypothesized* that a centralized defect would mimic the limb length discrepancy seen in pediatric cases of growth plate injury.

II. To identify in vitro culture conditions to reproducibly induce chondrogenesis in Sprague Dawley rat bone marrow derived stem cells in 3D hydrogel constructs.

Stem cells offer an attractive and abundant source of cells for osteochondral tissue engineering. It is becoming more evident that growth factors delivered in series or combination enhance gene expression and enhance matrix deposition of chondrogenic factors [1-4]. It has also been noted that the degree of monolayer expansion (passaging) has an effect on their differentiation potential [1, 2]. We *hypothesized* that Sprague Dawley rat bone marrow derived stem cells (BMSCs) can be induced to undergo chondrogenesis when exposed to a specific combination of growth factors including fibroblastic growth factor-2

(FGF-2) and transforming growth factor beta 1 (TGF-β1) in three-dimensional (3D) hydrogel scaffolds and that their differentiation potential was passage dependent.

III. To test the ability of hydrogel constructs implanted into transphyseal defects to inhibit growth plate fusion and restore growth plate function.

Blocking bone bar formation in growth plate defects is the major feature of current clinical treatment methods of this type of injury. This may be achieved using an material that is injectable and polymerizes *in situ*. The inclusion of cells has been shown to restore a growth plate phenotype to the injured area, but not to fully correct growth disturbance. Therefore, we *hypothesized* that: 1) injection of an *in situ* gelling agarose in centralized defects in the distal femurs of Sprague Dawley rats will inhibit limb length shortening caused by a growth plate defect by reducing bone bridge formation through the defect region and 2) delivery of stromal cells that have been pre-differentiated down the chondrogenic pathway into a growth plate defect will decrease limb length discrepancies and restore growth plate structure and function.

CHAPTER 2

BACKGROUND AND LITERATURE REVIEW

Growth Plate Structure and Function

The growth plate is a cartilage-like tissue that is responsible for the elongation of long bones during childhood and adolescence through a process known as endochondral ossification (EO). The growth plate can be divided into five zones: resting cell zone, proliferative cell zone, prehypertrophic cell zone, hypertrophic cell zone, and calcified cartilage (**Figure 2.1**). In the resting zone, a small number of relatively quiescent cells are embedded in a matrix rich in aggrecan and collagen type II. As they further differentiate and enter the proliferative zone, cells are rapidly dividing, flattened, and arranged in columns. During the transition from the proliferating phenotype into the prehypertrophic zone, cells begin to enlarge. In the hypertrophic zone, the cells undergo a 5-10 fold increase in intracellular volume (responsible for 44-59% of long bone growth), secrete a specialized matrix including collagen type X, and express high levels of alkaline phosphatase (ALP). The final stage of chondrocyte maturation is terminal differentiation during which the extracellular matrix is mineralized and the cells undergo apoptosis. This process leaves a calcified scaffold onto which osteoblasts brought in by invading vasculature lay down primary bone. During EO, this calcified cartilage is later remodeled into secondary trabeculae [2, 3].

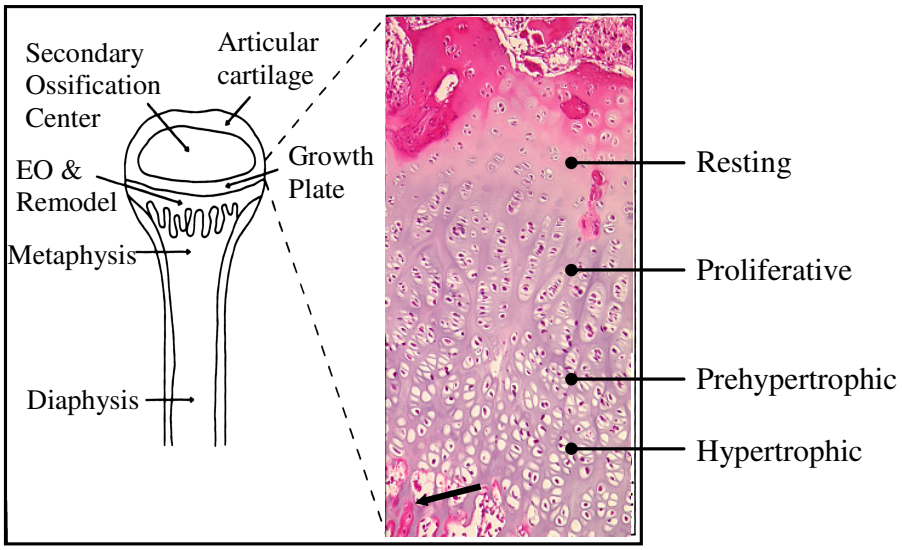

Figure 2.1. Schematic of the epiphysis of long bones.

The outset image of the growth plate is a histological section stained with hematoxylin and eosin. The resting zone cells are sporadically distributed throughout a collagen type II and aggrecan rich matrix. The proliferative cells are arranged in columns and have a flattened appearance. In the prehypertrophic zone, the cells are beginning to separate and secrete matrix. The large hypertrophic cells are visible above the vertical struts of calcified cartilage covered with new bone (arrow).

Recent studies have shed considerable light on the molecular regulation of endochondral ossification and revealed remarkable similarities in the mechanisms of fetal development and adult fracture repair [4]. The maturation of chondrocytes through each zone of the growth plate is tightly controlled through a feedback loop formed from the interaction of specific autocrine and paracrine signaling molecules synthesized by the chondrocytes. The predominant factors in the feedback loop that regulate cell maturation in the growth plate are parathyroid hormone related protein (PTHrP), Indian hedgehog (Ihh), and transforming growth factor – β (TGF-β). Prehypertrophic cells secrete Ihh in response to bone morphogenetic protein – 6 (BMP-6) secreted by hypertrophic cells. Ihh stimulates the cells of the perichondrium to release TGF-β. TGF-β then acts on the cells

of the perichondrium and appositional cartilage cells to increase expression of PTHrP. In response to increased PTHrP synthesis, the number of prehypertrophic cells expressing Ihh decreases. As the hypertrophic cells reach terminal differentiation and undergo apoptosis, the late prehypertrophic cells mature to hypertrophy and begin to secrete BMP-6 [5, 6]. A simplified model of this pathway is outlined in (**Figure 2.2**). In addition to the aforementioned factors, there is also evidence that chondrocyte phenotype is modulated by other systemic and local signaling molecules including the bone morphogenetic proteins (BMPs), the insulin-like growth factors (IGF)/growth hormone axis, Wnt family members, fibroblastic growth factors (FGF), and integrin-linked kinases [7-11].

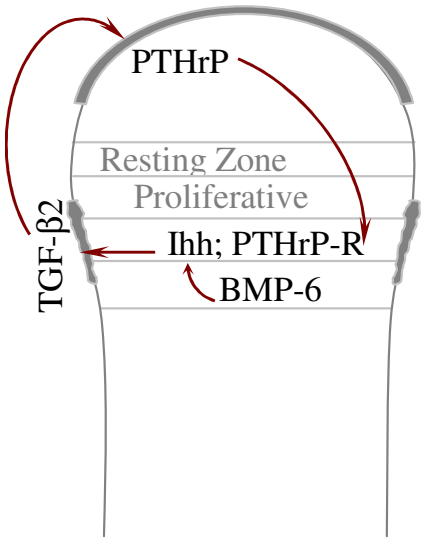

Figure 2.2. Growth plate feedback loop.

Growth Plate Injury

Approximately 42% of male children and 27% of female children experience a broken bone by the age of 16 and it is estimated that 20% of these fractures will involve the growth plate [12-14]. Injury to the growth plate may result in full or partial closure of the epiphysis through the formation of a mineralized bone bridge through the defect region that connects the epiphyseal bone to the metaphysis [14-16]. In addition to damage during fracture, injury to the growth plate may also result from the removal of osteosarcomas, the treatment of bone cysts, diabetes, chemotherapy, juvenile arthritis, and limb stabilization in the case of osteopetrosis imperfecta [17-20]. Damage to epiphyseal cartilage may result in an angular deformity if the injury occurs within the peripheral regions of the tissue and in a limb length discrepancy if the defect is centrally located [15, 21]. Abnormal loading due to these joint incongruities may cause life-long disabilities [16].

There are several classification systems for growth plate injury [22, 23], but the standard system used was developed by Salter and Harris in 1963 (**Figure 2.3**) [24]. Type I fractures involve the growth plate, but not the epiphyseal or metaphyseal bone. In Type II fractures, the line of fracture is through the growth plate and extends through the metaphysis breaking off a triangular piece of bone. Type III fractures run vertically through the epiphyseal bone and obliquely through a portion of the growth plate. Type IV fractures are due to vertically oriented splitting compression forces and cause a fracture of both the epiphysis and metaphysis. These fractures cannot be seen in radiographs. Types IV and V typically lead to growth disruption and although type V

injuries are quite rare, they are the most devastating due to destruction of the hypertrophic zone [14, 25, 26]. Premature fusion of the growth plate is more common in the distal femur and tibia regardless of how the injury was obtained. The distal femur is infrequently injured, but has the highest incidence of premature closure in case studies [14, 16]. Because this region contributes 55-70% of overall growth to the femur, premature fusion of this area can result in significant shortening of the limb [16].

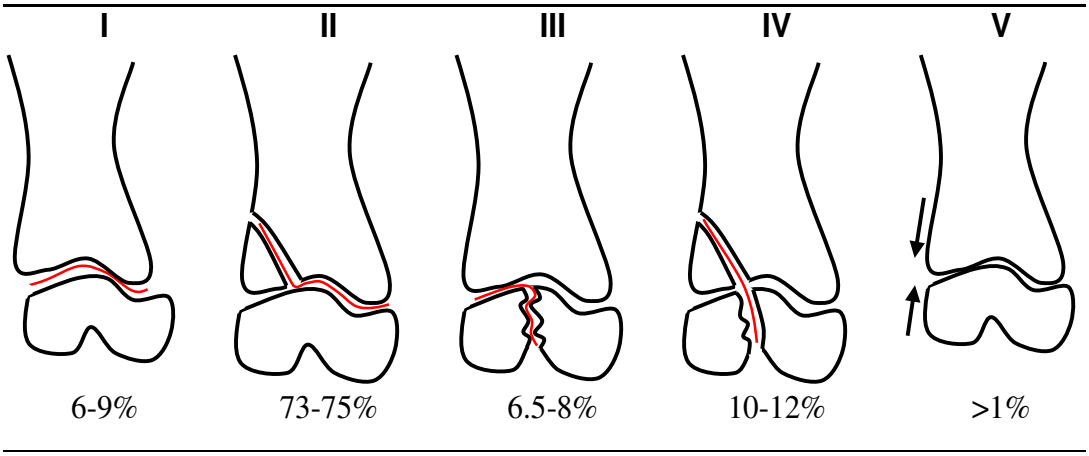

Figure 2.3. Salter-Harris classification of growth plate defects.
Red lines indicate plane of fracture. Values beneath each image is the frequency of occurrence [14]

Imaging of Growth Plate Injury

One of the major challenges with growth plate injury treatment is diagnosing the morphology of the growth plate after injury. Radiographical analysis (x-rays) is the first mode of analysis in the clinic, but images are hard to interpret and not all bridges, especially fibrous ones, will be visible [27, 28]. Diagnosis is based on epiphyseal

displacement or widening and haziness of the epiphyseal and metaphyseal margin along the growth plate [14].

Currently, the most common analysis method used in the clinical setting is magnetic resonance imaging (MRI) with fat-suppressed 3D spoiled gradient-recalled echo [27, 29-32]. Using this technique, the growth plate appears in intense contrast to the surrounding bone [14]. Defects within the growth plate, whether they be filled with bony or fibrous tissue, appear as a dark disruption within the tissue [14]. Recently, methods for 3D reconstruction of injured epiphyses from MR images have been developed [27, 29-31], however, this technique remains an expensive and time-consuming method with lower resolution than CT technologies [31]. Additionally, children under six years of age must be sedated for MR imaging [32]. It has also been noted that some coronal and sagittal images of the normal knee show discontinuity of the physeal cartilage (drop-out sign), which may be mistaken for premature closure [33, 34], and clinicians may have to wait up to 8 months before a bone bridge is apparent in a MR image [35].

Computed tomography (CT) images are used to fully evaluate growth plate injuries that have been found by radiographic analysis [14]. Methods to create joint 3D models of fractured epiphyses are in practice to aide in surgical planning for fractures, slipped femoral epiphyses, and bone bridge removal [14, 36, 37].

Treatment of Growth Plate Injury

Acute injuries that traverse the growth plate (Salter types III and IV) typically result in the formation of a bony bridge that is visible on radiomicrographs and MR

images [27, 28]. The most common treatment of minor growth plate injuries – those where the bone bridge size is <40% of the growth plate and the prospective growth period is at least 2 years – is the Langenskiöld procedure [1]. It involves removal of the bone bridge and insertion of autologous fat into the empty space to prevent reformation of the bone bridge. The fat is typically sutured to the growth plate or perichondrium to prevent migration of the graft. This procedure is labor intensive and, despite standardization of the technique in the field, clinical success is unpredictable, ranging from 15-38% [1]. Fat is prone to bone reformation after bleeding at the graft surface, fibrous degeneration and shrinking, dislocation of the graft, or necrosis in the center of the graft [1, 38, 39]. Alternate materials have been interposed in the defect including frozen hyaline cartilage, iliac apophysis, and nonbiologic materials such as methylmethacrylate, bone wax, and silastic [38, 40]. Although cartilage is reported to be more effective than fat in preventing growth retardation and angular deformity, none of the aforementioned materials fully restores function to the growth plate [39, 41].

For severe deformities, an alternative method, microsurgically revascularized epiphyseal plate transfer, is utilized. Here, a section of autologous growth plate and flap of skin is transferred from another anatomical site to the injured area and the vasculature from the skin is anastamosed to major blood vessels in the surrounding recipient site. The most common anatomical sites for growth plate harvest are the head of the fibula, lower scapula, and iliac crest [42, 43]. While this procedure does restore growth function to the growth plate by ensuring adequate blood flow to the area, a requirement for proper endochondral ossification, it is complex and labor intensive, the growth rate of the epiphysis is site dependent [44], donor site morbidity is prevalent [42, 44], and

transplanted growth plates do not adapt easily to the recipient site [42, 43, 45, 46]. In the case of allogenic epiphyseal graft transfer, immunosupression is required to restore growth function. However, the administration of a immunosuppressive regimen in non-life threatening situations is still controversial [44]. Therefore, limb discrepancies or angular deformities may still occur and distraction osteogenesis following skeletal maturity may be indicated.

More recently, a technique of slow distraction of the growth plate termed chondrodiastasis or hemi-chondrodiastasis has been developed to correct angular deformities [25]. In a rabbit animal model, Lee *et al*. demonstrated that this technique was able to correct angular deformities without having to remove the bone bridge [47].

Growth Plate Injury Animal Models

Several animal models of growth plate injuries have been developed and used to test clinical approaches to growth plate repair with variable results. Jouve *et al.* implanted allogenic growth plate chondrocytes in type I collagen gel into rabbit growth plate defects [48]. The implanted constructs remained viable after six weeks, produced a proteoglycan rich extracellular matrix, and began to display a columnar cellular organization similar to the surrounding growth plate tissue. However, neither prevention of bone bridge formation nor growth restoration was demonstrated. In an ovine model, Foster *et al*. also studied transplantation of allogenic growth plate chondrocytes into growth plate defects [49]. Isolated chondrocytes were cultured at high density until constructs containing a cartilaginous matrix were produced. Chondrocyte columniation

and endochondral ossification were observed 8-12 weeks post-implantation and reformation of a bone bridge was prevented. However, cell survival was highly variable perhaps due to a consistent local immune response to the implants and growth restoration was not demonstrated. In another rabbit model, Zhou *et al*. found that growth plate chondrocytes cultured on polylactic acid scaffolds to produce an engineered growth plate prevented bone bridge formation and partially restored growth [50].

More recently, models that employ the implantation of chondrogenic stem cells have emerged. Hui *et al.* found that fibrin alone resulted in the formation of a bone bridge and higher limb length discrepancies compared to mesenchymal cells seeded in fibrin in a rabbit model of growth plate injury [51]. Chen *et al.* reported that agarose alone did not inhibit angular deformity or premature fusion [52]. In both cases, the inclusion of MSCs into the gels rescued growth function. Both studies demonstrated the reformation of a growth plate histologically, however, no data was provided to demonstrated integration of the regenerated growth plate with the native tissue or if the growth rate of the implant tissue matches that of the native region [51, 52]. Additionally, delivery of MSCs alone did not inhibit bone bridge formation or regenerate the growth plate [53].

Several small animal studies of growth plate injury have also been reported. In a 5 week old Sprague Dawley rat model, Garces *et al.* found that a 1 mm defect drilled into the growth plate from the surface of the femur resulted in no significant differences in length or growth-plate height between injured bones and their controls. Defects were filled by a bone bridge that grew wider as time passed after the surgical procedure [54]. In a murine model, Lee *et al*. demonstrated that the growth plate defect healing begins

with fibrous tissue deposition followed by infiltration of mesenchymal cells and, finally, bone bridge formation from the rim of the defect inward [25]. This time-course of tissue infiltration was also observed in a tibial model of centralized defects developed by Xian *et al*. in rats [21]. Both authors also showed that bone bridge formation within the growth plate defect occurred through the intramembraneous pathway [21, 25]. To further characterize this process, Xian *et al*. have also examined the time-course of inflammatory cytokine expression, chondrogenesis, and endochondral ossification, within the injured growth plate using gene expression and immunohistological means [55-57].

Rats have been widely used to study endochondral ossification in the fracture callus [58, 59], as a model for osteoporosis [59, 60] and arthritis [19], and to study the effects of irradiation and systemic diseases on growth plate morphology [17, 18, 61]. Therefore, a wealth of information exists about the effects of various disruptive models on growth plate biochemistry and many antibodies and primer sequences have been developed. In fact, recent studies of the rat genome have shown that rodents are closer to humans than cats, pigs, or zebrafish [62]. The rats' small size also make them ideal for the quantitative characterization of the physical effects of growth plate injury using the micro-CT.

Cartilage Tissue Engineering

As demonstrated in previous animal models, cartilage tissue engineering is an attractive option for the treatment of growth plate defects [48, 50-52]. From decades of articular cartilage tissue engineering studies, a wealth of information has emerged about

chondrocyte response to environmental cues *in vitro* in numerous scaffold types. Unfortunately, the limited sources for primary chondrocyte isolation and their well characterized expansion limitations make this cell type an unlikely candidate for tissue engineering applications [63-65]. Mesenchymal progenitor cells offer an alternative cell resource with nearly unlimited expansion potential capable of supplying large quantities of cells. However, the success of any tissue engineered construct requires the correct marriage of scaffolds, growth factors, and cells for optimal matrix production and integration into the defect site.

Scaffolds

In tissue engineering, the criteria for scaffold design, in general, is that the material must exhibit biocompatibility and be biodegradable, provide mechanical support during the healing process while degrading to match tissue replacement, maintain the cell phenotype, and support deposition of matrix [66, 67]. When addressing biocompatibility, consideration must be given to not only how the recipient tissue will respond to the intact scaffold, but also to its degradation products as the tissue regenerates [66, 68, 69].

Several types of biodegradable scaffolds are being investigated by articular cartilage tissue-engineering researchers. These include woven scaffolds like polyglycolic acid (PGA) and polylactic acid (PLA), gels made from natural proteins like collagen, fibrin, chitosan, agarose, and alginate, and natural scaffolds (autologous or allogenic tissues) [66, 68, 70].

Materials derived from polyhydroxyacids are attractive because they have been approved by the US Food and Drug Administration (FDA) for application *in vivo* for many years [66, 68-70]. Polyglycolic acid (PGA) and polyL-lactic acid (PLLA) are easily extruded and have been well studied for cartilage applications [66]. They support cell attachment and matrix production of several different cell types involved in osteochondral tissue engineering [66, 69]. They have been shown to support significant matrix accumulation by young bovine chondrocytes in a rotating wall and perfusion bioreactors *in vitro* [71, 72], however, the results from several animal models is variable. [66, 68]. Although the viscoelastic properties of neocartilage developed on these meshes tends to approach that of some native cartilages, they are not likely to withstand physiological load or integrate with native tissues [66].

The recovery of the chondrocytic phenotype in hydrogels such as alginate and agarose has also been well characterized [73-79]. In these matrices, chondrocytes that have dedifferentiated due to monolayer expansion are induced to re-express cartilaginous matrix molecules [63, 64, 80]. The cross-linked network of hydrogels mimics the natural extracellular matrix and the high water content of hydrogels facilitates the exchange of nutrients and gases [81]. Hydrogels are also attractive because their high hydration provides the construct with initial mechanical stability and allows diffusion of nutrients and waste products to and from the encapsulated cells [82]. The ability of these gels to be injected into a defect site and polymerized *in situ* make hydrogels ideal for easy delivery clinically and molding into any shape [83]. Gels containing collagens and proteoglycans are the most popular natural scaffolds using in orthopaedic tissue engineering research based on numerous studies demonstrating the ability of these matrix

proteins to enhance chondrocyte function [69, 84-88]. However, the mechanical fragility of these scaffolds limits their usefulness in load bearing applications [83].

Recent studies have demonstrated that another US FDA approved polymer, photopolymerizable polyethylene glycol-based (PEG) hydrogels [66], support chondrogenesis and constructs up to 8mm in thickness can be produced [89-95]. The degradation rates and initial mechanical properties can be distinctly controlled and scaffolds with specific microarchitectures (i.e. multilayered stratified constructs) can be created using this system. These properties are attractive for the development of tissue-engineered constructs that recapitulates the complex microarchitecture of cartilaginous tissues [69, 96].

Natural scaffolds such as periosteum and osteochondral grafts derived from both autographic and allogenic sources have been used in the clinical setting for years to repair cartilaginous defects [68, 97, 98]. The cells of the inner layer of periosteal tissue, called the cambium, have been shown to be able to undergo chondrogenesis *in vitro* [99-102]. In combination with the osteogenic outer layer, the periosteum is an attractive scaffold for future osteochondral tissue engineering applications.

Growth factors

Many of the factors that direct cartilage matrix synthesis also regulate the process of chondrogenesis [5, 103]. Therefore, understanding the roles of specific signaling molecules in the growth plate may aid in controlling the phenotype of cells in tissue-engineering applications developed *in vitro* prior to *in vivo* implantation. The phenotype

of chondrocytes in the growth plate is tightly regulated by interactions between autocrine and paracrine factors secreted by chondrocytes and cells from the surrounding tissues [103]. Numerous investigators are currently conducting *in vitro* studies to elucidate the effects of growth factors [5, 103-107], glucocorticoids [108-110], steroid hormones [111, 112], and matrix molecules on growth plate chondrocytes [113]. Ballock *et al*. showed that growth plate cells will spontaneously form a growth plate-like tissue including a columnar arrangement of flattened proliferating cells and hypertrophic cells *in vitro* [114]. It has also been shown that BMP-2, 4, and 7 are capable of inducing hypertrophy [6], while TGF-β1 has been shown to inhibit hypertrophy in growth plate cells placed in aggregate culture [114, 115]. The addition of exogenous PTHrP to growth plate cultures increases expression of MMP-3 and 9 [116] and inhibits hypertrophy, possibly through genomic regulation of Ihh expression [117, 118]. The response of growth plate cells have also been shown to be dependent on maturation state [119]. Over the years, Boyan and colleagues have increased our understanding of the role of vitamin D_3 metabolites in the regulation of endochondral ossification and regulation of the growth plate phenotype. They have demonstrated the maturation-dependent response of growth plate cells to 1α,25-$(OH)_2D_3$ and 24R,25-$(OH)_2D_3$ as well as the intercellular mechanisms of their response to PTH, TGF-β1, and BMP-2 [120, 121]. The numerous studies in this area on the response of chondrogenic cells to in vitro culture conditions aids in the selection of environments in which the desired cell phenotype can be regulated, which will, in turn, determine how cells implanted into a growth plate defect respond to the complex biochemical environment and restore growth function.

Cell Sources

While primary growth plate cells from mice, rat, and chick have been studied *in vivo* to further understand development and examine the effects of various growth factors on the maturation cycle of chondrocytes, little work has been done to investigate the applicability of these cells for cartilage tissue engineering. In studies comparing chondrocytes from different sources, growth plate cells exhibited the ability to secrete a cartilaginous matrix *in vitro* and *in vivo* [122, 123]. Bentley *et al*. compared the ability of allogenic epiphyseal and articular derived chondrocytes to heal a full thickness osteochondral defect in rabbits. The authors found that epiphyseal chondrocytes exhibited superior filling of the defect and integration into the surrounding tissue over articular chondrocytes. While articular-derived cells did secrete a metachromatic matrix that stained intensely for sGAGs, the resulting tissue was surrounded by fibrous tissue and immune cells [122]. In another study comparing porcine auricular, articular, costochondral derived cells seeded in a fibrin matrix, Xu *et al*. found that all of the cell types secreted similar matrices high in sGAG content. However, constructs containing costochondral cells maintained their original shape better than auricular chondrocytes, which overgrew, and articular chondrocytes, which significantly shrank over time. Additionally, costochondral and auricular constructs had superior biomechanical properties to those made with articular chondrocytes [123].

Clinically, epiphyseal chondrocytes are introduced into a growth plate defect through whole physeal transfer, and animal studies have shown that this process is superior to fat interposition at preventing bar bridge formation and angular deformities

[124, 125]. However, studies have also shown that the cells of inserted epiphysis does not respond to the biochemical feedback loop that regulates chondrocyte maturation and, therefore, the rate of growth of the graft may not match the host site [42, 43, 45, 46]. In a study in rabbits by Abad *et al*., the authors found that if the epiphysis was inserted upside down, the cells graft continued to undergo endochondral ossification in the same direction and did not integrate with the surrounding tissue [126].

The feasibility of implanting isolated epiphyseal cells into growth plate defects also requires more investigation. A study by Lee *et al*. showed that chondrocytes isolated from the resting zone of rib cartilage and cultured in pellet culture for 14 days secreted a cartilaginous matrix and exhibited growth plate morphology. When implanted into a growth plate defect, graft growth and endochondral ossification continued. However, the ability of these constructs to prevent limb shortening or angular deformities was not investigated [127]. Therefore, it is unknown whether a growth plate graft created *in vitro* will adapt to the local biochemistry of the host growth plate any better than an autologous whole physeal transfer. In animal models that did investigate these parameters, the treatment did not completely prevent bone bar formation or correct angular deformities [48, 49]

Despite the superior matrix production and integration reported with tissue engineered constructs using growth plate chondrocytes *in vivo*, the use of these cells clinically is limited by lack of significant sources for cell isolation, the donor site morbidity associated with that harvest, and limited ability for expansion *in vitro* [126].

When autologous cartilage tissue or cells are used in the repair process, it is often difficult to harvest a large number of chondrocytes without causing substantial additional

damage due to donor site morbidity [115, 128]. Ample cell numbers may be obtained through *in vitro* monolayer expansion, or passaging, of the desired cells. Unfortunately, passaging causes chondrocytes to dedifferentiate, a condition marked by decreased expression of two necessary cartilage matrix components: type II collagen and sulfated glycosaminoglycans (sGAGs), as well as increased expression of undesirable type I collagen [63-65, 129]. Therefore 3D culture techniques have been developed in scaffolds, including gels and polymers, that maintain their rounded morphology and stabilize their phenotype [67].

Numerous methods have been investigated to modulate the phenotype of articular chondrocytes *in vitro*. It is well recognized that dynamic seeding and culture of chondrocytes yields constructs with superior matrix content and biomechanical properties compared to static culture [67, 130] and it is likely that bioreactor technologies will close the gap between research and clinical application of tissue engineering strategies to cartilage injury [115]. Studies have also focused on the TGF-β, FGF, and IGF families of growth factors for modulation of chondrocyte behavior *in vitro* [115]. Despite the advances made so far in tissue-engineering application for cartilage repair, the zonal variation of cartilaginous tissues has not been mimicked and *in vivo* applications of articular cartilage cells involve delivery of a homogeneous distribution of a heterogeneous population of articular cartilage surface, middle, and deep cells [67].

The results of treatment of growth plate defects in animal models with articular cartilage cells has been variable. When these cells were delivered to an injury that involved 66% of the growth plate in collagen gels, angular deformation was reduced compared to fat grafts, but bone still formed between the construct and native tissue

[131]. Lee *et al*. delivered chondrocytes in agarose to treat an injury involving 50% of the growth plate in a murine model. The authors found that the implanted cells contributed to the formation of a functional growth plate with some residual angular deformity [25].

Adult stem cells have harvested from a variety of tissues including trabecular bone, muscle, fat, synovium, amniotic fluid, placenta, umbilical cord, and bone marrow [132-143]. Each cell type exhibits different phenotypical behavior *in vitro* depending on the extraction, expansion, and differentiation methods used by the investigator. In general, stem cells have higher expansive abilities than primary cells *in vitro* and can be differentiated into the chondral, osseous, and adipogenic phenotypes [144]. There is overlap of cell surface markers of the adult stem cells from different tissues, but no criteria has been elucidated that defines a stem cell [83]. Of the adult stem cell types, bone marrow derived stem cells (BMSCs) have been the most studied for orthopaedic applications [83]. In a study comparing the multipotential capabilities of marrow- and adipose-derived stem cells, Liu *et al*. found that BMSCs may be a better choice for cartilage and bone tissue engineering than adipose-derived cells [145].

The clonal nature of BMSCs was first revealed in the 1960's [146]. The bone forming properties of rat BMSCs was later reported by Friedenstein [147]. Since then, the multipotential ability of these cells has been demonstrated [148-150]. Marrow-derived progenitor cells from several species including rabbit, goat, canine, bovine, and human can be induced to differentiate along the chondrogenic lineage *in vitro* and *in vivo* [151-155]. The chondrogenic potential of stem cells have been found to be associated with expression of CD105, a TGF-β receptor [83, 156] and members of the TGF-β

family, particularly TGF-β1, have been shown to promote chondrogenic differentiation in a variety of species [157, 158].

BMSCs make up 0.001-0.01% of nucleated cells in the bone marrow and therefore require *in vitro* expansion [83]. As with primary chondrocytes, extensive passaging of BMSCs has been shown to decrease the ability of cells to produce a functional matrix under differentiating conditions [63-65]. Tsutsumi *et al*. examined the effects of passaging on the ability of bone marrow stromal cells to differentiate down the mesenchymal pathway and found that treating the cells with 1 ng/ml of FGF-2 during monolayer expansion increases the rate of cell division, abrogates the negative effects of passaging, and enhances differentiation [148]. Hanada *et al*. also showed that FGF-2 increased BMSC osteogenesis [159] and numerous studies have shown FGF-2 to be mitogenic for many different cell types [158, 160-162]. These studies demonstrate that FGF-2 positively affects BMSC mitogenesis and differentiation.

In recent studies where stem cells have been used to treat growth plate defects, investigators found that the delivery of MSCs into the gel systems rescued growth function. These studies demonstrated the reformation of a growth plate histologically, [51, 52]. It has also been reported that a delivery vehicle for the MSCs was required to inhibit bone bridge formation and regenerate the growth plate [53].

Summary

Damage to the growth plate due to injury, disease, or surgical intervention may lead to limb length discrepancies due to premature fusion of whole or part of the physis.

These deformities not only impair the function of the individual as they grow, but may lead to future orthopaedic problems or injuries resulting from abnormal loading of the affected joints. Once the growth plate is fused, these conditions may only be corrected with expensive and painful procedures such as distraction osteogenesis and, in extreme cases, total joint replacement. Therefore it critical to treat these defects while the patient is still growing. While previous studies of growth plate defects in animal models have demonstrated that stem cells inserted into growth plate defects can reduce or correct angular deformity and limb length discrepancy, few studies have examined correction of a centralized defect. Furthermore, to our knowledge, no one has performed a detailed analysis on the relationship of changes growth plate morphology to subsequent length discrepancies. Therefore, the overall *objective* of this research project is to quantitatively evaluate the application of tissue engineering methods to the treatment of growth plate defects in a small animal model. Combining clinically relevant tissue engineering techniques and materials, the interdependence of monolayer expansion, hydrogel culture, and growth factor regimen on rat BMSC chondrogenesis was studied. A method was then developed to deliver chondrogenic progenitor cells to the injured growth plate. Using micro-CT imaging, growth plate morphological parameters were quantitatively assessed and correlated with whole bone growth kinetics during natural healing and with surgical intervention. This research is *significant* because it: 1) presents *novel* techniques with which the alterations to growth plate morphology due to injury and treatment may be *quantitatively* evaluated and 2) *enhances* our understanding of the factors that determine BMSC behavior under chondrogenic differentiation conditions *in vitro*.

Chapter 3

CHARACTERIZATION OF A SMALL ANIMAL GROWTH PLATE INJURY MODEL USING MICROCOMPUTED TOMOGRAPHY

Introduction

The growth plate is the cartilaginous region at the ends of long bones responsible for their longitudinal growth. Approximately 42% of male children and 27% of female children experience a broken bone by the age of 16 and it is estimated that 15-20% of these fractures will involve the growth plate [12, 13, 163]. Growth plate cartilage is biomechanically weaker than articular cartilage and has limited ability for self repair [13]. Therefore, fractures involving epiphyseal cartilage may result in an angular deformity if the injury occurs within the peripheral regions of the tissue an in a limb length discrepancy if the defect is centrally located [15, 164]. In addition to damage during fracture, injury to the growth plate may also result from the removal of osteosarcomas, the treatment of bone cysts, diabetes, chemotherapy, juvenile arthritis, and limb stabilization in the case of osteopetrosis imperfecta [17-20]. Abnormal loading due to these joint incongruities may have life-long consequences [16].

The growth plate consists of five zones – the resting cell zone, proliferative cell zone, pre-hypertrophic cell zone, hypertrophic cell zone, and calcified cartilage. Each zone consists of chondrocytes at different stages along the endochondral differentiation pathway. The maturation states of these cells are controlled by growth factors in a feedback loop that includes parathyroid hormone related protein (PTHrP), transforming growth factor-β (TGF–β), and Indian hedgehog (Ihh) in a process called endochondral

ossification. At terminal maturation, hypertrophic chondrocytes calcify the extracellular matrix and undergo apoptosis, leaving behind a mineralized scaffold for new bone formation. Terminal chondrocytes also secrete factors that stimulate blood vessel infiltration and regulate osteoblastic activity [165].

Acute injuries that traverse the growth plate (Salter types III and IV) typically result in the formation of one or more bone bridges that are visible on radiomicrographs and MRI images [27, 28]. These bridges may extend from the epiphysis to the metaphysis [1]. The most common treatment of minor growth plate injuries – those where the bone bridge size is <40% of the growth plate and the prospective growth period is at least 2 years – is the Langenskiöld procedure [1, 15]. It involves removal of the bone bridge and insertion of autologous fat into the empty space to prevent the bone bridge from reforming. This procedure is labor intensive and, despite standardization of the technique in the field, clinical success is unpredictable, ranging from 15-38% [1]. This variability may be the result of the propensity of fat to support bone formation after bleeding at the graft surface, fibrous degeneration and shrinking, dislocation of the graft, or necrosis in the center of the graft [1, 38, 39].

An alternative method, microsurgically revascularized epiphyseal plate transfer, is used to treat severe deformities. Here, a section of autologous growth plate and a flap of skin is transferred from another anatomical site to the injured area and the vasculature from the skin are anastamosed to major blood vessels in the surrounding recipient site [42, 43]. This procedure restores growth function to the growth plate by ensuring adequate blood flow to the area, a requirement for proper endochondral ossification. However, the procedure continues to be limited because it is very complex and labor

intensive, the growth rate of the epiphysis is site dependent [44], donor site morbidity is prevalent [42, 44], and transplanted growth plates may not adapt easily to the recipient site [42, 43, 45, 46]. Therefore, limb discrepancies or angular deformities may still occur and distraction osteogenesis following skeletal maturity may be indicated [44].

One of the major obstacles to growth plate injury treatment is assessing the morphology of the injured space. Radiographs are the first mode of analysis in the clinic, but images are difficult to interpret and not all bridges will be visible [27, 28]. MRI analysis with fat-suppressed three-dimensional (3D) spoiled gradient-recalled echo has superior diagnostic capabilities over radiographs [27, 29-32]. Unfortunately, clinicians may have to wait up to 8 months before a bone bridge is apparent in a MRI image [35]. It was also noted that some coronal and sagittal images of the normal knee show discontinuity of the physeal cartilage (drop-out sign), which may be mistaken for premature closure [33]. Due to these limitations, growth plate defect healing in animal models is typically defined as a restoration of whole bone growth or lessening of angular deformity on radiographs, and the changes to overall growth plate morphology are typically characterized using histomorphometric methods that may damage the local microarchitecture.

Microcomputed tomography (micro-CT) scans have been shown to improve accuracy of screw insertion clinically to fix epiphyseal fractures [36]. Using CT scans, 3D reconstructions of human limbs have also allowed detailed analysis of the epiphysis and femoral neck for treatment of a slipped capital femoral epiphysis [37]. These observations suggest that CT scans would allow clinicians to more accurately assess defect placement, treatment options, and changes in growth plate morphology over time.

Using 3D reconstructions from micro-CT images of rat tibiae, Martin et al. [166] have demonstrated that, as rats age, the natural process of growth plate closure is marked by an accumulation of mineralized struts or tethers that traverse the growth plate. These tethers form perpendicular to the plane of the growth plate, connecting the epiphyseal and metaphyseal bone surfaces. Tether formation has been noted on histological sections of fusing dog, pig, and human epiphyses [167]. Though the rat growth plate never fully fuses, the growth plate gets thinner and the number and volume of these tethers increases with time. In their report, Martin *et al*. were able to quantify both the number and volume of these tethers through micro-CT analysis [166].

Several animal models of growth plate injuries have been developed to test clinical approaches to diagnosis and repair of the growth plate. These include rabbit [40, 48, 50], sheep [49, 168], mice [25], and rats [21, 54, 169]. Using these models, the effects of numerous growth factors and insertion materials have been assessed with variable results. Alternate filler materials have included frozen hyaline cartilage, iliac apophysis, and nonbiologic materials such as methylmethacrylate, bone wax, and silastic [38, 40, 48]. Although cartilage is reported to be more effective than fat in preventing growth retardation and angular deformity, none of the aforementioned materials prevents reformation of the bone bar or restores function to the growth plate [39, 41].

The overall goal of this study was to demonstrate the utility of micro-CT as a non-invasive imaging modality for assessing growth plate injury and repair. Therefore, the first aim of this study was to establish a surgical defect model of growth plate injury in the distal femur of adolescent rats and characterize the changes in growth plate and bone lengths due to the presence of a centralized defect in the distal femur of adolescent

Sprague Dawley rats. Using micro-CT images, healing was determined by quantitatively monitoring bone bridge formation into the defect area as well as changes in growth plate thickness, volume, and natural closure dynamics (tether formation). Additionally, we hypothesize that the inhibition of bone bridge formation within the defects is required to prevent growth retardation and that prevention requires a scaffold that will completely occlude the defect. Therefore, the second aim of this study was to characterize the response of growth plate healing to injection of an *in situ* gelling agarose within the centrally localized defect.

Materials and Methods

Surgical Procedure

All procedures were performed under Georgia Institute of Technology IACUC approved guidelines. Sprague Dawley male rats (body weight 100-125 grams, approximately 5 weeks old) (Charles Rivers Laboratory, Wilmington, MA) were used in all studies. Animals were anesthetized using 5% isoflurane and prophylactic antibiotics were administered by subcutaneous injection. The skin over both knees sterilely prepared and draped, providing a sterile surgical field. A 2 cm midline incision was made on the anterior aspect of the right knee joint and a medial parapatellar arthrotomy performed. The patella was dislocated laterally to expose the trochlear groove of the distal femur. Using a hand drill, a central defect was created across the physes of the distal femur by drilling through the articular cartilage between the condyles, normal to the cross-sectional plane of the bone shaft, and then further up the intramedullary canal (**Figure 3.1**).

Preliminary micro-CT analysis of five-week-old limbs showed that the distance from the cartilage between the condyles to the growth plate is approximately 4 mm. Therefore, the depth of drilling into the metaphyses was controlled with a mechanical stop so that the defect did not enter the marrow cavity. The defect was then irrigated with a sterile saline solution. The patella was relocated to its original position and the medial joint capsule was closed with 4-0 vicryl suture. The skin was closed using wound clips and the surgical area was washed with hydrogen peroxide. The wound clips were removed 10-14 days post surgery. The left leg was left unoperated and used as the control for all analyses. In the first study, animals were euthanized by CO_2 asphixiation on days 28 (n=5), 56 (n=8), and 112 (n=5) post surgery to determine the timecourse of defect healing. In the second study, in addition to empty defects (n=4), defects were filled with a 1% solution of *in situ* gelling SeaKem GTG agarose (Cambrex, Rockland, ME) (n=6). Samples were harvested after 56 days and analyzed as described below.

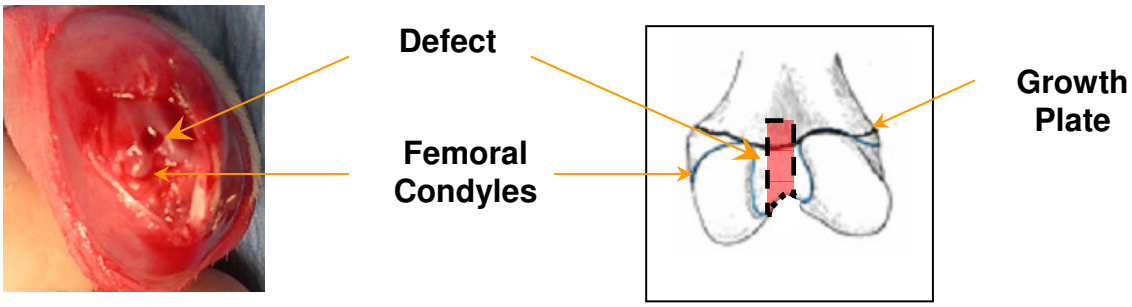

Figure 3.1. Growth plate surgical defect

Appearance of distal femur after growth plate defect created (left). Image demonstrating defect placement and depth (right).

Microcomputed Tomography

The epiphyseal region of the defect legs were scanned at a 20 μm voxel size on a VivaCT 40 system (Scanco Medical, Bassersdorf, Switzerland). The volume of bone infiltration into the defect (bone bridge formation) was measured by isolating a 2 mm x 15 slice (0.32 mm) cylindrical region within the original defect contained entirely within the growth plate as shown in **Figure 3.2A**. This parameter was termed the defect bone volume fraction. To quantify the effect of the defect on growth, whole femurs from the defect and contralateral control legs were scanned at a voxel size of 36 μm and the lengths of the whole bone and diaphysis of each femur were measured from the rendered 3D images. The diaphyseal length was defined as the distance from the lesser trochanter to the metaphyseal plate and the total length was defined as the distance from the greater trochanter to the edge of the femoral condyles (**Figure 3.B**). Finally, the growth plate was isolated from the surrounding bone tissue in the micro-CT images by manual contouring of 2D slices of sagittal images. The contoured regions were compiled to render 3D images (**Figure 3.2C**).

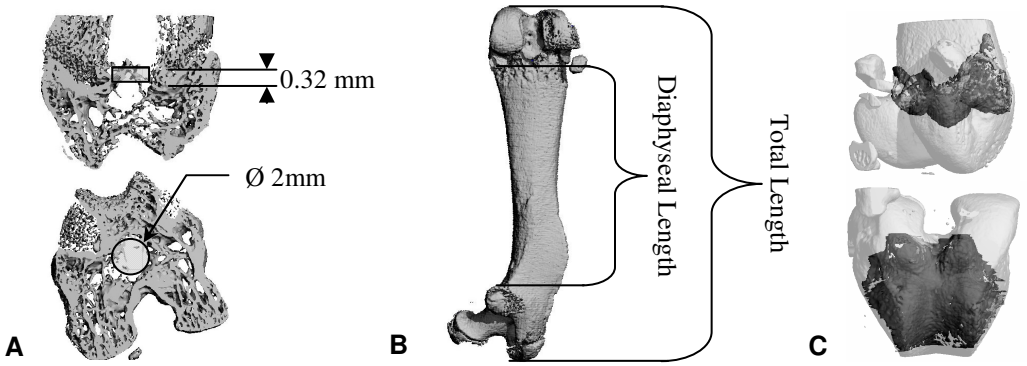

Figure 3.2. Micro-CT Analysis.

Images demonstrating (A) the method of determining the mineral content within the original defect. A controlled volume was used for each sample. (B) The diaphyseal and overall lengths of the contralateral and defect bones. (C) The location, position and morphology of the epiphyseal growth plate within the distal end of the femur. Note the four ridges that are located along the edges of the femoral-patellar groove.

In order to most accurately characterize the changes in growth plate morphology, the contoured areas were further analyzed to ensure that mineralized regions of bone and cartilage were removed. To achieve this, the contour areas of 2D images were decreased pixel by pixel (peeled) from the surface until an accurate representation of the growth plate was attained. From these images, total growth plate volume was calculated and thickness maps generated. Thickness measurements were obtained by expanding spheres at distinct voxels within the 3D volume. Total volume was determined by counting the number of voxels within the contoured region and multiplying the value by the voxel volume. To determine the effect of the defect on the natural course of growth plate closure in Sprague Dawley rats, the volume of mineralized tethers within the growth plate tissue but not including the bone bridge was quantified.

Histology

Whole femurs were fixed in 10% neutral buffered formalin at 4°C for 1 week and stored in 70% ethanol at 4°C until histologic processing. Samples were then decalcified in a 22% formic acid solution buffered with 10% sodium citrate and then embedded in paraffin. Four micron sections were taken through the cross-section and stained with haematoxylin and eosin (H+E).

Statistics

The effects of treatment on group means were assessed using the analysis of variance (ANOVA) general linear model. Statistical significance ($p<0.05$) between individual group means were determined using Tukey's *post hoc* test for multiple comparisons. All graphs represent the mean ± SEM unless otherwise noted.

Results

A preliminary experiment was performed to determine how close this model recapitulates the physiology of a centralized growth plate defects in humans, specifically bone bridge formation and limb length shortening. Animals were euthanized at 0, 7, 10, 14, 21, 28, and 35 days (n=1-2) after surgery and both femurs removed. There was no apparent difference in defect limb length compared to its contralateral control at any of the time points (not shown). Bone was seen to infiltrate the defect as early as day 10 and BVF within the defect increased in a non-linear manner with the most dramatic effects at days 28 and 35 (not shown).

Based on these results, a time-course study was performed in which healing was assessed at days 28, 56, and 112 days post surgery. At day 28, the total length of the contralateral control leg was higher than the defect leg. At days 56 and 112, total and diaphyseal limb lengths of the defect legs were shorter than their contralateral controls (**Figure 3.3A&B**). Overall, the defect resulted in a growth reduction of 63% between 28 and 56 days and 90% between 56 and 112 days.

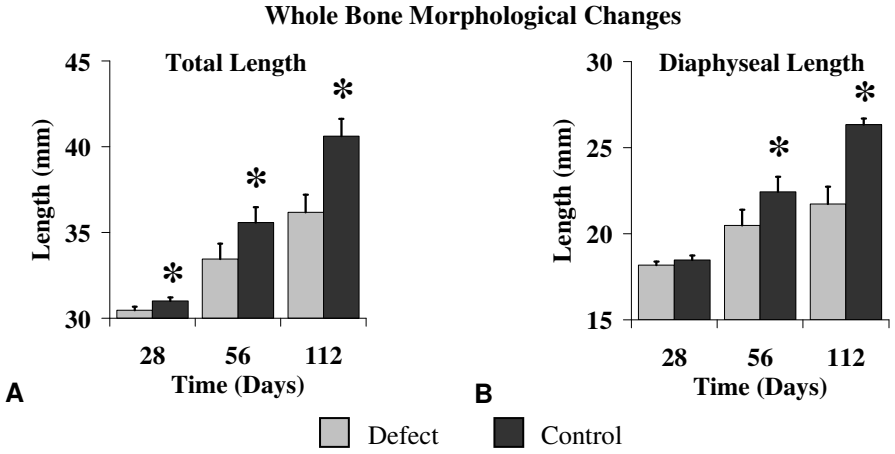

Figure 3.3. Growth plate defect decreases limb length.

Changes in the (A) total length and (B) diaphyseal length of the defect and contralateral control femurs over time as determined by micro-CT analysis. * indicates significant difference from the defect leg.

Optimization of growth plate morphological parameters

Figure 3.4 Figure 3.**A** demonstrates the effects of the peel protocol for 0, 3, and 5 pixel peels. This method has a significant effect on the measured parameters, predominantly at 56 days (**Figure3.4**Figure 3.**B**). At day 56, there was a trend indicating that removal of 5 pixels increased the average growth plate thickness whereas growth

plate volume decreased significantly as the peel number increases. The tether BVF decreased drastically after the initial peel, but did not change significantly thereafter. Based on this analysis, all of the growth plate morphological results were obtained from growth plate images analyzed with a peel of three.

Defect results in a thinner growth plate with increased tether volume

Day 112 growth plates were too thin to reproducibly isolate from the surrounding bone tissue. The growth plate became thinner over time and the presence of a defect through the tissue resulted in a significant reduction in thickness as compared to contralateral controls by day 56 (**Figure 3.5A** & **Figure 3.6**). The defect BVF (bone bridge formation within the defect) did not increase significantly between any of the time-points (**Figure 3.5B**). In contrast, the tether BVF was significantly higher in the defect limb by day 56 (**Figure 3.5C** & **Figure 3.6**). Histological staining of day 56 samples confirmed bone infiltration into the defect. In addition, the defect resulted in disorganization of the cellular morphology of the growth plate (**Figure 3.7A**). The proliferative and hypertrophic zones were highly disorganized compared to their contralateral controls by day 56. Formation of tethers was also confirmed by haematoxylin and eosin staining (**Figure 3.7B**).

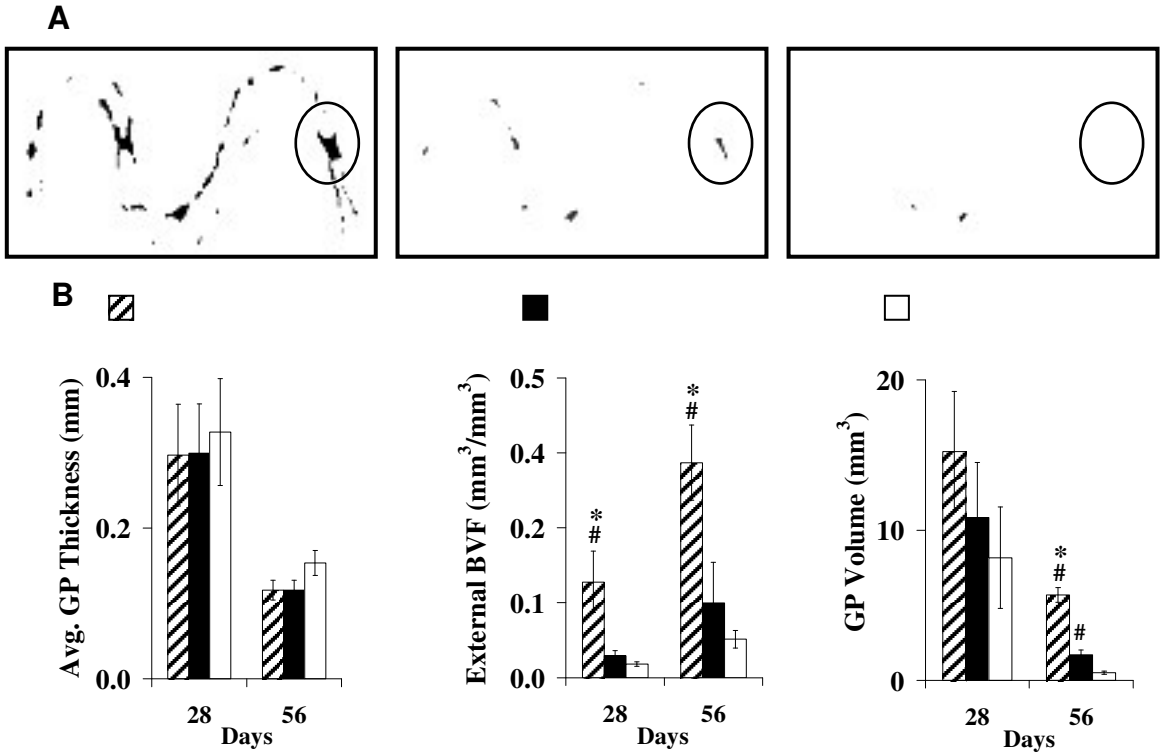

Figure 3.4. Optimization of growth plate morphological parameters.

(A) Images demonstrating the effects of the number of pixels removed from 2D contours (peels) on the representation of growth plate thickness, BVF, and total volume. The number below the image indications the number of pixels removed from the outside edges of the contours used to generate the image. The circled region is a mineralized tether that disappears as the peel number increases. (B) The effects of the different peels on the quantitative estimate of growth plate morphological parameters. * indicates significant difference from the 3 pixel peel and # difference from the 5 pixel peel.

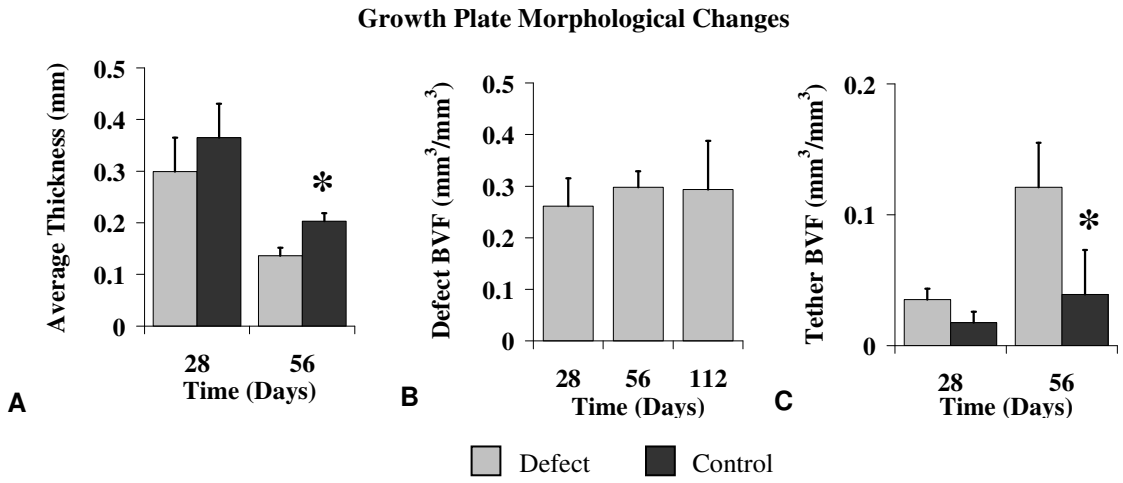

Figure 3.5. Growth plate morphology.

Morphological changes in the defect and contralateral control growth plates over time as determined by micro-CT analysis. (A) Change in average thickness of the growth plate over time. (B) Defect Volume Fraction – Infiltration of bone into the original defect site (bone bridge). (C) Tether Volume Fraction – Volume of mineralized tether formation through the growth plate outside of the centralized defect region as an indication of the degree of closure over time. * indicates significant difference from the defect leg.

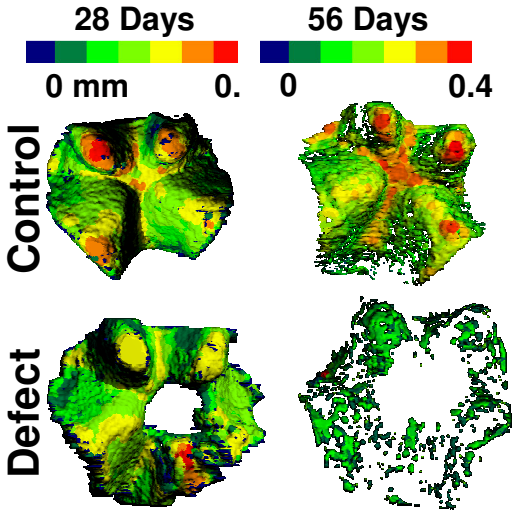

Figure 3.6. Growth plate thickness maps.

Growth plate thickness maps of defects and contralateral controls at 28 and 56 days. Images were generated by compiling 2D contours into 3D images. The defect region was not included in the contours. The white regions within the maps outside the large centralized defect area indicate the location of mineralized tissue (tether) formation through growth plate. Note the difference in the scale bars for the thickness maps at 28 and 56 days.

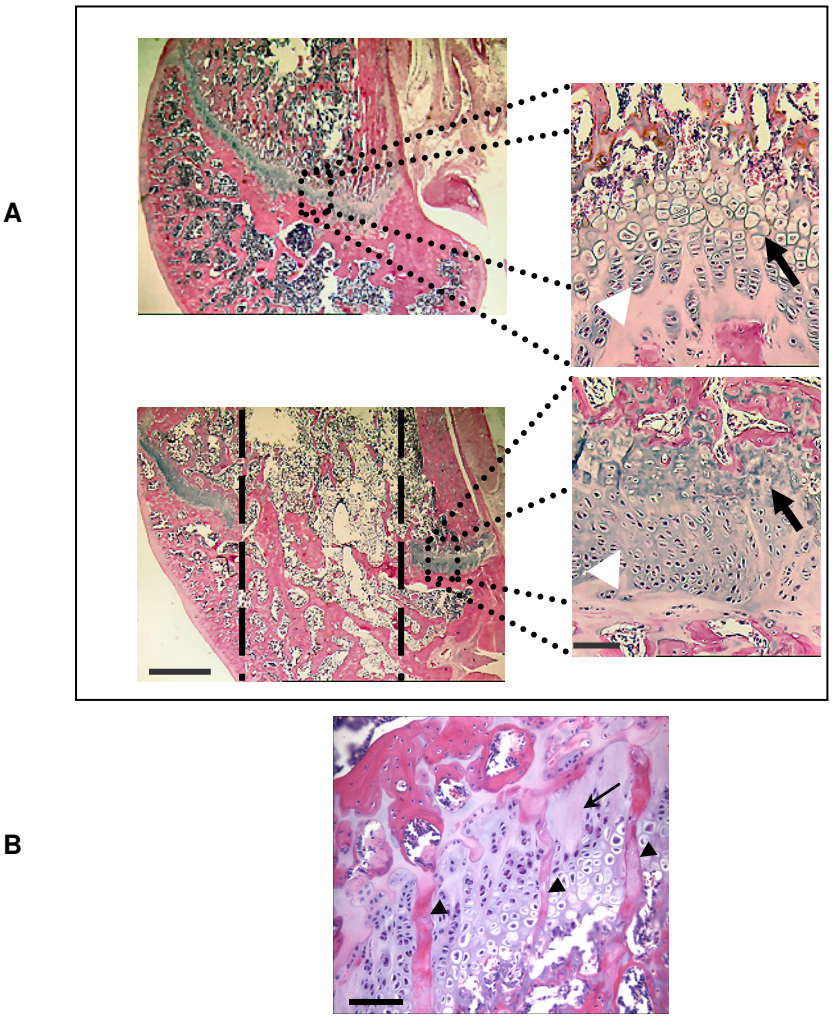

Figure 3.7. Growth plate defect results in cellular disorganization within the growth plate.

(A) Histological analysis of 56 day samples confirmed bone infiltration into the defect. Insets show the growth plate at higher magnification. Note the loss of proliferative cell columns (white arrowheads) and hypertrophic cells (black arrowheads). (B) Mineralized tethers formed through the growth plate connecting the epiphyseal and metaphyseal bone (arrow heads). Scale bar = 400μm on entire epiphysis images. Scale bar = 50μm on magnification of growth plate.

Positive correlations between whole bone and growth plate morphological parameters

To assess whether the limb length was a significant predictor of the growth plate thickness, volume, and/or tether BVF, these parameters were expressed as the percent difference between the defect and control legs. We found that total limb length was positively correlated in a non-linear fashion with the growth plate thickness (R^2=0.88; **Figure 3.8A)** and with the tether BVF (R^2=0.78; **Figure 3.8B**). The growth plate volume was directly correlated to growth plate thickness (R^2=0.96; **Figure 3.8C**) and the percent difference in growth plate volume was positively correlated to the percent difference in limb length (R^2=0.61; **Figure 3.8D**).

Injection of an in situ gelling agarose decreases limb length discrepancy

At day 56, gel insertion had a significant effect on growth plate defect healing. In both the gel filled and empty groups, the defect legs were significantly shorter than control legs (**Figure 3.9A**). However, the defects filled with agarose were significantly longer then their empty counterparts. This resulted in a decrease in limb length discrepancies from 9.74±0.86% in the empty defect to 5.02±1.19% in those defects filled with agarose for 56 days (not shown; p=0.02). The defect growth plates were thinner than the contralateral control limbs in all cases (**Figure 3.9B**). However, there was also a trend toward increased average growth plate thickness of the agarose treated defects compared to those defects left empty (p=0.07). The tether BVF was higher in defect legs (**Figure 3.**Figure 3.**9C**) and there was no difference between empty and agarose treated groups. The defect BVF was the same with or without agarose (not shown). Histological analysis of the defect region showed the presence of agarose remnants with little cellular

infiltration and some regions of mineralization, but no evidence of growth plate regeneration (**Figure 3.9D**).

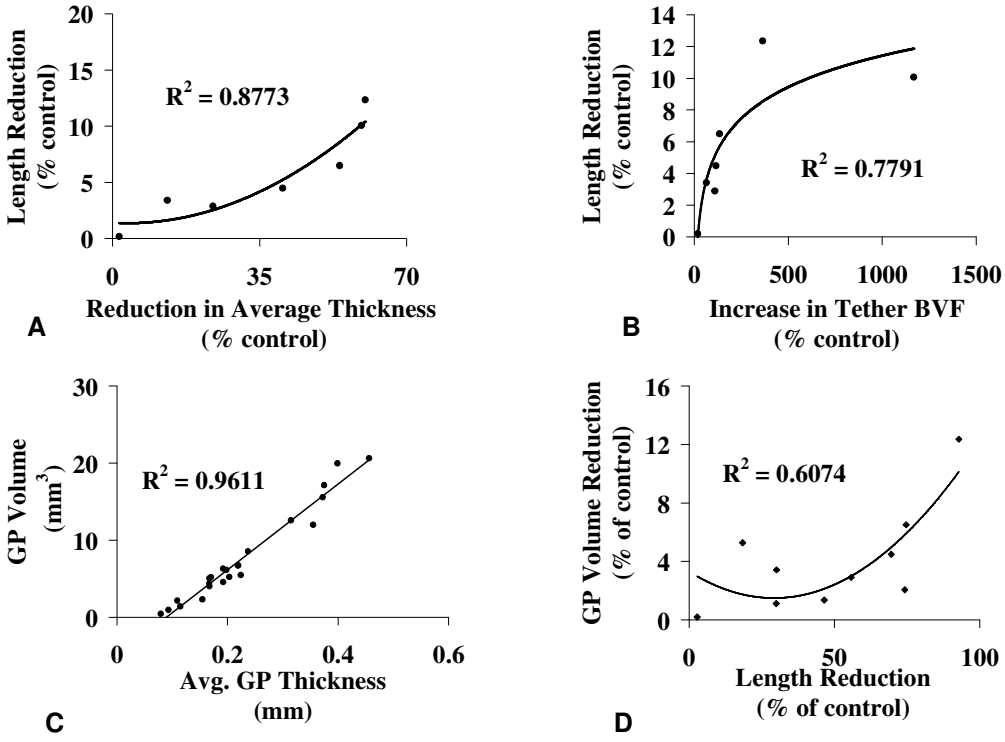

Figure 3.8. Positive correlations between whole bone and growth plate morphological parameters.

Correlations between the % difference in total length and (A) % difference in growth plate thickness legs and (B) % difference in tether bone volume fraction. Correlations between the growth plate volume and (C) the average growth plate thickness and (D) the % difference in length of the defect limbs.

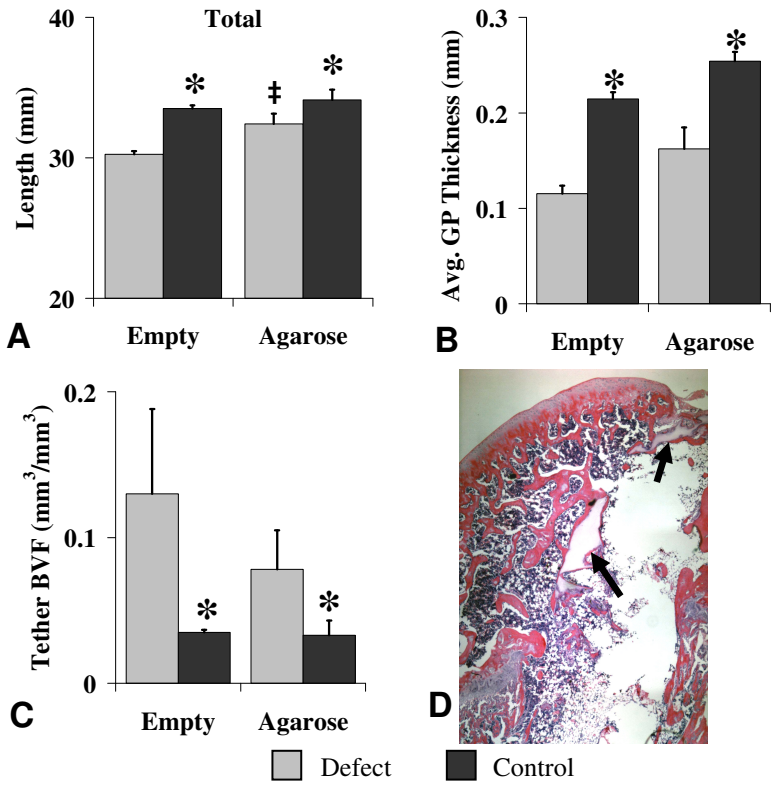

Figure 3.9. In situ gelling agarose decreases limb length discrepancy.

Whole bone and growth plate morphological parameters after 56 days. Defects were either left empty or filled with 1% agarose. (A) total length, (B) average growth plate thickness, (C) tether BVF, and (D) H+E stain of an agarose treated defect. * indicates significant difference from the defect leg; ‡ indicates difference of agarose filled defects from the empty defect leg. Black arrows indicate islands of agarose gel surrounded by bone within the original defect site. Scale bar = 100µm.

Discussion

In this study, a small animal model of growth plate injury was developed and characterized using microcomputed tomography and basic histology. Specifically, we were able to quantify the time-course of bone formation within the defect, changes in the average thickness and volume throughout the growth plate, as well as changes in the

closure dynamics of the rat growth plate by measuring the formation of mineralized tethers throughout the tissue. We have demonstrated that limb length was significantly reduced when the defect was left empty for 28 days. After 56 days, the average growth plate thickness was significantly decreased and the degree of growth plate fusion as measured by mineralized tether formation was increased. We also found that limb length is correlated with growth plate thickness, volume, and degree of tether formations. Overall these parameters can be used to establish the severity of the injury and aid in developing treatment options.

This model replicates the major features of a growth plate injury that traverses the tissue – formation of a bone bridge and limb length discrepancies – that is comparable to results found in other rodent models investigating the molecular mechanisms of bone bridge formation [21, 25, 55-57]. In a murine model, Lee et al. demonstrated that the defect begins with fibrous tissue deposition with infiltration of mesenchymal cells and that the bone bridge forms from the rim of the defect inward [25]. This time-course of tissue infiltration was also observed in a tibial model of centralized defects developed by Xian *et al*. using a rat model [21]. Both authors also showed that bone bridge formation within the growth plate defect occurred through the intramembraneous pathway [21, 25]. To further characterize this process, Xian et al. have also examined the time-course of inflammatory cytokine expression, chondrogenesis, and endochondral ossification, within the injured growth plate using gene expression and immunohistological means [55-57]. However these time-course studies were only qualitatively characterized using histological techniques [21]. In the current study, we were able to quantitatively monitor the changes in growth plate morphology over time. In the future, the marriage of

molecular and morphological models will be required to thoroughly investigate therapeutic options for growth plate injury.

Previous studies performed in our lab indicate that, in empty defects, limb length is positively correlated with the bone volume fraction of the bone bridge and not negatively as expected (unpublished data). Additionally, there was no significant difference in the amount of bone formed in the defect between empty and agarose filled samples after 56 days even though the injection of agarose into the defect reduced limb length discrepancy by ~50% after 56 days. The results of this study suggest that the mechanisms contributing to the observed limb length shortening was likely the observed cellular disorganization of the growth plate rather than formation of the bone bridge. Histological analysis showed thinner, more disorganized resting and hypertrophic zones. These zones are the predominant mechanism of growth within long bones, with the rate of growth determined by cell proliferation and the final intracellular volume of the hypertrophic chondrocytes [165]. This hypothesis is supported by several studies demonstrating that disorganization of the growth plate due to injury, chemotherapy, or irradiation is linked to limb shortening [17, 61, 164]. In a histomorphometric study in Sprague Dawley rats, Damron et al. showed that a single dose of gamma radiation to the proximal tibia resulted in a marked loss in growth rate due to rampant cellular disorganization and loss of reproductive potential of cells in the proliferative zone [17]. Xian et al. demonstrated that a single dose of 5-FU, a chemotherapy agent used in both children and adults, resulted in decreased proliferation of chondrocytes after 2 days. Although the activity and organization of the growth plate returned to normal after 10 days, there was considerable reduction in the overall length of the bone [164]. We also

found that increased limb length discrepancies was highly correlated to the volume of mineralized tether formation throughout the growth plate. However, further investigation is required to determine whether this tether formation is independent of the disorganization of growth plate cells.

Therapeutic strategies that are being investigated for the treatment of growth plate injuries include utilizing articular chondrocytes, growth plate cells, mesenchymal stem cells derived from different sources, and the addition of growth factors. Unfortunately, none have provided complete restoration of growth plate function [48-50, 52, 53, 163, 168-170]. When 1% agarose was used to treat the defect in our model, the limb length discrepancy between the defect and its contralateral control leg was decreased by almost 50% and the growth plate was 22% thicker on average compared to defects left empty for 56 days. Despite these positive effects, there was no evidence of regeneration of a functioning growth plate within the 56 day period in either group. Similar results were seen tissue by Hui et al. who found that fibrin alone resulted in the formation of a bone bridge and higher limb length discrepancies compared to mesenchymal cells seeded in fibrin in a rabbit model of growth plate injury [51]. Chen et al. also reported that agarose alone did not inhibit angular deformity or premature fusion [52]. In both cases, the inclusion of MSCs into the gels rescued growth function. However, no data has been provided to demonstrated integration of the regenerated growth plate with the native tissue or if the growth rate of the implant tissue matches that of the native region [51, 52]. Additionally, delivery of MSCs alone did not inhibit bone bridge formation nor regenerate the growth plate [53].

Biomolecular studies and observations from our micro-CT data suggest that bone formation occurs from the outer rim of the defect towards the center. Furthermore, bleeding around most filler materials serve as a scaffold onto which the bone bridge still forms [25] (unpublished observations). This could potentially explain why full recovery of growth functions has yet to be reported. Our results combined with these studies suggest that a carrier is needed to act as a plug to prevent bone bar formation while supporting tissue formation, but then a cellular component is required to regenerate a functioning growth plate. Future studies in will include the addition of a blood clotting agent to reduce bleeding, and hence infiltration of osteogenic factors from the marrow into the site. This step will facilitate the conformation of *in situ* gelling agarose to the defect space and increase contact between the native tissue and encapsulated factors.

Conclusions

We have demonstrated that micro-CT images may be used to quantitatively monitor changes in growth plate thickness, volume, and fusion after growth plate injury in addition to changes in whole bone morphology. With this model we have also shown the interrelationship between several growth plate morphological factors and limb length discrepancies. Using these predictive parameters, CT scans may be used develop treatment criteria for growth plate injury. CT images are currently used to aide in surgical planning for fractures and slipped femoral epiphyses. Methods to create 3D models of joints already exist, however these procedures yet to be extended towards the assessment of growth plate defects [36, 37].

CHAPTER 4

HYDROGEL EFFECTS ON BONE MARROW STROMAL CELL RESPONSE TO CHONDROGENIC GROWTH FACTORS

Introduction

Cartilage is an avascular tissue with low cellularity and a limited capacity for self-repair. When cartilage is injured or has undergone degeneration, there is little cellular invasion into the damaged region and the intrinsic repair response is insufficient to completely restore the tissue to its former functional state [171]. Tissue engineering strategies, in which cells are seeded within a biomaterial scaffold and cultured *in vitro*, present a possible treatment option for cartilage defects. The success of tissue-engineered cartilage requires the correct marriage of cells, scaffolds, and growth factors for optimal matrix production and integration into the defect site.

A significant challenge in cartilage tissue engineering is retrieving an adequate number of cells to develop the construct. If autologous tissue or cells are used in the repair process, it is often difficult to harvest a large number of chondrocytes without causing substantial additional damage due to donor site morbidity [128]. Ample cell numbers may be obtained through *in vitro* monolayer expansion, or passaging, of the desired cells. Unfortunately, passaging causes chondrocytes to dedifferentiate, a condition marked by decreased expression of two necessary cartilage matrix components: type II collagen and sulfated glycosaminoglycans (sGAGs), as well as increased expression of undesirable type I collagen [63-65, 129]. The identification of alternative cell sources and appropriate *in vitro* conditions to produce implantable 3D constructs that

effectively repair cartilage defects is therefore a high priority. Bone marrow stromal cells (BMSCs) have been identified as a potential source for the treatment of musculoskeletal defects [95]. BMSCs are a multipotential cell population that can be stimulated to differentiate into cells from the mesenchymal lineage including bone, cartilage, and fat under specific *in vitro* culture conditions [148-150].

BMSC chondrogenesis has been achieved using several types of *in vitro* culture systems, including woven polymers and hydrogel constructs, with the most popular system being scaffold-free (aggregate or pellet) culture [148-150, 154, 157, 172-175]. Hydrated materials offer an attractive alternative to pellet or pre-manufactured polymer scaffold culture because their cross-linked network mimics the natural structure of extracellular matrices *in vivo* and their high water content facilitates the exchange of nutrients and gases [176, 177]. Additionally, the recovery and maintenance of the chondrocytic phenotype of primary articular chondrocytes in hydrogels such as alginate and agarose have been well characterized [75-77, 178-181]. Alginate and agarose solutions may also be injected and polymerized *in situ*, making them attractive options for arthroscopic repair of lesions [182]. While alginate and agarose have similar macroscopic properties and are sometimes used interchangebly, recent evidence suggests that cell-scaffold interactions result in remarkably different cell behavior in response to biochemical and mechanical stimulation [180, 183-185].

Much work in recent years has focused on establishing the correct growth factor regimen in order to achieve chondrogenesis of BMSCs with cocktails typically including transforming growth factor-β1 (TGF-β1) [148, 157, 186]. Furthermore, fibroblastic growth factor-2 (FGF-2, also known as basic FGF) has been shown to enhance

mesenchymal differentiation of stromal cells at late passage numbers [148, 187] and in BMSCs isolated from older animals [188]. Dexamethasone, a synthetic glucocorticoid, has also been shown to be required for chondrogenesis of stem cells isolated from human bone marrow and rat calvaria [189, 190].

Although several different approaches have been investigated to stimulate BMSCs down the chondrogenic pathway [148, 149, 154, 171-173, 183, 191, 192], few studies have investigated the influence of scaffold material on the response of BMSCs to biochemical conditions that stimulate chondrogenic differentiation. The aim of this study was to investigate the influence of alginate and agarose encapsulation on the chondrogenic response of BMSCs to FGF-2, Dex, and TGF-β1 treatment *in vitro*.

Materials and methods

Cell isolation and expansion

Bone marrow stromal cells were retrieved using a technique previously described [193]. Briefly, six female 45-day old Sprague Dawley (Charles Rivers Laboratory, Wilmington, MA) rats were euthanized by CO_2 asphyxiation and their femurs and tibiae removed under IACUC approved guidelines. The epiphyses were removed from the proximal and distal ends of the bones using a bone cutter. Bone marrow was flushed from diaphyses with α-MEM supplemented with penicillin/streptomycin (100U/100μg/ml; Invitrogen Carlsbad, CA) and a selected lot of fetal bovine serum (FBS; Hyclone, Logan, UT) using a 20 gauge needle attached to a 10 ml syringe. The cell suspension was centrifuged at 1,200 RPM for 20 minutes, resuspended in media, and

plated at one leg/100 mm dish (Corning, Corning NY) for 30 minutes. Unattached cells were collected, replated in 150 cm^2 T-flasks at a density of $150x10^6$ cells/flask, and covered with 35ml of media. Media was changed after four days to remove non-adherent cells. The cells grew in circular patches that became confluent after eight days, which were termed primary confluence (P0). The cells were then lifted from the surface using 0.05% trypsin/0.53mM EDTA (Invitrogen Carlsbad, CA), replated at a density of $1x10^6$ cells/150 cm^2 flask, and again grown to confluence (P1). This process was repeated up to 3 times to reach P4. Those cultures treated with rhFGF-2 [FGF+] (R & D Systems Minneapolis, MN) received fresh growth factor added to the media at a concentration of 1ng/ml at the time of passage from P1 until P4.

Hydrogel culture

For all experiments, 2% Pronova UP LVG sodium alginate (FMC Biopolymer Drammen, Norway) and 2% Agarose type VII (Sigma, St. Louis, MO) solutions were used. Gels were prepared by mixing the alginate or agarose powder with calcium and magnesium free phosphate buffered saline (PBS). The mixtures were autoclaved for 20 minutes to dissolve the powder and sterilize the solutions.

Cylindrical gels were cast in a custom designed mold (see **Appendix B** for mold design and seeding protocol). The mold consisted of a solid base and top piece containing cylindrical holes machined from 0.25 inch thick polycarbonate. A 0.2 μm cellulose-acetate membrane (Cole-Parmer, Vernon Hills, IL) supported by an 80 μm stainless steel mesh (McMaster Carr, Atlanta, GA) was placed between the top and bottom pieces. The membrane was wet with either a solution containing 102 mM $CaCl_2$,

100 mM NaCl, and 50 mM HEPES to crosslink alginate gels or PBS to support agarose gels while they polymerized. At the specified passage, FGF+ and FGF- cells were suspended in the specified hydrogel at a seeding density of $20x10^6$ cells/ml. The gel plus cell solutions were pipetted into each well of the mold and allowed to polymerize for 30 minutes at room temperature. The resulting gels measured either 4 or 8 mm in diameter and were 2 mm thick. Gels were rinsed in high glucose DMEM supplemented with 1% antibiotic/antimycotic (100 U penicillin G, 100 μg streptomycin sulfate, 0.025 μg amphotericin B/ml; Invitrogen Carlsbad, CA) after polymerization. The constructs were then placed into either basal medium (DMEM supplemented with 1% ITS+ (BD Biosciences, Bedford, MA), 1% antibiotic/antimycotic, 0.1 mM non-essential amino acids (Invitrogen Carlsbad, CA), and 50 μg/ml ascorbic acid-2-phosphate (AA-2P; Sigma, St. Louis, MO), basal medium supplemented with dexamethasone-21-phosphate (Dex) or TGF-β1 plus Dex in the concentrations outlined below. Gels were covered with 1-2 ml of media and cultured in a humidified atmosphere of 5% CO_2 at 37°C. Media was changed every 2-3 days for the duration of the experiments. Fresh AA-2P was added to the culture at every media change. Dex or TGF-β1 + Dex were also added fresh at every media change in those groups indicated.

Experimental design

Experimental groups for all studies are outlined in **Table 4.1**. In the first study, we examined the combined effects of growth factor treatment during monolayer expansion and alginate culture at P2 and P4 (*Study A*). At each passage point, the cells were divided into 4 groups: Monolayer expansion with (Groups A1 and A3) or without (Groups A2 and A4) 1ng/ml FGF-2 supplemented media and then, after encapsulation in alginate, exposure to 10 nM Dex alone (Groups A1 and A2) or 10ng/ml TGF-β1 + 10 nM Dex (Groups A3 and A4). Samples were harvested after 21 days of culture for biochemical and immunohistochemical analysis. Next, we examined the effects of Dex concentration and hydrogel material on the production of cartilaginous proteins and cell viability (*Study B*). P2, FGF+ cells were seeded in alginate or agarose and treated with 10 ng/ml TGF-β1 and either 0, 0.1, 10, or 1000 nM Dex . Samples were harvested after 21 days for biochemical and live/dead analysis. Finally, we investigated the effects of hydrogel on the chondrogenic response to a specific growth factor regimen: 1ng/ml FGF-2 treatment during monolayer expansion and 10ng/ml TGF-β1 + 10 nM Dex treatment in 3D culture (*Study C*). P2, FGF+ and FGF- cells (Groups C1, C2 , and C4 and Groups C3 and C5, respectively) were seeded in alginate or agarose. They were then cultured in either basal medium (ITS alone) (Group C1), 10nM Dex alone (Groups C2 and C3), or 10ng/ml TGF-β1 + 10 nM Dex (Groups C4 and C5). Samples were harvested on days 14 and 21 for biochemical, histological, and live/dead analysis.

Table 4.1 Experimental groups

	Groups	Monolayer Expansion		Hydrogel Culture		
		Passage[a]	FGF-2	Type	Dex (nM)	TGF-β1 (ng/ml)
Study A	1	2	+	Alginate	10	--
	2	2	-			
	3	4	+		10	10
	4	4	-			
Study B	1	2	+	Alginate and Agarose	0	10
	2	2	+		0.1	10
	3	2	+		10	10
	4	2	+		1000	10
Study C	1	2	+	Alginate and Agarose	ITS alone	
	2	2	+		10	--
	3	2	-			
	4	2	+		10	10
	5	2	-			

a All FGF+ received 1ng/ml FGF-2 from P0 until the passage number indicated

Biochemistry

To assess the accumulation of a cartilaginous matrix, sGAG production was measured using the DMMB dye assay developed by Farndale *et al.* [194] and including modifications reported by Lee and Bader [195]. Total DNA was quantified using Hoechst 33258 dye (Sigma, St. Louis, MO) as described by Kim *et. al* [196]. On day 14 or 21, whole alginate gels were digested with proteinase k in a buffer containing 100 mM sodium phosphate and 5 mM EDTA at 60°C for 16 hours. Whole agarose gels were first heated at 70°C in ammonium acetate until softened, then cooled to 41°C for 1 hour before adding 1.5 U/ml agarase. Samples were incubated at 42°C overnight to break up the agarose and then digested with proteinase k for 16 hours at 60°C.

Immunohistochemistry

Immunohistochemistry was used to confirm the production of the cartilage specific proteins aggrecan and collagen type II. Alginate gels were rinsed in 100 mM barium chloride for 30 minutes under agitation to permanently crosslink the gels. After rinsing in PBS, 1 mm sections were cut from the center of both alginate and agarose samples, placed in 48 well plates, and fixed in 10% NBF for 10 minutes. All of the following steps were performed on a shaker plate. Samples were rinsed with PBS and permeabilized with 0.01% Triton-X (Sigma, St. Louis, MO) for 5 minutes. Samples were then treated with 0.05 U/ml chondroitinase (Sigma, St. Louis, MO) for 30 minutes at 37°C. After rinsing, samples were blocked with 1% BSA (Sigma, St. Louis, MO) in PBS for 10 minutes. Either primary monoclonal mouse anti-type II collagen (II-II6B3; Developmental Studies Hybridoma, Iowa City, IA) or polyclonal rabbit anti-aggrecan (AB1031; Chemicon, Temecula, CA) antibodies (diluted 1:1 and 1:40 respectively in 1% BSA/PBS) were then applied to the samples and incubated at room temperature for 1 hour. Secondary antibodies conjugated to Rhodamine Red (collagen) and Alexa Fluor 488 (aggrecan) (Molecular Probes Eugene, OR) were diluted 1:200 in 2% serum and 1% BSA. Hoechst 33258 dye (Sigma, St. Louis, MO) was also included in this solution at a concentration of 10 ng/ml to counterstain the cell nuclei. Samples were incubated in the secondary antibody solution under low light conditions for 1 hour at room temperature. Images were taken on a Zeiss LSM 510 confocal microscope at excitation/emissions of 365 nm/458 nm for Hoechst, 573 nm/590 nm for Rhodamine Red, and 496 nm/518 nm for Alexa Fluor 488. Negative controls, incubated with secondary antibodies only, were also imaged to determine background staining.

Cell Viability

The Live/Dead Assay (Molecular Probes) was used to follow the progression of cell death within the gel samples over time. The protocol was adapted from recommendations provided by the manufacturer. Briefly, for each treatment group, the remainder of the gel from which the immunohistochemistry sample was excised was incubated in a solution containing 4 mM ethidium bromide and 4 mM calcein for 45 minutes. After rinsing in PBS, gels were imaged on a Zeiss LSM 510 confocal microscope. Viability was determined by imaging three samples along the cross-section, rim, bottom, and top regions. Twenty consecutive 5 μm thick images were taken from the cross-section of each sample and the number of live and dead cells in each image was counted using ImagePro software.

Statistical Analysis

The effects of culture conditions on group means were assessed using the analysis of variance (ANOVA) general linear model. Statistical significance ($p<0.05$) between individual group samples was determined using the Tukey *post hoc* test for multiple comparisons. All graphs represent the mean ± SEM unless otherwise noted.

Results

Passage dependent FGF-2 and TGF-β1 modulation of BMSC chondrogenesis

In our first study, the influence of passage number and FGF-2 treatment on rat BMSC chondrogenesis in alginate was examined. Treatment with FGF-2 during monolayer expansion did not affect the DNA content of constructs after 21 days in 3D culture except for P4 cells treated with Dex alone (**Figure 4.1A**). FGF-2 treatment significantly enhanced TGF-β1 stimulated chondrogenesis at P2, however this effect was lost at P4 (**Figure 4.1B**). Exposure of constructs to TGF-β1 during 3D culture increased sGAG/DNA measurements at both P2 and P4. Over all the groups, FGF-2 treatment during monolayer expansion and TGF-β1 treatment in alginate culture of P2 cells for 21 days resulted in the greatest deposition of sGAG. In addition to sGAG accumulation, collagen type II expression detected by IHC qualitatively confirmed chondrogenesis of rat BMSCs in response to TGF-β1 (not shown). Based on the results of this study, P2 cells were subsequently used to examine the effects of growth factor treatment regimen and hydrogel type on rat BMSC chondrogenesis.

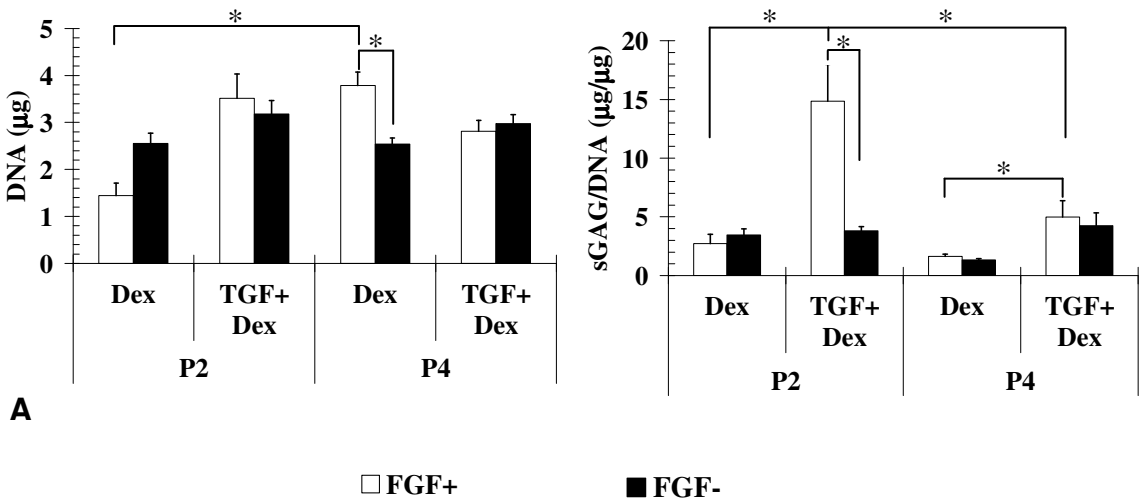

Figure 4.1. Effects of passaging on DNA and sGAG levels

Cells expanded to P2 or P4 in the presence or absence of FGF-2 were seeded in alginate and cultured for 21 days. (A) Total DNA and (B) sGAG normalized by total DNA (n=4-6).

BMSC response to Dex treatment is scaffold dependent

In preliminary experiments, we observed that hydrogel constructs exposed to Dex appeared to have decreased cell viability. To more closely examine the effects of Dex on BMSC viability and cartilaginous matrix deposition, a dose response study was performed (**Figure 4.2**). At day 21, Dex treatment significantly decreased viability in agarose but not alginate constructs ($p<0.008$). Images taken on the rim, top, bottom, and cut face of each construct demonstrated consistent distribution of live and dead cells. In all agarose groups receiving Dex, there was an approximately 20% decrease in the number of live cells (**Figure 4.2A**). No dose-dependent effect of Dex on cell viability was observed in either hydrogel group. The samples receiving 10 nM Dex had an approximately 2 fold higher accumulation of sGAG over all other groups in both hydrogel types (**Figure 4.2B**). Although normalized data are presented to highlight the

relative differences observed within the two hydrogel systems, alginate overall supported a higher level of sGAG accumulation compared to agarose ($p<0.0012$).

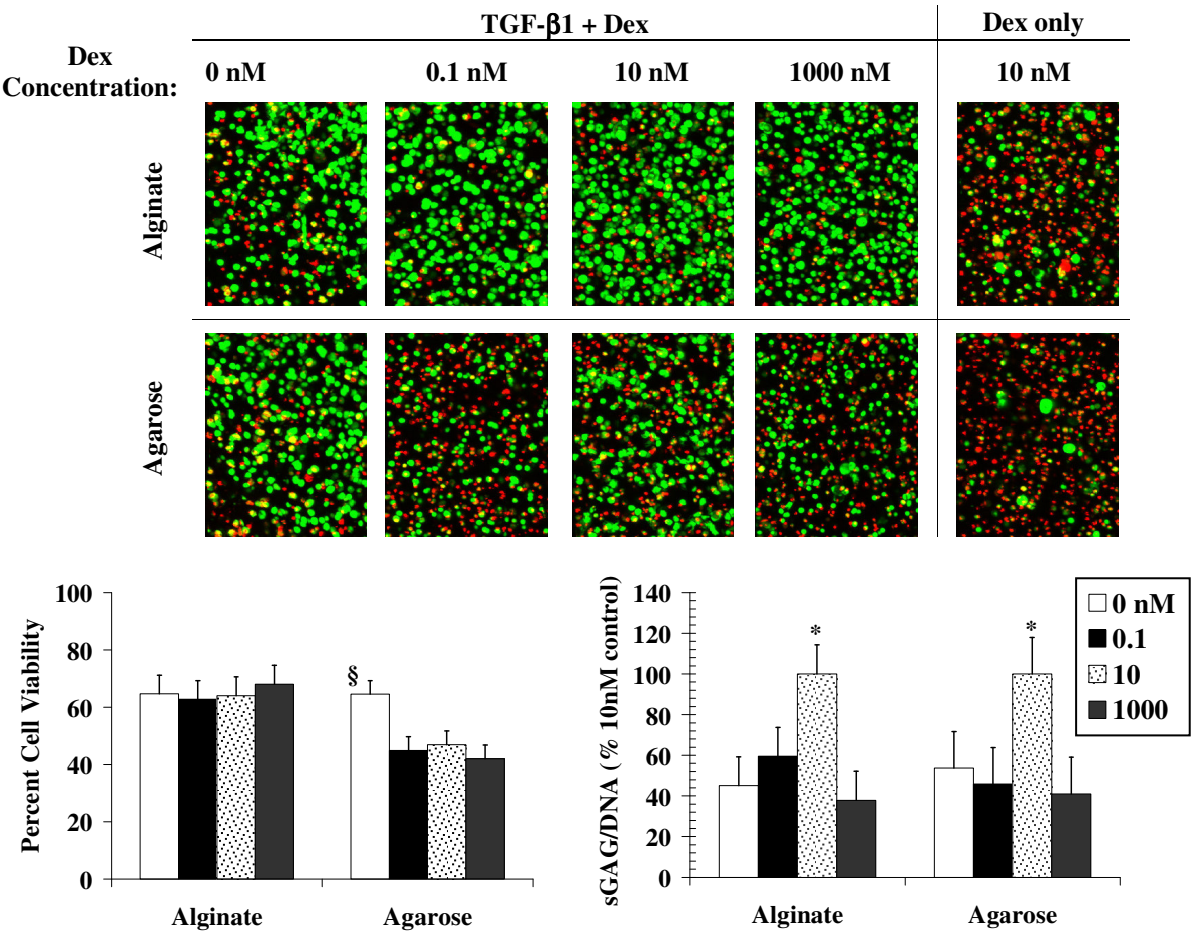

Figure 4.2. Dex dose response results

[Top] Live dead staining of day 21 alginate and agarose gels treated with 0, 0.1, 10, or 1000 nM Dex with or without the addition of TGF-β1. Live and dead cells fluoresce green and red respectively. The yellow regions are overlapping live and dead cells. Original magnification was 10x. **[Bottom]** Cells expanded to P2 in the presence of FGF-2 were seeded in alginate or agarose and cultured for 21 days in the presence of TGF-β1 and the dosage of dex indicated. **(A)** Addition of Dex to agarose samples resulted in a 20% decrease in cell viability compared to agarose samples that received no Dex treatment (n=5-6, § → $p<0.008$). **(B)** sGAG/DNA presented as the percent of the 10nM Dex group (n=7-8).

BMSC response to chondrogenic growth factor regimen is scaffold dependent

Having determined that P2 BMSCs treated with 10ng/ml TGF-β1 and 10nM Dex result in the highest accumulation of a cartilaginous matrix in alginate and agarose culture, we next examined the effects of hydrogel choice on the chondrogenic response of these cells to the entire growth factor regime: 1ng/ml FGF-2 during expansion to P2 and 10 ng/ml TGF-β1 + 10 nM Dex during 3D culture.

In both alginate and agarose constructs containing FGF+ cells, DNA content decreased in the ITS and Dex groups but remained similar in the TGF-β1 + Dex group between days 14 and 21. TGF-β1 + Dex treatment of FGF- cells stimulated a consistent increase in DNA between days 14 and 21 whereas Dex treatment alone had no effect on DNA content (**Figure 4.3A & C**).

In alginate, FGF+ and FGF- groups treated with TGF-β1 + Dex had significantly more sGAG/DNA than either ITS or Dex alone at both days 14 and 21. Alginate samples also had greater sGAG accumulation by day 21 compared to day 14 samples for all TGF-β1 treatment groups (**Figure 4.3B**). Additionally, FGF+ cells in alginate had increased sGAG accumulation over FGF- samples by day 21 only when exposed to TGF-β1 + Dex.

Agarose samples treated with TGF-β1 + Dex demonstrated significantly more sGAG accumulation compared to ITS or Dex treatment alone only at day 21 (**Figure 4.3D**). In contrast to culture in alginate, FGF+ cells produced significantly less sGAG than FGF- cells in agarose by day 21. At day 21, the amount of sGAG produced in FGF+ cells in alginate gels and FGF- cells in agarose gels cultured with TGF-β1 + Dex were not statistically different.

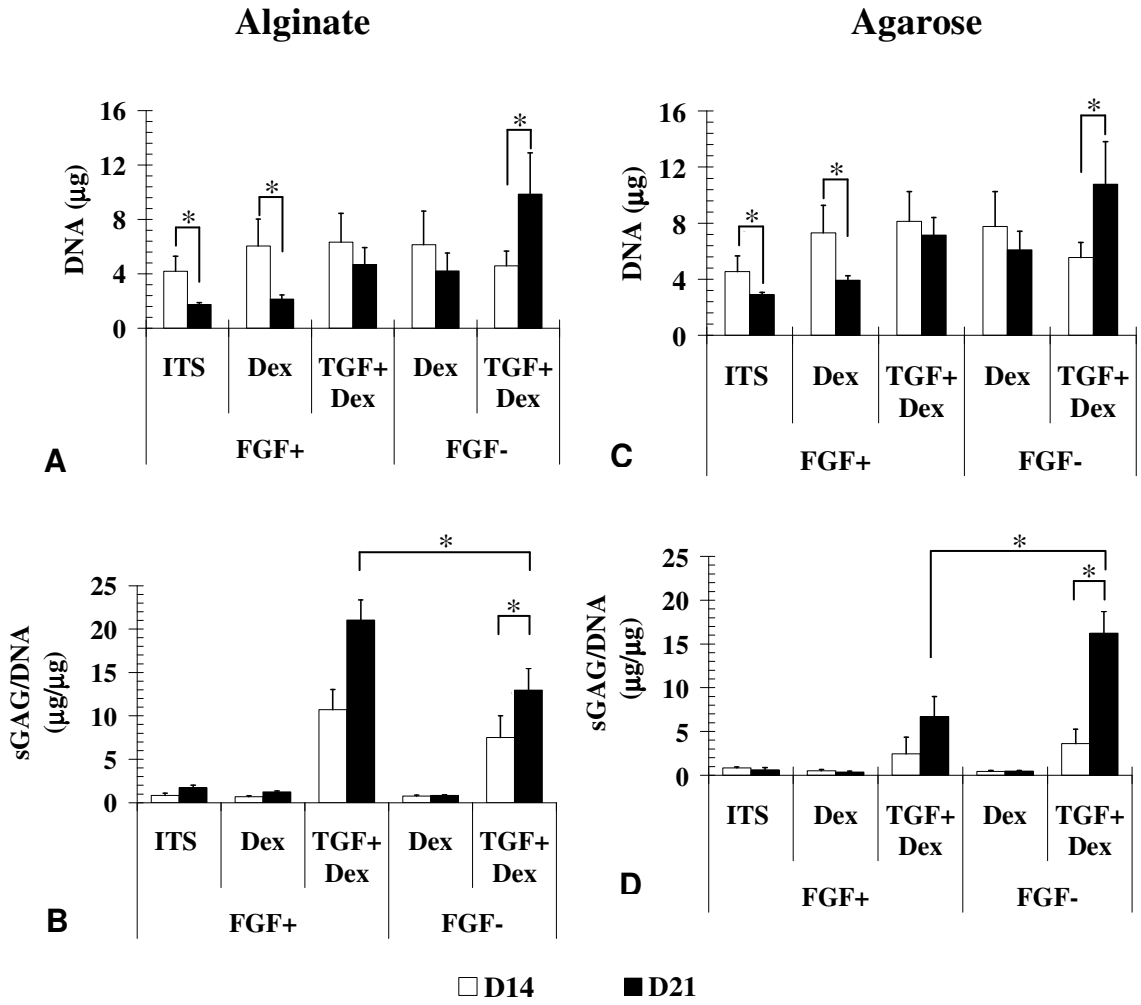

Figure 4.3. sGAG and DNA production

Cells expanded to P2 in the presence or absence of FGF-2 were seeded in alginate or agarose and cultured for 14 and 21 days. **(A&C)** Total DNA and **(B&D)** sGAG normalized by total DNA (n=10-12).

The live/dead images shown **Figure 4.4** again demonstrate the negative effects of Dex on cell viability, particularly in agarose. In alginate, FGF treatment during monolayer expansion and TGF-β1 treatment in 3D culture promote cell viability even in

the presence of Dex. In agarose, neither FGF treatment nor TGF-β1 treatment appear to prevent loss of cell viability in constructs exposed to Dex over the 21 day culture period.

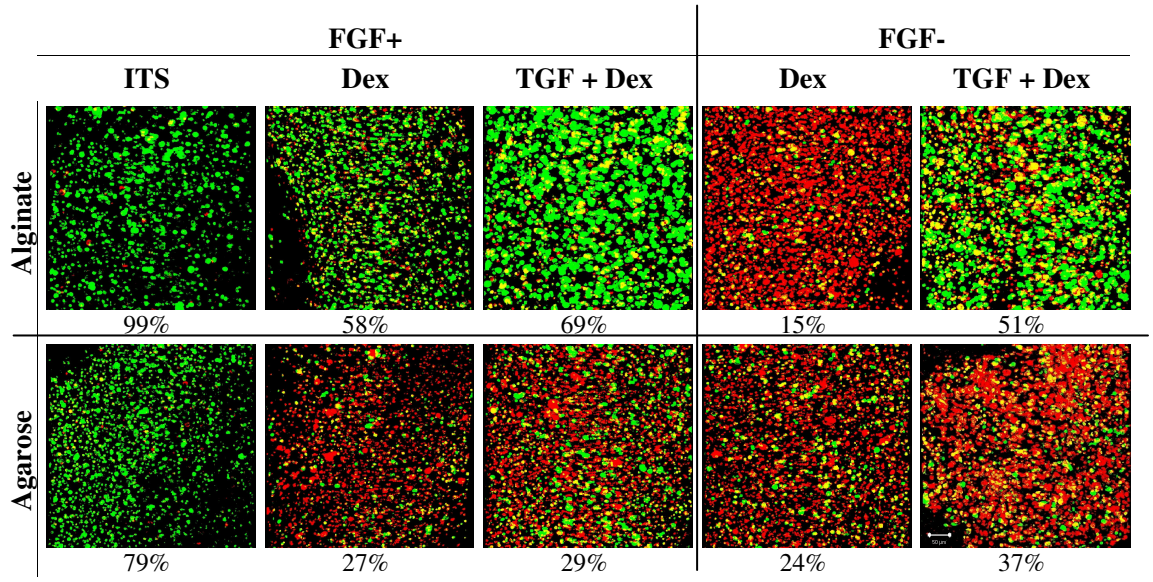

Figure 4.4. Live dead staining of alginate and agarose gels after 21 days of culture. The value below each image is the percent live cells as determined from image analysis of 20 consecutive confocal sections. Original magnification was 10x.

Aggrecan and collagen type II protein expression were most intense in TGF-β1 treated alginate and agarose samples. Both proteins were localized to the pericellular matrix of individual cells or cell clusters (**Figure 4.5**). There were no observable qualitative differences in aggrecan and collagen II expression in any of the TGF-β1 treated groups at either day 14 or 21, whether or not the cells were treated with FGF-2 during monolayer expansion.

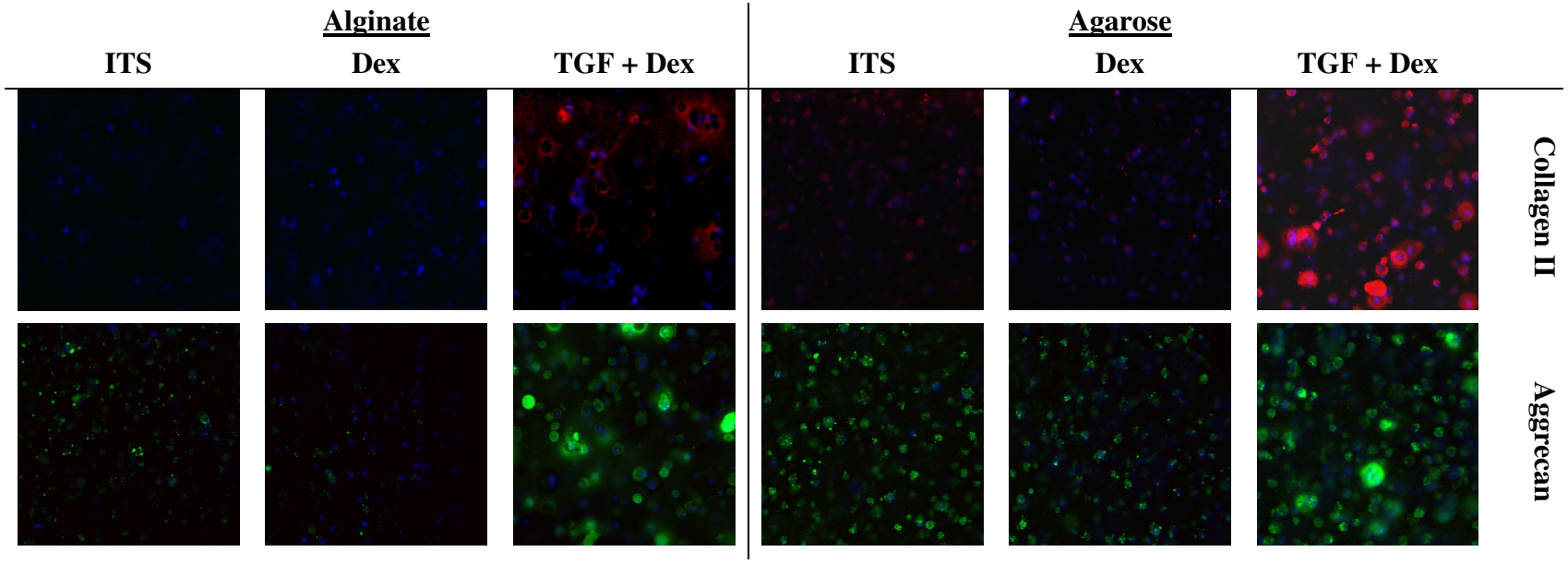

Figure 4.5. Immunohistochemical detection of collagen type II and aggrecan.

Hydrogel samples containing cells treated with FGF-2 during monolayer expansion and TGF-β1 during 3D culture. All images were taken at the 21 day timepoint. Both proteins were localized in the pericellular regions surrounding single cells or cell clusters. Cell nuclei were counterstained with Hoechst dye and fluoresce blue. Original magnification 10x.

Discussion

Ectopic and orthotopic small animal models are used extensively to evaluate cell-based strategies for tissue repair and regeneration. This study was a first step towards developing a small animal model in which bone marrow stromal cell based strategies may be initially tested for cartilage therapies. The purpose of this study was to evaluate interactions between hydrogels and biochemical factors that stimulate chondrogenic differentiation of rat BMSCs. Both alginate and agarose are promising scaffolds for cartilage tissue engineering. However, these hydrogels are sometimes used interchangeably in tissue engineering research. This study demonstrates that the chondrogenic response of BMSCs to biochemical chondrogenic stimuli is scaffold dependent. Specifically, we found that rat BMSCs expanded in monolayer in the presence of FGF-2 resulted in a higher accumulation of a cartilaginous matrix in alginate culture in response to TGF-β1 treatment compared to TGF-β1 treatment alone. Conversely, FGF-2 expanded cells seeded in agarose accumulated less matrix than those cells exposed to TGF-β1 alone. Additionally, we found that matrix accumulation was highest when an intermediate level of Dex (10nM) was added to the chondrogenesis media for both alginate and agarose culture. However, Dex was also found to decrease cell viability in agarose constructs while having no effect on the viability of cells encapsulated in alginate.

Although both alginate and agarose are composed of complex polysaccharides, their components give them very different physicochemical properties. Alginate contains varying amounts of 1,4'-linked β-D-mannuronic acid and α-L-guluronic acid and the pore

size, diffusivity, and mechanical properties are determined by guluronic acid content and the method of polymerization [197]. The resultant gel is negatively charged. Agarose is a neutral species composed predominantly of alternating units of β-D-galactopuranosyl and 3,6-anhydro-α-L-galactopuranosyl [198]. Due to the charge disparity between alginate and agarose as well as the differences in the structure achieved by their polysaccharide units during polymerization, the diffusion of molecules through these gels may be distinctive. A study by Leddy *et al.* found that the porosity of 2% alginate and agarose were similar, however, the movement of negatively charged particles, such as the dexamethasone-21-phosphate used in these experiments, through alginate compared to agarose was not examined [199]. It is possible that alginate resists the diffusion of negatively charged particles into and out of the matrix exposing the encapsulated cells to a dissimilar biochemical microenvironment compared to agarose.

Specific interactions between alginate and positively charged proteins have been reported in the literature [200]. These interactions are likely to also result in an altered cellular biochemical microenvironment in alginate compared to agarose samples cultured under identical conditions *in vitro* [200]. TGF-β1 has been shown to bind to alginate by replacing Ca^{2+}, resulting in inactivation of the protein [200]. Wee *et al.* have shown that when TGF-β1-alginate is incubated in a low pH environment (e.g. waste buildup during metabolism) and then exposed to neutral conditions (e.g. media change), active TGF-β1 is rapidly released from the alginate [200]. Cells seeded in alginate may therefore be exposed to varying levels of activated TGF-β1 depending on local pH.

The propensity for positively charged proteins to bind to alginate may also increase the probability that cellular interactions with the scaffold will occur and

therefore alter their response to any growth factor regimen. This phenomenon may explain why cells treated identically in monolayer have dissimilar responses to chondrogenic stimuli in alginate compared to agarose. Surfaces and gels designed to contain specific proteins or present RGD sequences to cells have been shown to directly affect cell behavior [201, 202]. Furthermore, the binding of chondrocyte integrins to ECM molecules results in the intracellular formation of focal adhesion plagues, which is a prerequisite for cells to respond to growth factors such as FGF [203, 204]. Studies comparing the *in vitro* response of chondrocytes to culture in various types of hydrogels have been reported [180, 183-185], but few have investigated the complex interactions of chondrocytes or BMSCs with these hydrogels on a sub-cellular level.

Rat BMSCs have been used extensively *in vitro* to study the response of mesenchymal cells to osteogenic stimuli [159, 205-207]. However, chondrogenic differentiation of this cell population has only recently been examined, often with mixed results. Hanada *et al.* found that they could not stimulate chondrogenesis in rat BMSCs using TGF-β1 in a pellet culture system [99], whereas Neuhuber *et al.* found that chondrogenesis could be stimulated using the pellet system with TGF-β3, BMP-2, and the addition of 1% FBS [149]. We found that rat BMSCs placed in alginate after primary confluence (P0) did not demonstrate significant sGAG production or collagen type II expression with TGF-β1 treatment (unpublished data). This may explain the difficulties reported with chondrogenic stimulation of BMSCs derived from Sprague Dawley rats [99], however the monolayer treatment for the previous studies was not reported. Studies examining the effects of passaging on stem cells derived from various tissues have demonstrated that the treatment of these cells in monolayer can effect their response to

differentiating conditions [148, 208]. We therefore examined the effects of passaging on rat BMSCs with a focus on the effects of FGF-2 stimulation. We found that P2 cells underwent chondrogenesis in media conditions that P0 cells did not and that FGF-2 treatment during monolayer expansion enhanced cartilaginous matrix accumulation over untreated cells.

BMSCs have been shown to express the FGF-receptor [209] and the mitogenic effect of FGF-2 has been demonstrated in several cell systems including bone marrow progenitor cells derived from rabbit [148] and humans [148, 186, 209] as well as monolayer expansion of primary mammalian chondrocytes [186, 210, 211]. In agreement with these studies, we observed that FGF-2 treatment of rat BMSCs during expansion increased their rate of proliferation. Additionally, FGF-2 expansion to P2 stimulated increased subsequent sGAG production in alginate culture but did not have a significant effect on cells passaged to P4. The interaction of FGF-2 and TGF-β1 in our system also corresponds with the previously reported response of rabbit and human BMSCs to chondrogenic factors. The authors found that through multiple passages, cell expansion in the presence of FGF-2 resulted in greater sGAG accumulation in pellets treated with TGF-β1 [148]. In contrast, we found that the beneficial effects of FGF-2 on proliferation and sGAG accumulation of rat BMSCs decreased rapidly with passage number.

The mechanism through which FGF-2 enhances differentiation of BMSCs is not yet known. Hanada *et al*. hypothesized that FGF-2 increased the number of cells responsive to biochemical stimuli including Dex [159]. Martin *et al.* demonstrated that during monolayer expansion, bovine articular chondrocytes exposed to FGF-2 maintained

a spread morphology due to the disassembly of actin filaments. These cells more readily recovered the chondrocytic phenotype compared to cells that did not receive FGF treatment [192]. In our study, rat BMSCs treated with FGF-2 also exhibited a more spread morphology than those that were not cultured in the presence of FGF-2. This observation suggests that actin fiber arrangement within these cells prior to placement in a chondrogenic environment may have a role in rat BMSC chondrogenesis similar to primary articular cartilage chondrocytes.

In both alginate and agarose, 10nM Dex resulted in the highest accumulation of a cartilaginous matrix. These results are consistent with previous studies that demonstrate that Dex is either required for chondrogenesis or enhances matrix accumulation of cartilaginous proteins. Grigoriadis *et al*. found that stem cells derived from rat calvaria required Dex treatment to undergo chondrogenesis and that cell clustering and matrix accumulation were dose dependent [190]. Derfoul *et al.* found that Dex treatment of human BMSCs upregulated sGAG production as well as increased the gene expression of aggrecan, dermatopontin, and collagen type XI. The authors also reported that Dex enhanced TGF-beta-mediated upregulation of collagen type II and cartilage oligomeric matrix protein [189]. However, we also found that Dex resulted in a 20% decrease in cell viability in agarose cultures but not alginate cultures. This scaffold dependence may again be due to differences in the diffusion of Dex through alginate compared to agarose or specific interactions of Dex with the hydrogels that is yet unknown.

The precise mechanism through which Dex reduced cell viability has not been elucidated, but it has been shown to have a role in the regulation of chondrocyte phenotype and maturation in the growth plate [212], possibly through manipulation of the

IGF-I pathway [7, 108]. Work by Chrysis *et al*. using a human chondrocytic cell line demonstrated that Dex treatment *in vitro* increased the rate of apoptosis and that treatment with IGF-I abrogated this effect [213]. Our results also indicate that growth factor treatment, in our case FGF-2 and TGF-β1, may lessen the effects of Dex-induced cell death in alginate culture, but has no effect on reducing cell death in agarose.

Conclusions

This study demonstrates that TGF-β1 induced chondrogenic differentiation of rat BMSCs can be achieved in 3D hydrogel systems. This response is cell passage dependent and expansion in the presence of FGF-2 enhances cartilaginous matrix accumulation within 2% alginate over time whereas FGF-2 pretreatment decreases matrix accumulation by BMSCs in 2% agarose. Furthermore, Dex treatment is required for maximal matrix deposition but can reduce cell viability in agarose.

CHAPTER 5

DELIVERY OF CHONDROGENIC STROMAL CELLS IN AN INJECTABLE HYDROGEL FOR THE REPAIR OF GROWTH PLATE DEFECTS IN A SMALL ANIMAL MODEL

Introduction

The incidence of fractures in children have become more prevalent in recent years and, therefore, so has growth plate injuries [13]. Due to the variability of treatment options, growth disturbances caused by damage to physeal tissue still remains an issue in the orthopaedic field [1, 13, 56, 214-216]. This challenge has inspired the development of several animal models to investigate treatment strategies with a focus on the application of cartilage tissue engineering strategies to reform the damaged region of the growth plate and restore growth function. These include the insertion of articular chondrocytes, growth plate chondrocytes, and stem cells [48, 49, 51, 52, 124]. In Specific Aim I, we showed that the delivery of an *in situ* gelling agarose to a centralized growth plate defect in a rat animal model decreased limb length discrepancies, but did not fully restore function to the injured area. These results indicate that additional biological components are needed to fully restore growth function.

Previous studies in animal models have demonstrated reformation of a growth plate tissue within the defect region when stem cells are introduced into a defect. A scaffold is required for the full effect. Comparison of adipose, ???, and BMSCs showed BMSCs are the best for cartilage fixing. Histology and radiography at est for analysis. We therefore wanted to quantitatively evaluate the healing of growth plate defects using

the model and techniques developed in SA I to determine the differentiation based effects of introducing stem cells with in the defect.

In Specific Aim II, we demonstrated that chondrogenesis of female Sprague Dawley rat BMSCs is dependent on cell passage, hydrogel culture environment, and growth factor regimen [217]. However, due to noted sex-specific response of progenitor cells to differentiation protocols *in vitro* and *in vivo* [218], we chose to use male cells for implantation into the growth plate defect animal model. We have demonstrated that male rat BMSCs are also capable of chondrogenesis differentiation using the optimal conditions found in Specific Aim II (**Appendix C**). Studies in our laboratory have also demonstrated sex-based differences in the response of male rat BMSCs to alginate culture. These studies demonstrate that, although these cells do undergo chondrogenesis when encapsulated in alginate, their viability decreases rapidly in this system (see **Appendix D**).

Recently, interest has developed in applying a multi-step approach to chondrogenic pre-differentiation of bone marrow derived stem cells (BMSCs) [156, 219]. Worster *et al*. found that equine BMSCs first stimulated with TGF-β1 in high density monolayer and then seeded in fibrin discs continued to accumulate sulfated glycosaminoglycans (sGAGs) once placed in hydrogel culture and that additional IGF-I stimulation in 3D culture enhanced matrix production [3]. Using human BMSCs, Matsuda *et al*. found that a cocktail of TGF-β3, IGF-I, and dexamethasone stimulate higher levels of aggrecan mRNA than cells seeded in 3D gel/polymer amalgams and that chondrogenic pre-differentiation of cells in 2D prior to seeding in 3D enhanced overall collagen II and aggrecan mRNA expression [220]. These studies demonstrate not only

that BMSCs undergo chondrogenesis in high density monolayer, but also that the chondrogenic phenotype is maintained after transfer to 3D culture and that pre-differentiation in monolayer increased expression of chondrogenic markers and matrix accumulation over 3D culture alone.

The overall objective of this specific aim was to deliver BMSCs pre-differentiated to the chondrogenic phenotype to centralized growth plate defects in the distal femur of Sprague Dawley rats for the correction of a growth disturbance. The first aim of this study was to develop a method to initiate chondrogenic differentiation of male rat BMSCs that could then be seeded into a gel system for injection into cartilaginous defects. We hypothesized that stem cells stimulated to undergo chondrogenesis in high density monolayer would retain their chondrogenic phenotype after transfer into an injectable *in situ* gelling agarose *in vitro*. The second aim was to deliver these cells to a growth plate defect via agarose injection. Using the techniques and animal model developed in Specific Aim I, we quantitatively examined changes in growth plate and whole bone morphology in response to delivery of agarose and BMSCs. We hypothesized that the degree of healing of the defect will depend on the differentiation state of the implanted cells.

Materials and Methods

In vitro chondrogenesis of rat BMSCs in high density monolayer

Cell isolation

Bone marrow stromal cells were retrieved using a technique previously described [193]. Briefly, six male 45-day old Sprague Dawley (Charles Rivers Laboratory, Wilmington, MA) rats were euthanized by CO_2 asphyxiation and their femurs and tibiae removed under IACUC approved guidelines. Bone marrow was flushed from diaphyses with α-MEM supplemented with 1% antibiotic/antimycotic (100 U penicillin G, 100 μg streptomycin sulfate, 0.025 μg amphotericin B/ml; Invitrogen Carlsbad, CA) and a selected lot of fetal bovine serum (FBS; Hyclone, Logan, UT) using a 20 gauge needle attached to a 10 ml syringe. The cell suspension was centrifuged at 1,200 RPM for 20 minutes, resuspended in media, and plated at one leg/100 mm dish (Corning, Corning NY) for 30 minutes. Unattached cells were collected, replated in 150 cm^2 T-flasks at a density of $150x10^6$ cells/flask, and covered with 35ml of media. Media was changed after four days to remove non-adherent cells. The cells grew in circular patches that became confluent after eight days, which were termed primary confluence (P0). The cells were then lifted from the surface using 0.05% trypsin/0.53mM EDTA (Invitrogen Carlsbad, CA) and frozen until the experiment was performed.

In Specific Aim II, we demonstrated that female rat BMSC chondrogenesis was passage dependent. Male cells exhibited a similar dependence in the chondrogenic environment. Preliminary studies demonstrated that male cells expanded to P2 rapidly

die once placed in a chondrogenic environment whereas P1 cells remain viable. Therefore, all experiments in this specific aim were performed using P1 cells. For the final expansion, cells were plated at a density of $6.67x10^3$ cells/cm^2 in either 185 cm^2 T-flasks for hydrogel seeding or 6 well plates (35mm dish) for a time-course analysis of chondrogenesis in monolayer. During this expansion, the passaging media was supplemented with 1ng/ml FGF-2 (R & D Systems Minneapolis, MN).

Monolayer chondrogenesis

At confluence (P1), cells were switched to a basal chondrogenesis medium (high glucose DMEM with 1% antibiotic/antimycotic, 0.1 mM non-essential amino acids (Invitrogen Carlsbad, CA), and 50 μg/ml ascorbic acid-2-phosphate (AA-2P; Sigma, St. Louis, MO) supplemented with 2% FBS and either 10ng/ml TGF-β1 or 1ng/ml FGF-2. Samples were given 1.5ml media everyday. Media samples and cells were taken on days 0, 1, 2, 3, and 5 for sGAG and gene expression respectively.

Hydrogel culture

A solution of 1% SeaKem Agarose (Fisher Scientific) was prepared by mixing the agarose powder with calcium and magnesium free phosphate buffered saline (PBS). The mixture were autoclaved for 20 minutes to dissolve the powder and sterilize the solution.

Three-dimensional constructs were produced with either P1 cells released from monolayer culture with trypsin or cells that were stimulated in high density monolayer with TGF-β1 for 2 days. To isolate pre-differentiated cells, 185 cm^2 T-flasks were treated with a cocktail of 0.3% dispase and 0.2% collagenase (Invitrogen) made up in α-MEM.

Flasks were agitated at 37°C for 30 minutes to release the cells. Cells were then passed through a 70μm filter and the solution diluted with 3 volumes of α-MEM containing 10% FBS. The cells were collected by spinning at 1200 RPM for 7 minutes, resuspended in PBS, and counted on a hemacytometer. The cells were then resuspended in PBS at a density of $40x10^6$ cells/ml.

Cylindrical gels containing either undifferentiated P1 cells or TGF-β1-treated cells were cast as previously reported [217]. Briefly, cells in PBS were combined 1:1 with 1% SeaKem® agarose for a final cell density of $20x10^6$ cells/ml in 0.5% SeaKem® agarose. The gel plus cell solutions were pipetted into a well of a custom designed mold and allowed to polymerize for 30 minutes at room temperature. The resulting gels measured 4 mm in diameter and were 2 mm thick. Gels were rinsed in high glucose DMEM (DMEM-HG) supplemented with 1% antibiotic/antimycotic after polymerization. The constructs were then placed into basal chondrogenesis medium with the following supplements: (A) 10% FBS, (B) 1% ITS+ (BD Biosciences, Bedford, MA), or (C) 1% ITS+ and 10ng/ml TGF-β1. Gels were covered with 1 ml of media and cultured in a humidified atmosphere of 5% CO_2 at 37°C. Media was changed every 2-3 days for the duration of the experiments. TGF-β1 was added fresh at every media change.

sGAG in the Media

sGAG release into the culture media was measured using the DMMB dye assay developed by Farndale *et al.* [34]. Media samples (1ml) were lyophilized overnight and resuspended in 200μl water. sGAG content was compared to standards containing known amounts of chondroitin sulfate.

Cell Viability

For monolayer cultures, cells from 35mm wells were trypsinized, resuspended in 3ml media, and counted using trypan blue exclusion. Cell viability within agarose constructs were determined using the Live/Dead Assay (Molecular Probes). The protocol was adapted from recommendations provided by the manufacturer. Briefly, samples were incubated in a solution containing 4 mM ethidium bromide and 4 mM calcein for 45 minutes. After rinsing in PBS, gels were imaged on a Zeiss LSM 510 confocal microscope.

Histology

Agarose construct were taken down on days 7, 14, and 21 for histological analysis. Samples were fixed in 10% neutral buffered formalin at 4°C for 1 week and stored in 70% ethanol at 4°C until histologic processing. Four micron sections were taken of paraffin embedded samples through the cross-section and stained with safrinin-O (Saf-O).

RNA Isolation and Quantitative RT-PCR

Cells in monolayer culture were rinsed with PBS and then covered with 350μl RLT buffer (Qiagen) containing 1% β-mercaptoethanol. The cells were then scraped from 35mm dishes and disrupted by passing through a Qiashredder according to the manufacturer's protocol (Qiagen). RNA was isolated using RNeasy spin columns according to the manufacturer's protocol. One microgram of DNase-treated RNA was

converted to cDNA using the Promega Reverse Transcriptase kit (Promega). Samples were probed for aggrecan, collagen type II, Sox9, and collagen type I using SYBR Green dye on a ABI PRISM 7700 system (Applied Biosystems) using the sequences listed in **Table 5.2.**

Table 5.2. Quantitative PCR Primers

Collagen Type II forward	CTC AAG TCG CTG AAC AAC C
Collagen Type II reverse	CTA TGT CCA CAC CAA ATT CC
Collagen Type I forward	ATG TTC AGC TTT GTG GAC
Collagen Type I reverse	GGA TGC CAT CTT GTC CAG
Aggrecan forward	AGG ATG GCT TCC ACC AGT GC
Aggrecan reverse	TGC GTA AAA GAC CTC ACC CTC C
Sox9 forward	ACT TCC GCG ACG TGG ACA TC
Sox9 reverse	TGT AGG TGA CCT GGC CGT G

Growth plate defect animal model

Surgical Procedure

All procedures were performed under Georgia Institute of Technology IACUC approved guidelines. Sprague Dawley male rats (body weight 100-125 grams, approximately 5 weeks old) (Charles Rivers Laboratory, Wilmington, MA) were used in all studies. Animals were anesthetized using 5% isoflurane and prophylactic antibiotics were administered by subcutaneous injection. The skin over both knees sterilely prepared and draped, providing a sterile surgical field. A 2 cm midline incision was made on the anterior aspect of the right knee joint and a medial parapatellar arthrotomy performed. The patella was dislocated laterally to expose the trochlear groove of the distal femur.

Using a hand drill, a central defect was created across the physes of the distal femur by drilling through the articular cartilage between the condyles, normal to the cross-sectional plane of the bone shaft, and then further up the intramedullary canal. The depth of drilling into the metaphyses was controlled with a mechanical stop so that the defect did not enter the marrow cavity. The defect was made 2mm deeper than in Specific Aim I so that the Gelfoam® inserted would be below the growth plate (see below). The defect was then irrigated with a sterile saline solution and treated as outlined below. The patella was relocated to its original position and the medial joint capsule was closed with 4-0 vicryl suture. The skin was closed using wound clips and the surgical area was washed with hydrogen peroxide. The wound clips were removed 10-14 days post surgery. The left leg was left unoperated and used as the control for all analyses. Animals were euthanized by CO_2 asphixiation on day 56 (n=4 per group) post surgery.

Gelfoam® (Henry Schein) was inserted into each defect after rinsing with saline to stop blood infusion into the defect (see **Appendix E** for the effects of Gelfoam® insertion into growth plate defects). The defect was then packed with gauze. After 20 minutes, the gauze was removed and the site was checked for bleeding. The defects were then either left empty, filled with 0.5% agarose, filled with 0.5% agarose containing BMSCs pre-differentiated with TGF-β1, or filled with 0.5% agarose containing P1 BMSCs. All cells were suspended at a density of $20x10^6$ cells/ml.

Microcomputed Tomography

The epiphyseal region of the defect legs were scanned at a 20 μm voxel size on a VivaCT 40 system (Scanco Medical, Bassersdorf, Switzerland). The volume of bone

infiltration into the defect (bone bridge formation) was measured by isolating a 2 mm x 15 slice (0.32 mm) cylindrical region within the original defect contained entirely within the growth plate as shown in **Figure 5.1A**. This parameter was termed the defect bone volume fraction (Defect BVF). To quantify the effect of the defect on growth, whole femurs from the defect and contralateral control legs were scanned at a voxel size of 36 μm and the lengths of the whole bone and diaphysis of each femur were measured from the rendered 3D images. The diaphyseal length was defined as the distance from the lesser trochanter to the metaphyseal plate and the total length was defined as the distance from the greater trochanter to the edge of the femoral condyles (**Figure 5.1B**). Finally, the growth plate was isolated from the surrounding bone tissue in the micro-CT images by manual contouring of 2D slices of sagittal images. The contoured regions were compiled to render 3D images (**Figure 5.1C**). From these images, total growth plate volume was calculated and thickness maps generated. Thickness measurements were obtained by expanding spheres at distinct voxels within the 3D volume. Total volume was determined by counting the number of voxels within the contoured region and multiplying the value by the voxel volume. To determine the effect of the defect on the natural course of growth plate closure in Sprague Dawley rats, the volume of mineralized tethers within the growth plate tissue but excluding the bone bridge with in the defect was quantified.

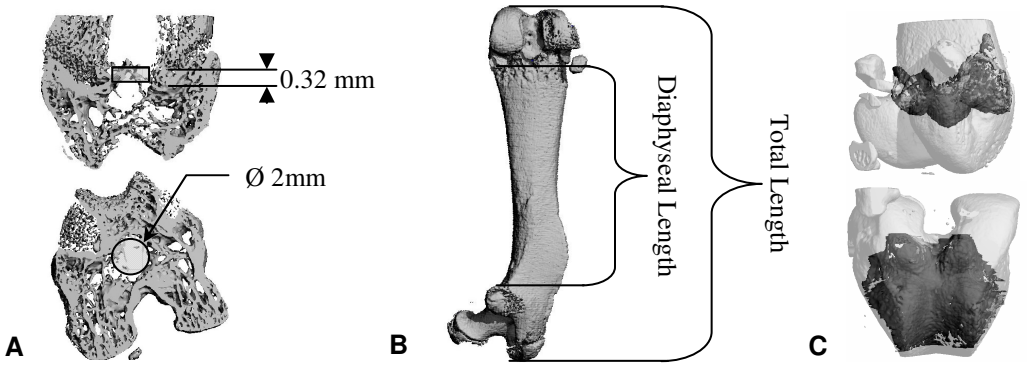

Figure 5.1. Micro-CT Analysis.

Images demonstrating (A) the method of determining the mineral content within the original defect. A controlled volume was used for each sample. (B) The diaphyseal and overall lengths of the contralateral and defect bones. (C) The location, position and morphology of the epiphyseal growth plate within the distal end of the femur. Note the four ridges that are located along the edges of the femoral-patellar groove.

Statistical Analysis

The effects of culture conditions on group means were assessed using the analysis of variance (ANOVA) general linear model. Statistical significance ($p<0.05$) between individual group samples was determined using the Tukey *post hoc* test for multiple comparisons. All graphs represent the mean ± SEM unless otherwise noted.

Results

TGF-β1 stimulates chondrogenesis in BMSCs in monolayer culture

Cells treated with TGF-β1 detached from the plates after 2 days and remained a floating monolayer until day 5. Due to this phenomenon, cell numbers could not be ascertained at day 5. BMSCs in high density monolayer showed very little proliferation after switching to chondrogenesis media in both FGF-2 and TGF-β1 treated samples over

the culture period. The decrease in cell numbers after day 1 was due to the inability of trypsin to adequately release the cells from the high density monolayer. The viability of the isolated cells remained high in both FGF-2 and TGF-β1 treated samples whether cells were released with trypsin or dispase and collagenase (**Figure 5.2**). sGAG released into the media was higher in TGF-β1 cultures until after day 2 (**Figure 5.3**). BMSCs treated with TGF-β1 also had significantly higher expression of aggrecan mRNA by day 1 and collagen type II by day 2. There was no significant expression of Sox9 or collagen type I until day 5 (**Figure 5.4**).

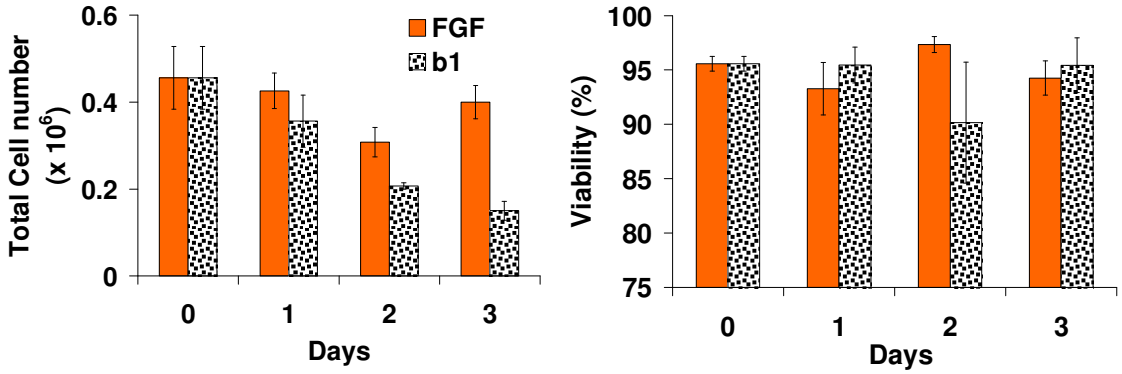

Figure 5.2. Total cell number and viability of cells in monolayer culture. Cells were trypsinized from 35mm plates and cell number and viability were determined by trypan blue exclusion (n=6).

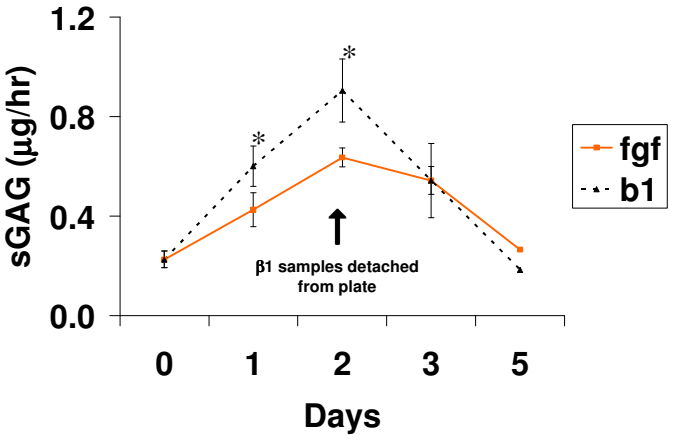

Figure 5.3. sGAG released into the media
* indicates difference from FGF treatment (n=6)

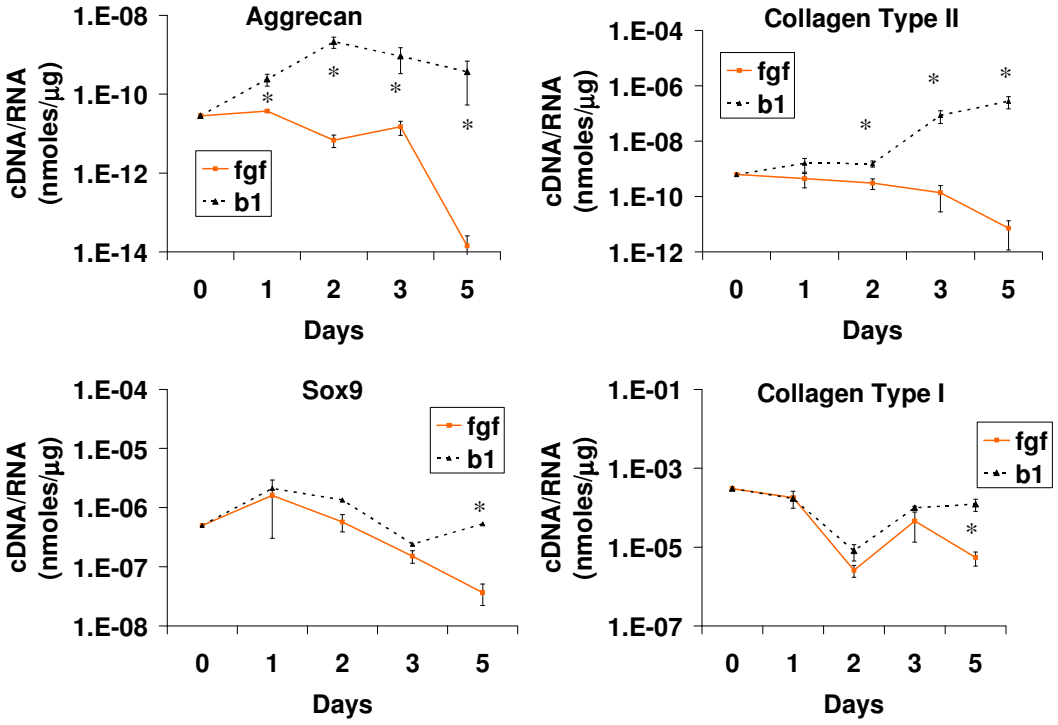

Figure 5.4. Time-course of mRNA expression of male BMSCs in alginate gels
* indicates difference from FGF treatment (n=8)

Cells released from day 2 TGF-β1 monolayer culture and P1 cells were seeded in agarose to determine if pre-differentiation of cells in monolayer culture influenced matrix accumulation in 3D. After 21 days of culture in agarose, very little matrix was produced by pre-differentiated BMSCs in serum, ITS, or with continued TGF-β1 stimulation. Light Saf-O was seen only in P1 BMSCs treated with TGF-β1 for 21 days in agarose culture (**Figure 5.5**).

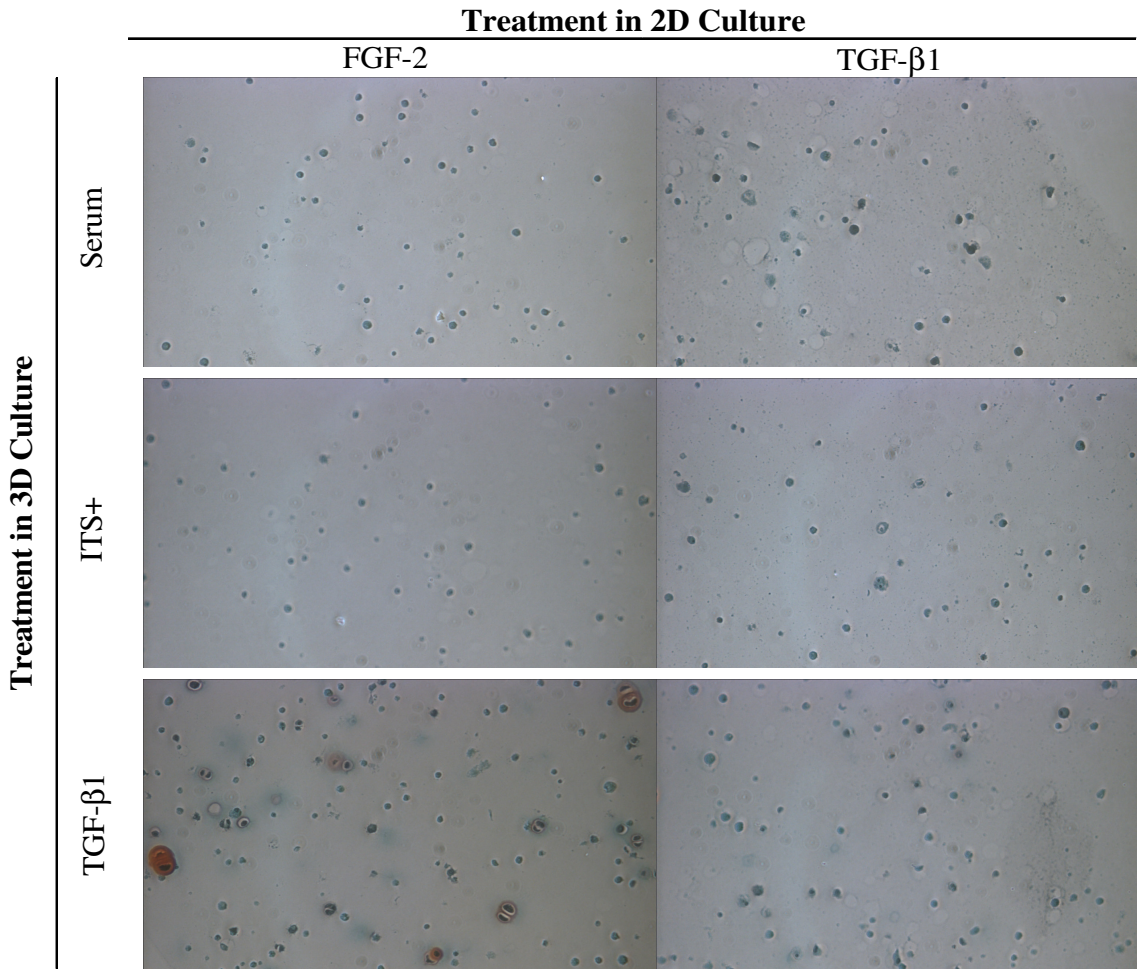

Figure 5.5. Safrinin-O staining of day 21 agarose embedded BMSCs.

P1 and cells pretreated in monolayer (2D culture) with TGF-β1 for 2 days (top) were embedded in agarose and further cultured in 10% FBS, ITS, or ITS + TGF-β1 for 21 days (side). Original magnification = 20x.

BMSCs effect growth plate healing in a differentiation dependent manner

To determine the effect of BMSC differentiation state on the healing of growth plate defects, P1 or pre-chondrogenic cells were suspended in 0.5% SeaKem® agarose (AGA+Undiff and AGA+B1, respectively) and delivered into the defect. These were compared to defects left empty or filled with agarose alone (AGA).

After 56 days post surgery, there were no differences in the volume fraction of the bone bridge formed within the defect in any of the treatment groups (**Figure 5.6**). The tether BVF of the defect growth plates in the empty and agarose alone groups was higher than their respective contralateral controls. Defects that received cells in addition to agarose showed no increase in tether formation over their contralateral controls (**Figure 5.7**). The volume fraction of tethers of the empty groups was greater than all of the agarose treated defect samples. The agarose group had a higher tether BVF than the agarose + undifferentiated cells group, but not the agarose + β1 treated cells group. All groups had a thinner defect growth plate than their contralateral controls, but there was no effect of injection of agarose or agarose and cells on this parameter (**Figure 5.8**). In all cases, the defect legs were shorter than their contralateral control leg. However, the defect limbs of the agarose alone group and the agarose + undifferentiated cell group were longer than their empty counterparts (**Figure 5.9**).

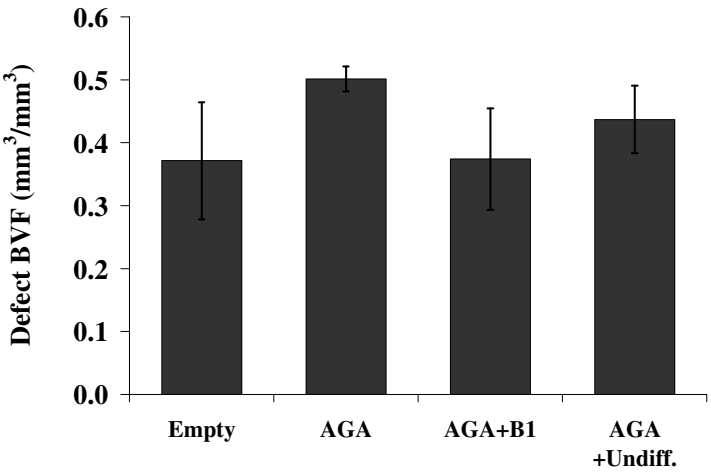

Figure 5.6. Bone volume fraction of bone bridge formation 56 days post surgery.

n=4

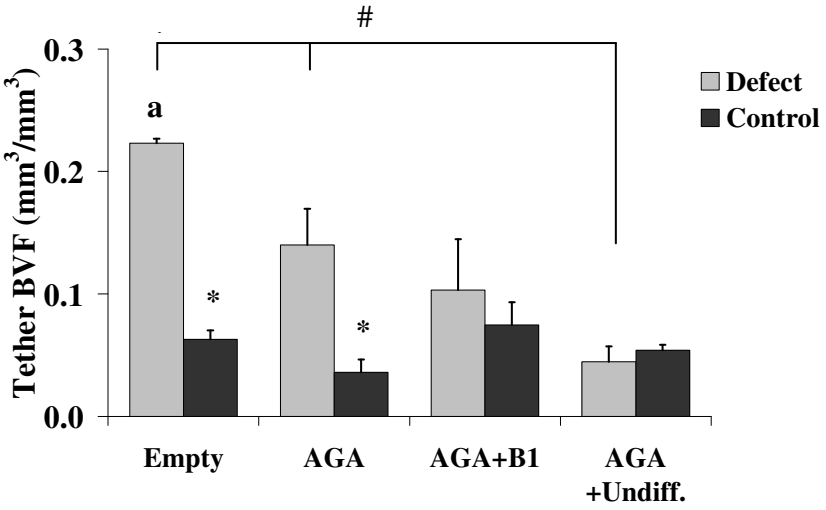

Figure 5.7. BVF of tethers throughout the growth plate.

* indicates difference from defect leg; # indicates difference from the AGA + Undiff group; **a** indicates difference from all other groups; n=4.

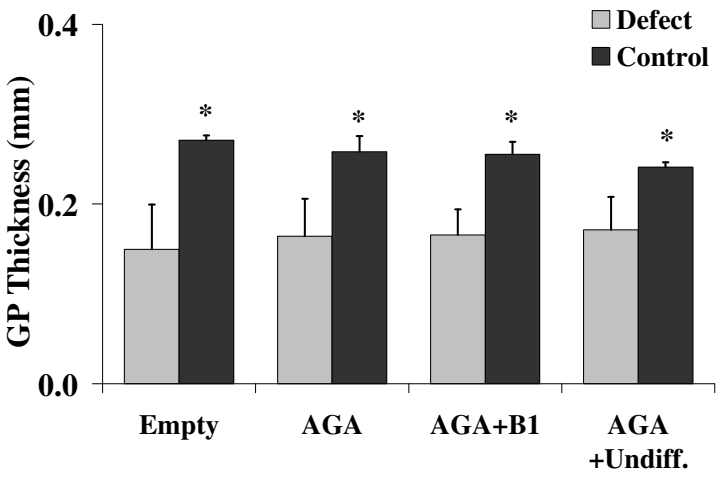

Figure 5.8. Average growth plate thickness.

* indicates difference from defect leg; n=4

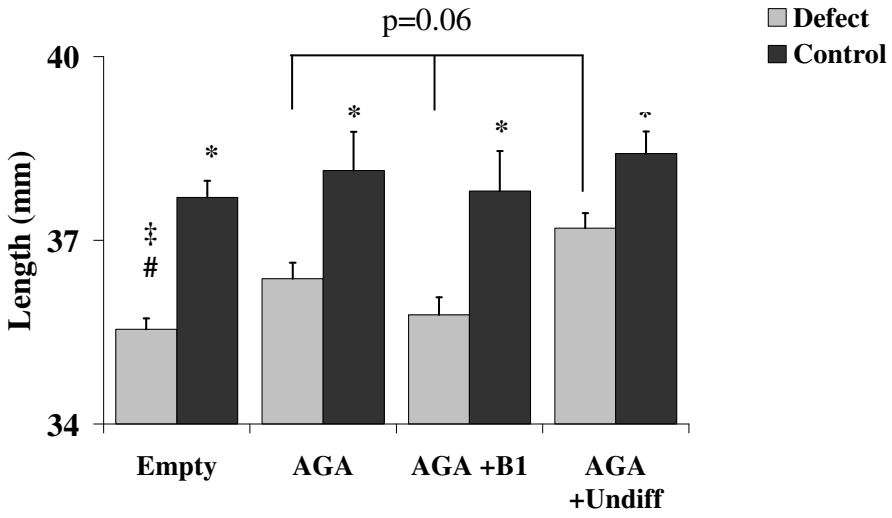

Figure 5.9. Total length of defect and control legs.

* indicates difference from defect leg; ‡ indicates difference from AGA group; # indicates difference from the AGA + Undiff group; n=4.

Discussion

In this specific aim we have shown that male rat BMSCs express the chondrogenic genotype and phenotype in high density monolayer with TGF-β1 stimulation. However, when these cells were placed in 3D agarose culture, they failed to produce a cartilaginous matrix even with continued TGF-β1 stimulation for 21 days. When 0.5% agarose with or without a cellular component was implanted into growth plate defects, there was no reduction of bone bridge formation within the defect or restoration of growth plate thickness. We also saw that there was no dependence of tether formation on the differentiation state of the implanted cells. However, a differentiation dependent response in length discrepancy was observed. Injection of undifferentiated BMSCs into growth plate defects resulted in a reduction of limb discrepancy over empty defects and we showed a trend indicating that implantation of these cells improved whole limb lengths over implantation of agarose alone or BMSCs pre-differentiated in high density monolayer culture prior to insertion *in vivo*.

The observed dependence of limb length discrepancy on BMSC differentiation state is likely related to the observed behavior of these cells in 3D culture *in vitro*. Although delivery of pre-differentiated BMSCs into this defect model inhibited tether formation to control levels within the growth plate, the treatment did not restore growth function to the injured limb. This is probably due to the inability of these cells to secrete a cartilaginous matrix once placed in agarose and further cultured *in vitro*. The same response may have occurred in agarose *in vivo*, thereby preventing the cells from reforming a functional growth plate and correcting limb growth. Interestingly,

implantation of undifferentiated BMSCs reduced limb length discrepancy compared to samples of empty defects (45% reduction) but not over limbs with defects filled with agarose alone (30% reduction compared to empty defects). Additionally, the resultant reduction in limb discrepancy due to implantation of undifferentiated cells is 40% more than that groups receiving pre-differentiated cells. Unlike pre-differentiated cells, undifferentiated cells demonstrated accumulation of some cartilaginous matrix after encapsulation in agarose and TGF-β1 stimulation for 21 days. *In vivo* chondrogenesis of these cells may have allowed them to achieve some reformation of growth plate-like tissue, which contributed to some restoration of growth function. Histological analysis of these samples is needed to further characterize the behavior of undifferentiated and pre-chondrogenic cells *in vivo*.

The transfer of BMSCs into growth plate defects did inhibit excess tether formation in this model, but unlike undifferentiated cells, pre-differentiated cells did not correct limb length discrepancies. In fact, the length of limbs treated with pre-differentiated BMSCs was less than those treated with agarose alone. In Specific Aim I, we found that increased tether formation was highly correlated with limb length discrepancy. The disconnection between these parameters may be due to the secretion of specific paracrine factors by the injected BMSCs. It has been noted that the differentiation state of various cell types will determine their response to growth factors *in vitro* [166]. It is possible that the response to autocrine and paracrine signaling between the native tissue and the implant was uniquely different for each cell type. This may have resulted in normal tether formation in both cases, but this did not lead to restored growth. The process of tether formation has not been well recognized in the

literature. Martin *et al*. used micro-CT imaging to measure the number and volume of tethers during normal growth of Sprague Dawley rats [166]. Tether formation has also been noted in the normal closure dynamics of dog, porcine, and human histological sections [167, 221]. Despite these studies, the biomolecular mechanisms through which tethers form or the change in tether formation due to injury has not been investigated. Studies examining the process of tether formation and cross-talk between the implant and native tissue is required to elucidate the relationship between tether formation and limb growth.

A number of aspects may have contributed to the lack of *in vitro* matrix production of chondrogenic BMSCs seeded into agarose gels including the passage point and culture conditions. Previously, we showed that chondrogenic differentiation of female rat BMSCs is passage dependant [217] and the passage dependence of BMSC differentiation has been previously reported in other species [148]. We have also have evidence that the chondrogenic differentiation potential of male and female cells is dissimilar (see **Appendix C**). Sex-based disparities in the osteochondral differentiation of muscle derived progenitor cells has also been noted [218]. Passage 1, male BMSCs expanded in the presence of FGF-2 were chosen for this study due to their ability to maintain high viability in agarose culture *in vitro* (see **Appendix D**). However, like female cells, there is likely an optimal point in male BMSC expansion for favorable chondrogenic matrix production. The cells remained viable throughout the *in vitro* culture period (data not shown), so it is unlikely that cell death is the cause of the lack of matrix secretion. Further optimization of the regimen of growth factor and/or steroid stimulation for monolayer expansion and 3D culture is required. Additional study is also

required to optimize retrieval of the cells once chondrogenesis is achieved as the dispase/collagenase digestion of the chondrogenic cell layer may have also contributed to the inability of these cells to secrete a cartilaginous matrix.

In this study, we have demonstrated a that delivery of BMSCs in agarose into centralized growth plate defects occurs in a manner dependent on the differentiation state of the cells. Undifferentiated BMSCs reduced limb length discrepancies whereas the BMSCs pre-differentiated to chondrogenesis using TGF-β1 did not. However, none of the treatment groups fully corrected limb length discrepancy. Recent studies have found that stem cells isolated from various tissues can contribute to growth plate healing *in vivo* [51, 52]. Similar to our study, Hui *et al*. demonstrated that BMSCs decreased limb length discrepancy, but did not completely restore function [51]. Chen *et al*. found that periosteal derived MSCs delivered in agarose generated a new growth plate and completely corrected angular deformity [52]. However, this was in a rabbit model where excision of the lateral portion of the defect was removed and little limb length discrepancy was seen [52]. Based on these studies and the results presented here, further work is needed to characterize not only the chondrogenic potential of MSCs from various sources, but also to determine the response of MSCs to the physiological factors that regulate growth plate chondrocytes.

Conclusions

In this specific aim, we have demonstrated that the potential for BMSCs to reduce limb length discrepancy due to a centralized defect through the growth plate of the distal

femur is dependent on the differentiation state of the cells. Specifically, delivery of pre-chondrogenic BMSCs did not restore growth function compared to empty defects. Trends indicate that delivery of undifferentiated cells reduced limb length discrepancy over pre-chondrogenic cells and agarose alone. Inclusion cells in the implant did reduce tether formation to control levels. However, this parameter did not correlate with limb length discrepancy. This result suggests that injection of cells restored the natural process of growth plate closure in rats. It also indicates that increased tether formation may be a by-product of growth plate injury and not associated with disruption of the growth potential of the tissue. Therefore, treatments that affect tether formation within the growth plate may not restore growth function.

CHAPTER 6

CONCLUSIONS AND FUTURE RECOMMENDATIONS

Conclusions

As delineated in previous chapters, growth plate injury may result in the formation of a bone bridge in the defect region that connects the epiphyseal and metaphyseal bone. This damage can result in a limb length discrepancy or angular deformity that may lead to life long disability. Patient reviews and animal models have demonstrated that current treatment methodologies, including fat interposition and whole physeal transfer, have limited success rates. These studies also illustrate that current imaging modalities to correctly diagnose these injuries in the clinical setting are lacking accuracy. Based on these findings, there is a need for a more effective treatment method for growth plate injuries. First, however, it is essential to define the relationship between injury to the growth plate, changes in growth plate morphology, and loss of growth potential. Therefore, the overall *objective* of this dissertation was to demonstrate the utility of microcomputed tomography (micro-CT) to *quantitatively* assess the changes in growth plate and whole bone morphology due to growth plate injury and to assess tissue engineering strategies to restore growth function in injured limbs. To accomplish this goal, a surgical model of a centralized growth plate defect was established in the distal femur of adolescent Sprague Dawley rats. Methods were developed using the micro-CT to *quantitatively* measure the volume fraction of the bone bridge within the defect, alterations in natural physeal growth dynamics (growth plate thickness, volume, and

closure dynamics through tether formation) and limb length discrepancy (whole bone and diaphyseal lengths). In parallel, the *in vitro* effects of monolayer expansion, culture environment, and growth factor regimen on bone marrow derived stem cell (BMSC) chondrogenesis were examined to develop a tissue engineering construct for treatment of growth plate defects. Finally, the animal model was used to assess the effectiveness of an *in situ* gelling agarose, with and without a cellular component, to restore natural growth plate morphology and growth function to the injured limb. Specifically, we examined the effect of the differentiation state of implanted BMSCs on the healing of these defects.

Due to several observations made during the course of this dissertation and recently in the literature, several changes had to be made to the study design before we could test the differentiation based effects of stem cell delivery into growth plate defects. In Specific Aim II, we demonstrated that TGF-β1 induced chondrogenic differentiation of female rat BMSCs in 3D hydrogel systems. This response was dependent on passage number, hydrogel scaffold choice, and growth factor regimen. Passage two (P2) cells accumulated more cartilaginous matrix in a chondrogenic environment than earlier passages. Expansion of BMSCs in the presence of FGF-2 enhanced cartilaginous matrix accumulation within 2% alginate over time whereas FGF-2 pre-treatment decreased matrix accumulation by these cells when encapsulated in 2% agarose. However, recent studies have show that the differentiation behavior of stem cells is also dependent on the sex of the animal from which the cells were derived and the sex of the animal in which they are implanted [218]. Therefore, the chondrogenesis of *male* cells was examined for implantation into our *male* animal model. The viability of male cells was also dependent on passage number and growth factor regimen. Passage 1 (P1) cells exhibited higher

viability in hydrogel culture compared to P2 cells and with FGF-2 treatment during expansion. However, after chondrogenic differentiation in hydrogel culture, only 20% of the cells retrieved for implantation were viable. Therefore, in the final study, a high density monolayer system was developed to achieve chondrogenesis of male cells. Ninety-five percent of pre-differentiated cells retrieved from this culture system remained viable. These cells were suspended in agarose for implantation into growth plate defects or continued culture *in vitro*.

In the course of developing our tissue engineered treatment strategy for growth plate injury, we observed that 1% SeaKem® agarose polymerized before a homogenous cell/hydrogel solution could be obtained and injected into defects. Therefore, cells were delivered to growth plate defects via a 0.5% agarose solution. We also observed that back pressure and bleeding within the defects inhibited adequate delivery of the *in situ* gelling agarose, limiting the effectiveness of this solution in conforming to the shape of the defect. In order to reduce bleeding and pressure, Gelfoam®, an antifibrolytic sponge used clinically to control bleeding within deep wounds, was inserted into the defect prior to injection of agarose.

The results of this dissertation indicate that prevention of bone bridge formation within a growth plate defect was not as significant as previously thought in preventing limb length reduction in response to growth plate injury. Only recently have stem cells been used to treat growth plate defects in an effort to reform a functional growth plate. The majority of the work in this field has focused on the implantation of a filler material to prevent bone bridge formation. In this work, bone bridge formation was not a significant predictor of defect healing as no correlations to changes in growth plate or

whole bone morphological parameters were found. Treatment of defects with 1% agarose reduced the limb discrepancy although it did not reduce the volume fraction of the bone bridge formation. These results indicate that blocking bone bridge formation may not be significant in restoring growth function to injured growth plates. These results may also explain the high variability (15-38%) of the Langenskiöld procedure in the clinical setting. Reformation of the growth plate has not been reported with use of this procedure – only whether or not the bone bridge has reformed.

Understanding the relationship between the parameters of growth plate morphology and final limb length will aid in developing treatment strategies. In this dissertation we examined the relationship between growth plate and whole bone morphological parameters in healthy and injured growth plates. A time-course study of our growth plate injury model demonstrated that a centralized defect caused significant stunting of the injured limb's growth up to 112 days post surgery. The percent reduction in limb length was found to be positively correlated to percent reduction in growth plate thickness (R^2=0.88), percent increase in tether bone volume fraction (R^2=0.78), and percent reduction in growth plate volume (R^2=0.61). These findings demonstrate that a centralized defect model in Sprague Dawley rats replicates limb length discrepancies of human growth plate injury in the distal femur and that limb length discrepancy is associated with changes in growth plate morphology.

Healing of growth plate injury was shown to be dependent on the density of *in situ* gelling agarose injected into the defect. At 56 days post surgery, injection of a 1% agarose solution into the defect resulted in a 50% decrease in limb length discrepancy compared to defects left empty. Growth plate thickness was also increased by 10% with

this treatment. However implantation of a lower density agarose (0.5%) solution only resulted in a 20% reduction in limb length discrepancy and had no effect on growth plate thickness. These results further support the correlation found between growth plate thickness and length discrepancy and indicate that 1% SeaKem® agarose contributed to the restoration of limb growth, probably through providing some support for normal function of the remaining growth plate tissue.

Correction of limb length discrepancy occurs in a manner dependent on the differentiation state of implanted BMSCs. Inclusion of cells in the implant reduced tether formation to the level of their contralateral controls irrespective of cell differentiation state. However, this parameter did not correlate with reduction of limb length discrepancy. Delivery of pre-chondrogenic BMSCs did not restore growth function compared to empty defects. Trends indicate that the delivery of undifferentiated cells reduced limb length discrepancy over pre-chondrogenic cells and agarose alone. These results suggest that treatment of growth plate injury with BMSCs restored the natural process of growth plate closure in rats. It also indicates that increased tether formation may be a by-product of growth plate injury and not associated with disruption of the growth potential of the tissue. Therefore, treatments that affect tether formation within the growth plate may not restore growth function.

In conclusion, we have developed a small animal model of centralized growth plate defects in adolescent Sprague Dawley rats that demonstrates limb length discrepancies similar to that seen in the clinical setting. We have also demonstrated that micro-CT imaging can be used to *quantitatively* monitor disruptions in the normal function of the growth plate. The changes in growth plate morphology due to injury

were found to be correlated to overall growth disturbances when the defect was allowed to heal without intervention. Using these techniques in combination with histological analysis, we have revealed preliminary mechanisms of limb length discrepancy due to growth plate injury. We showed that premature thinning of the growth plate was due to disorganization of the cellular microarchitecture of the tissue. There was a loss in proliferative cell columns and a decrease in the number of hypertrophic cells. Since the hypertrophic zone is responsible for 45-60% of limb growth [2, 3], the loss of these cells is likely to be the significant contributor to the stunted growth of the defect limb. Bone bridge formation occurred with or without treatment and had no effect on limb length discrepancies. Tether formation is reduced with injection of BMSCs, but does not appear to be associated with growth disruption. Consequently, treatments that focus on inhibiting bone bridge or tether formation are unlikely to correct limb length discrepancy. Future research should concentrate on maintaining the health of the remaining growth plate tissue.

The techniques developed here *contribute* to the field in that they offer an improvement over basic histology for *in situ* analysis of alterations in growth plate tissue morphology due to injury. Combining the animal model and the micro-CT analysis techniques developed in this dissertation with biological methods, such as *in situ* hybridization, will further our understanding of the mechanisms of growth plate repair and its relationship to limb deformities and can also aid in more accurate diagnoses of growth plate injury clinically as well as aid in surgical preparation for treatment of these defects.

Tissue engineering strategies using progenitor cells has gained interest in the research community for treatment of a wide variety of musculoskeletal injuries. In this work, we have shown that several factors of rat BMSC chondrogenesis were interrelated. Cell viability and matrix accumulation were dependent on passage number, hydrogel scaffold, and growth factor regimen. When BMSCs were implanted into growth plate defects, a dependence of limb length discrepancy on the differentiation state of these cells was observed. This response appears to be due to the inability of pre-chondrogenic BMSCs to continue to secrete a cartilaginous matrix when placed in hydrogel culture. This work has *contributed* to our understanding of the interdependence of factors such as sex of the animal, passage number, scaffold choice, and final tissue engineering application on progenitor cell response to a chondrogenic differentiation protocol. In future applications of BMSCs for cartilage tissue engineering, characterization of the interdependence of BMSC chondrogenic response to *in vitro* and *in vivo* conditions will aid in development of tailored tissue engineering strategies for tissue repair.

Future Recommendations

This research has provided an important step toward understanding the relationship between growth plate morphology and growth disruption. However, along the way several limitations have been uncovered and research questions raised. One of the main limitations of our animal model is that the growth plate isolation protocol is time consuming and not practical for clinical application. To address this issue, preliminary studies have been performed using Hexabrix™ (Mallinckrodt). Hexabrix™ is

an injectable, iodinated, water soluble contrast agent that is currently used clinically for angiography and arteriography. It has been safely used in children. Previous *in vitro* work has also demonstrated that quantitative assessment of 3D cartilage morphology is possible using Hexabrix™ and micro-CT imaging [222]. In the preliminary experiment, the distal ends of Sprague Dawley rat femur were immersed in a 25% (v/v) Hexabrix™ at 37°C for 30, 90, and 150 minutes. The growth plate were then isolated using a protocol developed from Scanco software to label and isolate the growth plate as show in **Figure 6.1**. The accuracy of this method was compared to the contouring method developed in Specific Aim I. The results are shown in **Figure 6.2**. Compared to the contouring method, the average thickness decreased significantly after 90 minutes in Hexabrix™. The volume measurement was not different. Based on these results, Hexabrix™ is a promising method by which the growth plate morphology can be accurately isolated. However, the process still requires further optimization.

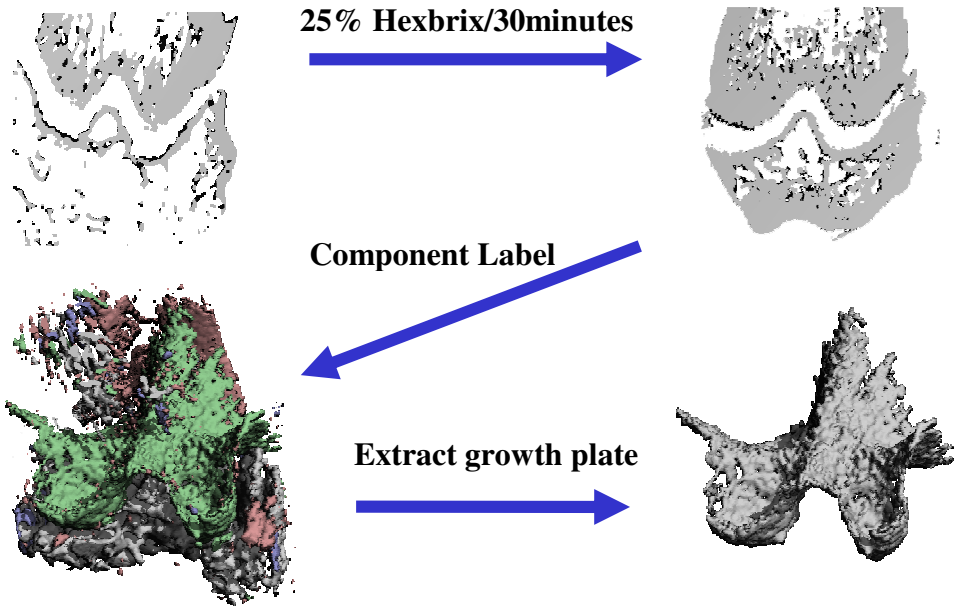

Figure 6.1. Illustration of isolation of the growth plate using Hexabrix™ and Scanco software

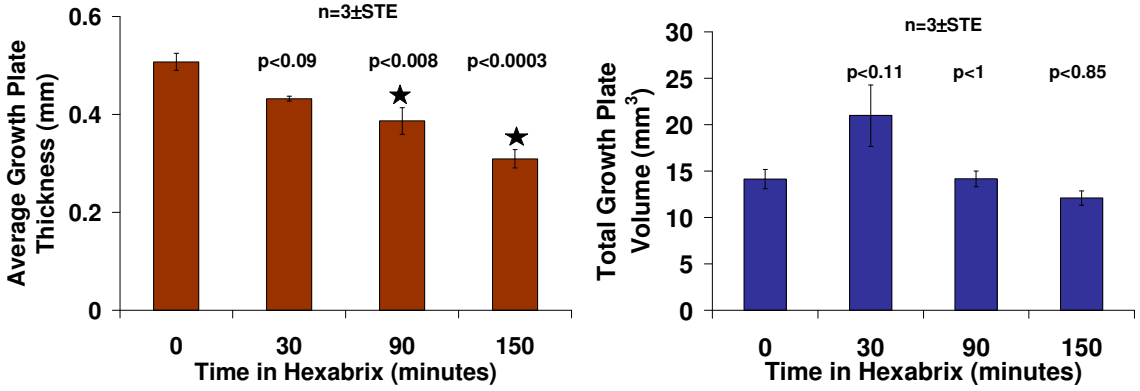

Figure 6.2. Changes in growth plate morphological measurements with increased time in Hexabrix™.

Another avenue of treatment for growth plate injury that was not explored in this dissertation is the delivery of growth factors into the defect. For instance, studies in craniosynostosis, a premature fusion of cranial sutures (cartilaginous tissue responsible for skeletal growth) that results in abnormal skull morphology, have identified TGF-β's

as having a dominant role in this disease [223-228]. Specifically, studies in this area have demonstrated that delivery of TGF-β3 to sutures in animal models of craniosynostosis rescues osseous obliteration of this tissue by altering TGF-β2 and TGFR-β2 expression [224, 225]. *In vitro* studies have also shown that TGF-β3 acts directly on osteoblasts, inhibiting their activity [229]. TGF-β3 also shown to stimulate chondrogenesis in progenitor cells *in vitro* [230]. Therefore the presence of this factor within a cell/agarose construct may contribute to BMSC differentiation as well as blocking bone infiltration. Based on these studies, a preliminary experiment was performed to examine the ability of TGF-β3 encapsulated in polymer nanoparticles to heal growth plate defects. Approximately 1ng of TGF-β3 was injected into growth plate defects via 1% SeaKem® agarose and the defect analyzed after 56 days. The results show defect limbs did not show a limb length discrepancy (**Figure 6.3**). However, there is no discernible effect when compare to defects left empty or filled with agarose alone. This study demonstrates that delivery of TGF-β3 into the defect may be beneficial to recovery of a normal limb length. Further analysis with a larger sample, higher doses, and, possibly, combination with BMSCs may show complete healing of a centralized growth plate defect with restored growth function.

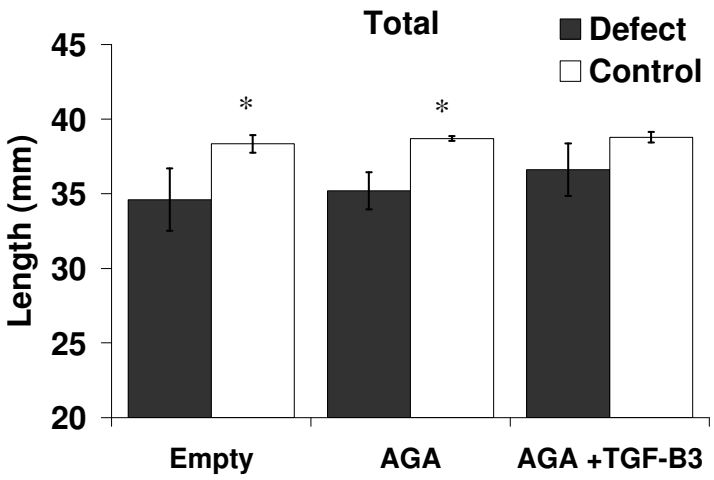

Figure 6.3. Effect of TGF-β3 loaded nanoparticles suspended in agarose on defect bone limb length.

n=3; error bars=±SEM; * indicates difference from defect leg

Finally the micro-CT method developed in this dissertation may be used to study growth plate abnormalities in diseases such as achondroplasia, the most common form of human dwarfism. This disorder has been shown to be due to point mutations in the transmembrane domain of fibroblastic growth factor receptor 3 (FGFR-3) [103, 231]. The morphological changes of the growth plate have been investigated through histomorphometric analysis of mouse knockout models [231, 232]. This method is both expensive and time consuming. With techniques developed in this dissertation, *in situ* analysis of knockout models is possible and will allow investigators to study the time-course of growth plate morphological changes in disease and with treatment. We have recently demonstrated that the micro-CT method developed in this dissertation can be readily adapted to mouse growth plate using a vitamin D receptor knockout model (VDR-/-) [233]. Significant differences in growth plate thickness, volume, and tether formation were found compared to wild type animals [233].

As enumerated in Chapter 2, many investigators are studying the control of progenitor cell differentiation for tissue engineering applications. Numerous combinations of growth factors and scaffolds have been tested and developed for this purpose. From this dissertation, four salient factors were found to play a role in the *in vitro* chondrogenic response of rat BMSCs: monolayer expansion, gender, hydrogel, and growth factor regimen. These factors in no way cover the wide spectrum of facets that regulate the behavior of BMSCs, but has raised some interesting avenues worth pursing. For instance, the mechanism of dexamethasone (Dex)-induced cell death in agarose cultures. Dex has been shown to have a role in the regulation of chondrocyte phenotype and maturation in the growth plate [212] and that it may be interconnected to the role of IGF [7, 108]. If BMSCs are to be introduced into the growth plate environment, than the effects of the factors that regulate growth plate morphology on differentiation and subsequent cell behavior requires further investigation. Specifically, determining whether the maturation of chondrogenic BMSCs can be controlled though exogenous exposure to PTHrP, IHH, TGF-β, and BMP-6 would further demonstrate the chondrogenic phenotype of these cells and allow investigators to better predict their behavior *in vivo*.

APPENDIX A

A. 1. Growth plate isolation from micro-CT scans

1. Evaluate the epiphysis of the leg of interest in a voi window (this give you a 3D image <u>without</u> doing any evaluations):
   a. In Session Manager, click on IPL_VIVACT

      → Change IPL_VOI_ONLY.com file to 1.2, 2, 92

   b. In the DECterm window type $ voi
      → evaluation window opens up
      → click "*evaluation 3D*"
      → select the slice range of interest and make sure the white voi box includes all of the regions of interest while still being as small as possible

      → ***set the number of pages to zero or you will get a textbook of nonsense from the printer***
      → evaluate (**record gobj file number if one is necessary; record the seg.aim number. You will develop several of both file types and will need to keep them in order**)

2. Rotation of epiphyses:
   a. Open 3D window
   b. File→Open→measurement number→seg.aim number
   c. Orient the image such that the the posterior side of the femur faces out of the screen, towards the viewer (in the +y direction).

      Note: The rotation and elevation shown in the upper left corner of the screen. These values
      correspond to the angles that the image must be rotated in the z and x directions, respectively.

      Note: Positive rotation is always counterclockwise around the + axis of interest

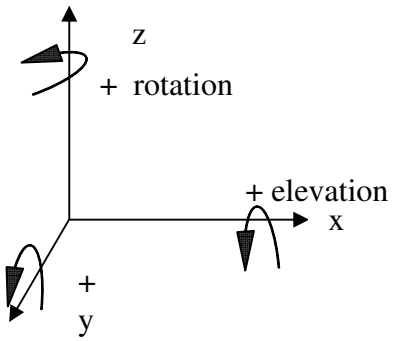

   d. To rotate image
      In DECterm window type $ IPL

IPL> read **in** DSK0…seg.aim (image to be rotated)
IPL> turn2d (around z-axis → ALWAYS DONE FIRST)
[in]> **in** [default values are in brackets and do not necessarily have to be changed]
[out]> out
[angle]> **rotation** value from 2c

- Hit enter until program is running

IPL> turn3d

[in]> out (from previous step)
[out]> rot (whatever you want)
[axis]> [default is x-axis: 0 90 90; y-axis: 90 0 90; z-axis 90 90 0]
[angle]> [default is 0.00] elevation angle from 2c if around x, rotation in the plane of the screen if around y (you'll have to approximate this one by eye).

- Hit enter until program is running

e. To make the size of image as small as possible, the empty space is removed:

IPL> bounding
[in]> rot (or whatever you named the last out file)
[out]> cut

- Hit enter until program is running

f. Write rotated file to disk

IPL> write cut DSK0…NEWNAME.aim (the NEWNAME should be the angles about which you rotated the image [e.g. X-10_Y5_Z130.aim])

g. Check rotation in the 3D window. Repeat turn2d and turn3d as needed until the epiphysis is oriented like the image in step c.

3. Creation of 2nd isq to contour growth plate.
   a. Rotate the image -90° around the x-axis
   b. Invert the image

IPL> read in DSK0…seg.aim (**or just use 'out' file from last step**)
IPL> set_value out 0 127

- Hit enter until program is running

Note: the image in 'out' has been replaced with the inverted image

c. Create new ISQ.

IPL> read in DSK0…seg.aim (**or just use 'out' file from the last step**)

IPL> from_aim_to_isq

aim_name [out]> **out**
isq_filename [default]> DSK0…isq (**MUST be the isq from the sample file which contains your seg.aim file; MUST delete the 1**)
square_flag [false]> leave at false (hit return)
original_position [true]>false (**MUST be false**)

- Hit enter until program is running

4. IF the new ISQ has more slices then the original:
   a. In DECterm window, create a new database and write down the new sample number applied by the system
   b. Then: $run_um:µCT_import
      Give the newly created isq file
      Enter the new sample number

5. Contour the growth plate
   a. Open new isq in a VOI evaluation window
   b. **SAVE OFTEN!** The buffer fills up quickly and you will lose data if you do not.
   c. Evaluate the growth plate
      i. Change the values in the IPL_VOI_ONLY.com file to 1.2, 2, 248
      ii. See 1b
   d. When all contours are drawn, delete all the .GOBJ files except those used to make the voi of the bone earlier and the very last GOBJ for the growth plate evaluation Write down the number GOBJ number. **YOU WILL NEED THEM LATER**.

6. Determine growth plate thickness

IPL> read in DSK0…seg.aim (growth plate seg.aim)
IPL> dt_obj
aim_name [in]> **in**
output [out]> out (whatever you want)
gobj_filename [default]> DSK0…gobj (**the growth plate evaluation file**)
peel_iter [-1]> this value must be determined prior to running this command

- Hit enter until program is running

IPL> write out DSK0…GP_THICKNESS.aim (yields the color thickness

map) → (can be viewed in the 3D window)

7. Determine bone volume fraction of the growth plate

IPL> read in DSK0…seg.aim (growth plate seg.aim)
IPL> vox
aim_name [in]> **in**
gobj_filename [default]> DSK0…gobj (**the growth plate evaluation file**)
peel_iter [-1]> this value must be determined prior to running this command

- Hit enter until program is running
- Record ov/tv and total volume (bone volume fraction)

A.2. RMC_GP_PREP.COM

Purpose: To rotate, invert, and convert to isq a seg.aim of an epiphysis. Script saves rotated and inverted files in the folder of the seg.aim in question. The input **MUST BE** a seg.aim file. If it is not, copy the file of interest and rename _seg.aim.

```
$!
$!          _/_/_/  _/_/_/     _/
$!           _/     _/     _/  _/           Image Processing Language
$!          _/     _/_/_/     _/
$!         _/     _/         _/             (c)  Andres Laib, Scanco
Medical AG
$!      _/_/_/  _/         _/_/_/_/
$!
$!
$!  IPL Batch Scanco
$!
$   if p1 .EQS. ""
$     THEN
$     write sys$output "Give C0001234.aim ! Exit"
$     exit
$   endif
$
$   define   org_file     'p1'
$   turn_file = p1 - F$PARSE(p1,,,"VERSION") - "_SEG.AIM" +
"_rotated.aim"
$   inverted = p1 - F$PARSE(p1,,,"VERSION") - "_SEG.AIM" +
"_inverted.aim
$   isq_file = p1 - F$PARSE(p1,,,"VERSION") - "_SEG.AIM" + ".isq"
$
$   show log org_file
$!
$   ipl_scanco_prog := $um:ipl_scanco_m.exe
$!
$   ipl_scanco_prog


/aim in org_file

/turn3d in out
 -turnaxis_angles   0 90 90
 -turnangle         -90

/bounding_box out cut

/write cut "turn_file

/set_value cut 0 127

/write cut "inverted

/from_aim_to_isq cut
 -isq_filename          "isq_file
 -square_flag           true
 -original_position     false
..
$ exit
```

APPENDIX B

Figure B.4. CAD Drawing of hydrogel seeding mold

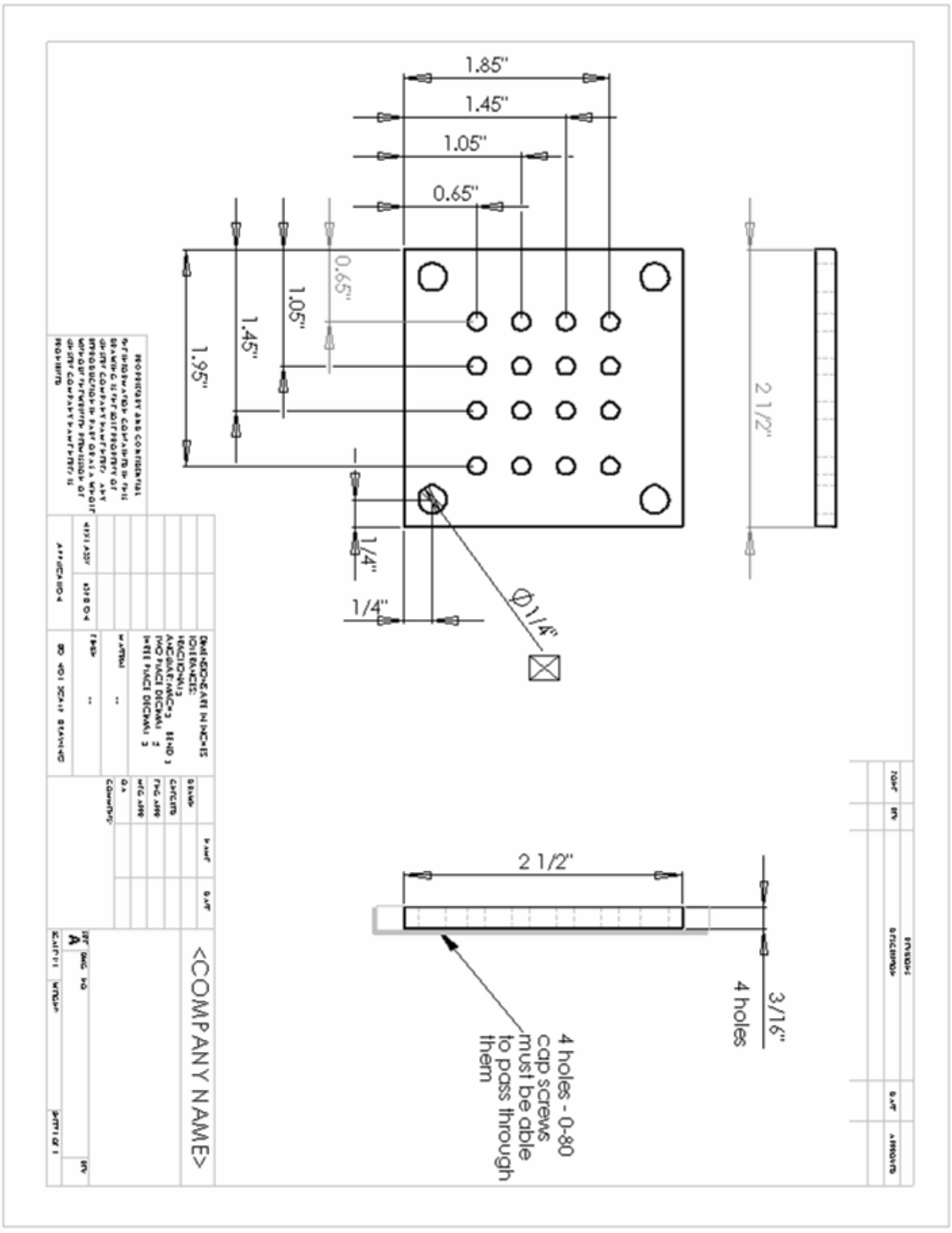

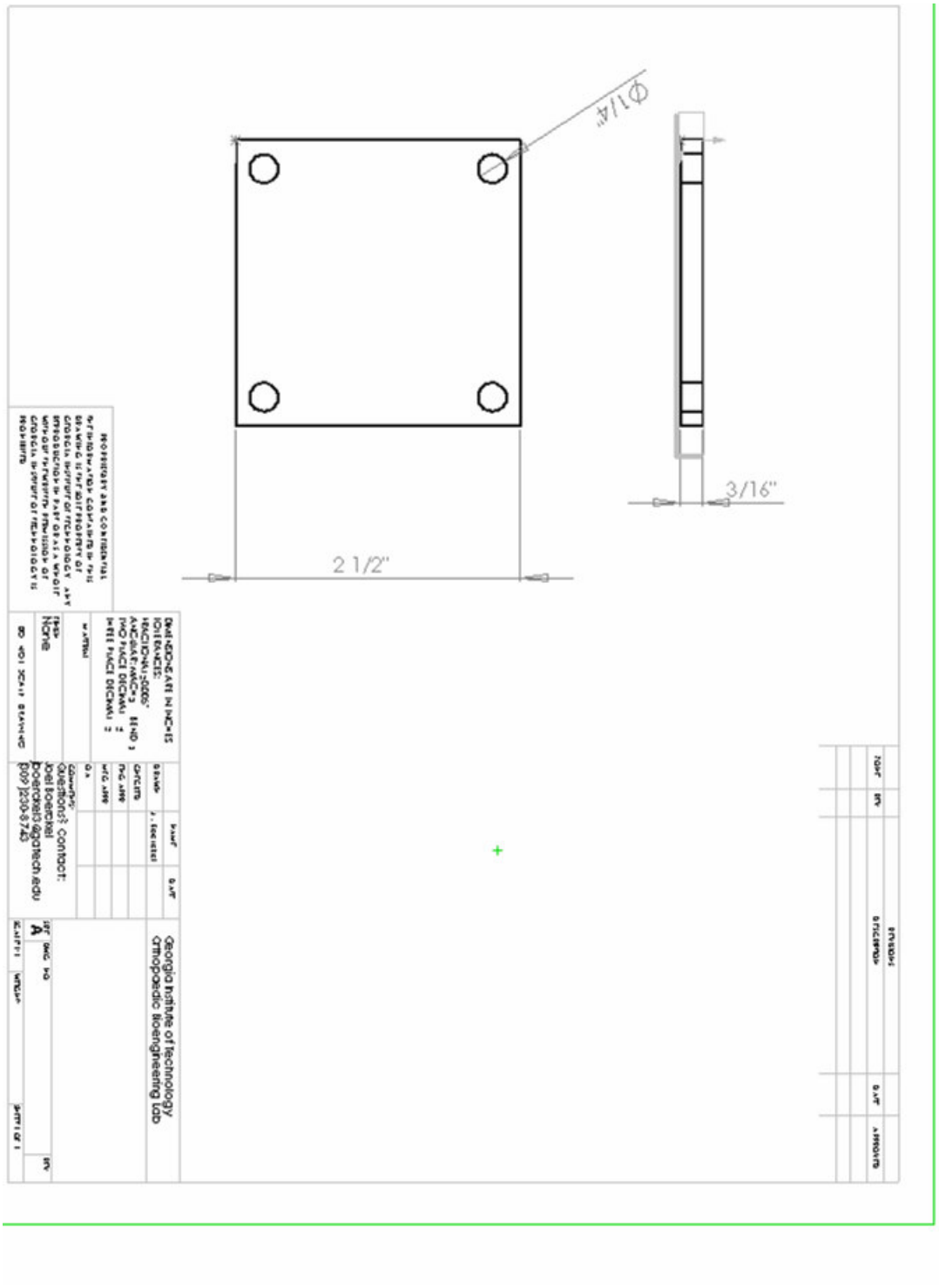

B.2. Hydrogel seeding protocol

Purpose

To promote rat osteoprogenitor cells to undergo chondrogenesis in alginate gels and agarose gels by stimulation with TGF-□1 and dexamethasone.

Materials

Sterile 3% Pronova alginate made up in ion free PBS and autoclaved for 20minutes [FMC BioPolymers]
Sterile 4% Type VII agarose made up in ion free PBS and autoclaved for 20minutes [Sigma]
10 Sterile molds set up for alginate gels (metal mesh + filter paper)
10 Sterile molds set up for agarose gels
TGF-β1 [R&D Systems #240-B] Lot#_____
DMEM-High glucose [Gibco # 11995-073]
10mM Non-essential amino acids (NEAA) [Gibco #11140-050]
100X Antibiotic/Antimycotic [Gibco # 15240-062]
L-proline [Sigma #P-1428]
Ascorbate 2-phosphate [Sigma # A-8960]
Dexamethesone [ICN #157565]
ITS [BD Labware #354352] Lot#_____
Selected lot of FBS [Hyclone FLL1524; heat inactivated]

Solutions

Alginate crosslinking solution: 102 mM $CaCl_2$, 100 mM NaCl, and 50 mM HEPES
1,000X Stocks: 40mg/ml L-proline, 50mg/ml AA-2P, 10µg/ml TGF-β1, 10µM/ml Dex. Store at -80°C.
DMEM+: to DMEM-HG, add, 1% NEAA, 1% Antibiotic/Antimycotic, 40µg/ml L-proline, and
1% ITS. This solution is good for 3 weeks at 4°C. At every feeding add, 50µg/ml AA-2P, and 10nM Dex.

Methods

Alginate

1. Wet filter paper on molds with the alginate crosslinking solution. Do this from the outside and allow to wick in.
2. Count cells. Determine how much 2% alginate solution will be needed to obtain a final density of $20x10^6$ cells/ml.
3. Spin down cells and resuspend in 1/3 of 2% alginate volume Ca^{2+}/Mg^{2+} -free PBS. Carefully 2/3 of 2% alginate volume 3% alginate to make a 2% solution.
4. Seed alginate gels as per the experimental protocol.
5. Place gels in 48-well plates.
6. Add 1ml of media to the gels.

7. Place 6 in individual, preweighed Eppendorf tubes. Take wet weights and store at -20°C until assay.
8. Stain 1 gel for the live/dead assay.
9. Replace media every other day.
10. Freeze remaining cells.

Agarose

1. Wet the filter paper with Ca^{2+}/Mg^{2+} -free PBS. Do this from the outside and allow to wick in. Place molds (6) and 100 and 1000µl tips in to incubator for at least ½ hr.
2. Resuspend cells in DMEM+ for a final seeding density of $40x10^6$ cells/ml. Maintain at 37°C at all times.
3. Microwave agarose for 10 sec.
4. Add 500µl of 4% agarose to 4 sterile 5 ml tubes and place in a beaker.
1. Place 1 tube of agarose at a time into a 42°C waterbath for no more than ½ hr. Also place a second container of water into bath to take into hood.
5. Place the beaker containing 42°C water in the hood.
6. Quickly add 500µl of the cell solution to a tube containing agarose using prewarmed tips and mix well. Place in the water bath in the hood.
7. Quickly seed agarose gels: draw up 27µl of agarose+cell solution and add to each well.
8. Repeat until all gels have been seeded (stagger 15 minutes).
9. Allow to polymerize in hood for at least 10 minutes.
10. Place gels in 48-well plates.
11. Add 1ml of each media to 24 of the gels.
12. Takedown 6 gels for day 0 analysis and stain 1 for the live/dead assay.
13. Replace media every other day.
14. Freeze remaining cells.

APPENDIX C

C.1. Chondrogenesis of male and female Sprague Dawley rat BMSCs

1. Purpose:
   To determine the response of male rat BMSCs to TGF-β1 stimulation compared to female rat
   BMSCs
2. Methods
   a. Cells were expanded to P2 in the presence of 1ng/ml FGF-2
   b. P2 cells were seeded in 2% alginate (25µl gels)
   c. Groups:
      ii. 10ng/ml TGF-β1
      iii. 10ng/ml TGF-β1 + 0.1nM Dex
      iv. Dex alone
3. Analysis:
   a. sGAG/DNA – DMMB dye assay
   b. Live/Dead assay
4. Results:
   a. sGAG/DNA – male cells accumulated more sGAG than female cells in response to TGF-β1 stimulation on days 14 and 21. With Dex, there was only a difference between the sexes at day 21.

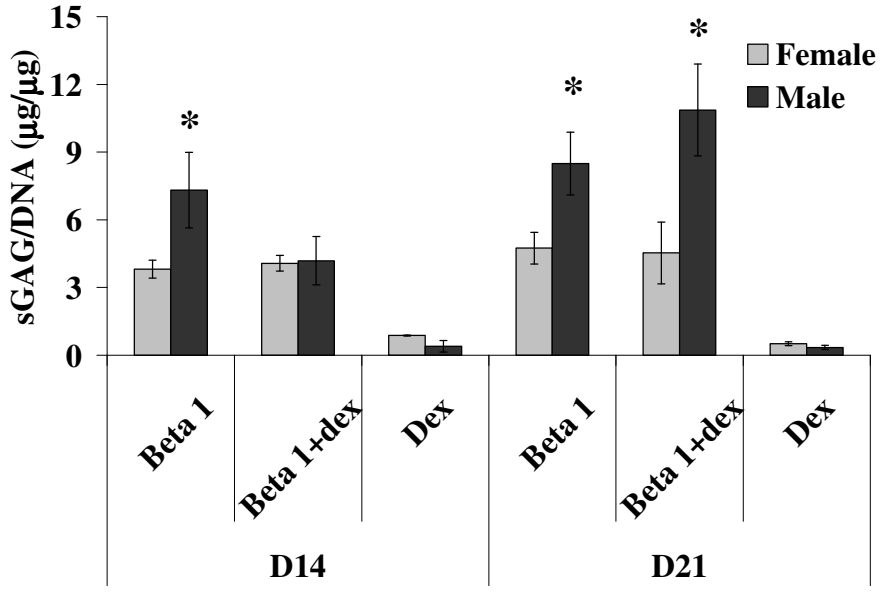

Figure C.1. sGAG production male and female BMSCs under chondrogenic conditions

b. Live Dead – Cell viability was high except in the Dex alone group

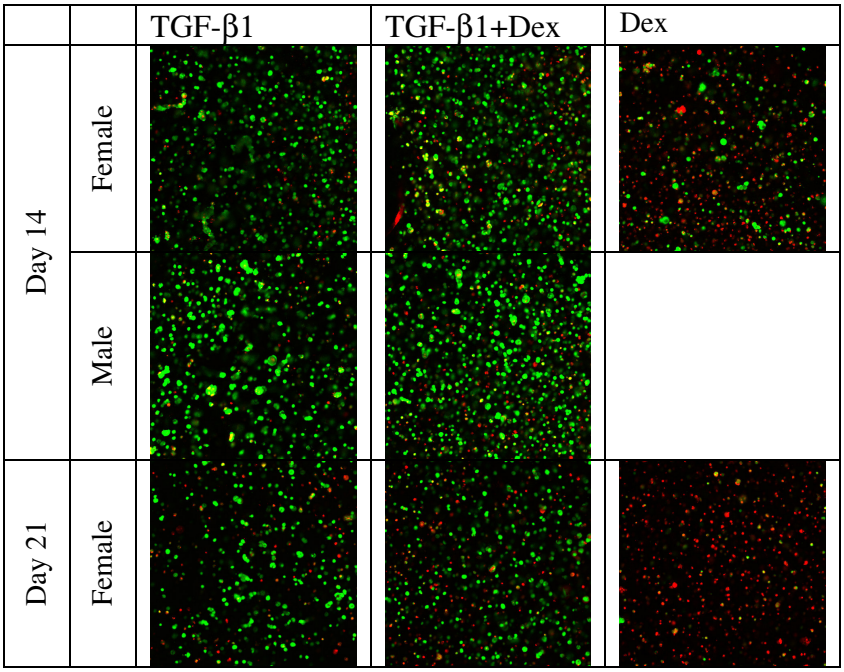

Figure C.2. Viability of male and female BMSCs under chondrogenic conditions

5. Conclusions:
   Male cells undergo chondrogenesis in 2% alginate at the same level or better than female cells.

APPENDIX D

D.1. Effects of various culture conditions on the viability of male BMSCs during chondrogenesis

1. Purpose to determine whether alginate culture or TGF-β supplementation causes death of male BMSCs during chondrogenesis
2. Methods
   a. Frozen P0 cells were plated in T-185 NUNC plates at a density of $1x10^6$ cells/plate. All plates were cultured in standard passaging media (α-MEM, 10% FBS, antibiotic/antimycotic) supplemented with 1ng/ml FGF-2 during monolayer expansion. At P2, cells were seeded in the following conditions:
      i. Plated in 6 well plates at a density of $6.7x10^6$ cells/cm^2 and culture in the following media conditions:
         1. Basal media
         2. Chondrogenic media (CGC) – inclusion of 10ng/ml TGF-β
         3. Basal or CGC media with unpolymerized 2% alginate
      ii. 2% Pronova alginate at a density of $20x10^6$ cells/ml in basal or chondrogenic media
      iii. 2% agarose at a density of $20x10^6$ cells/ml in basal or chondrogenic media.
   b. Cell viability was examined on days 1 and 7 using the Live/Dead Assay
3. Results (**Figures D.1**)
   a. Cells survived process of hydrogel encapsulation (Day 1)
   b. Cell viability was lost in monolayer and 3D hydrogel culture by day 7 with or without chondrogenic media.
2. Conclusions
   a. Neither hydrogel nor growth factor stimulation is the singular factor that determines the viability of male BMSCs in culture.

		Monolayer	Monolayer + Alginate	Cells seeded into alginate	Cells seeded into agarose
Day 1	Basal	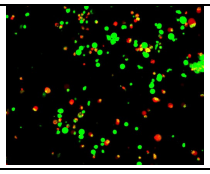	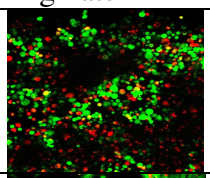	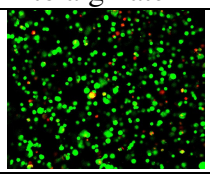	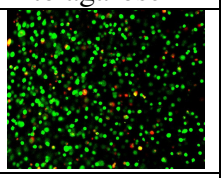
Day 7	Basal	No cells remaining	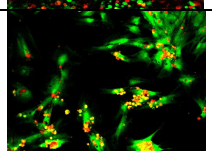	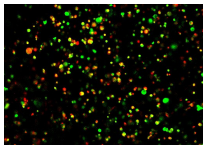	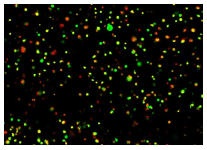
	CGC	No cells remaining	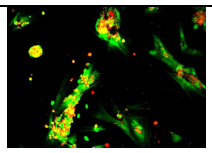	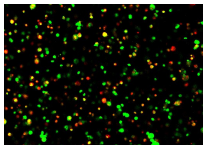	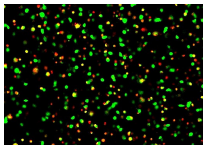

Figure D.1. Viability of male BMSCs under various culture conditions

D.2. Effects of passaging, culture plate, and growth factor supplementation on the viability of male BMSCs during chondrogenesis in alginate gels

1. Purpose to determine what culture condition affect cell male BMSC viability during chondrogenesis
2. Methods
   a. Frozen P0 cells were plated in T-185 NUNC plates at a density of $1x10^6$ cells/plate. All plates were cultured in standard passaging media (α-MEM, 10% FBS, antibiotic/antimycotic) supplemented with 1ng/ml FGF-2 during monolayer expansion. At P1 and P2, cells were seeded in 2% Pronova alginate at a density of $20x10^6$ cells/ml.
   b. 50μl gels were made in all cases. The following conditions were examined:
      i. Passage point – Cells at Passage 1 and 2 were used in all conditions
      ii. Incubator – cells were cultured in my incubator and another incubator that not previously used for chondrogenesis culture
      iii. Culture media – ITS alone and TGF-β (CGC)
      iv. Time in culture – viability was determined on days 1, 3, and 7
      v. Type of culture dish – gels were cultured in a group in $25cm^2$ T-flask. Gas exchange occurs through a filtered cap. Gels were cultured individually in a 24 well plate. Gas exchange occurs with the incubator air directly.
3. Results and Conclusions (**Figures D.2 and D.3**)
   a. Passage point – P1 cells appeared less spread and proliferated faster than P2 cells.
   b. Incubator – No differences were observed
   c. Culture media – TGF-β treated gels had more viable cells in each sample that ITS alone samples at P1. These differences were less apparent at P2.
   d. Time in culture – At P1, cell viability did not appear to decrease from day 1 to day 3, but does decrease from day 3 and day 7. P2 cell viability appeared to decrease rapidly from day 1 to day 3.
   e. Type of culture dish – individual culture in plates may have some benefit on cell viability, but the results are inconclusive.

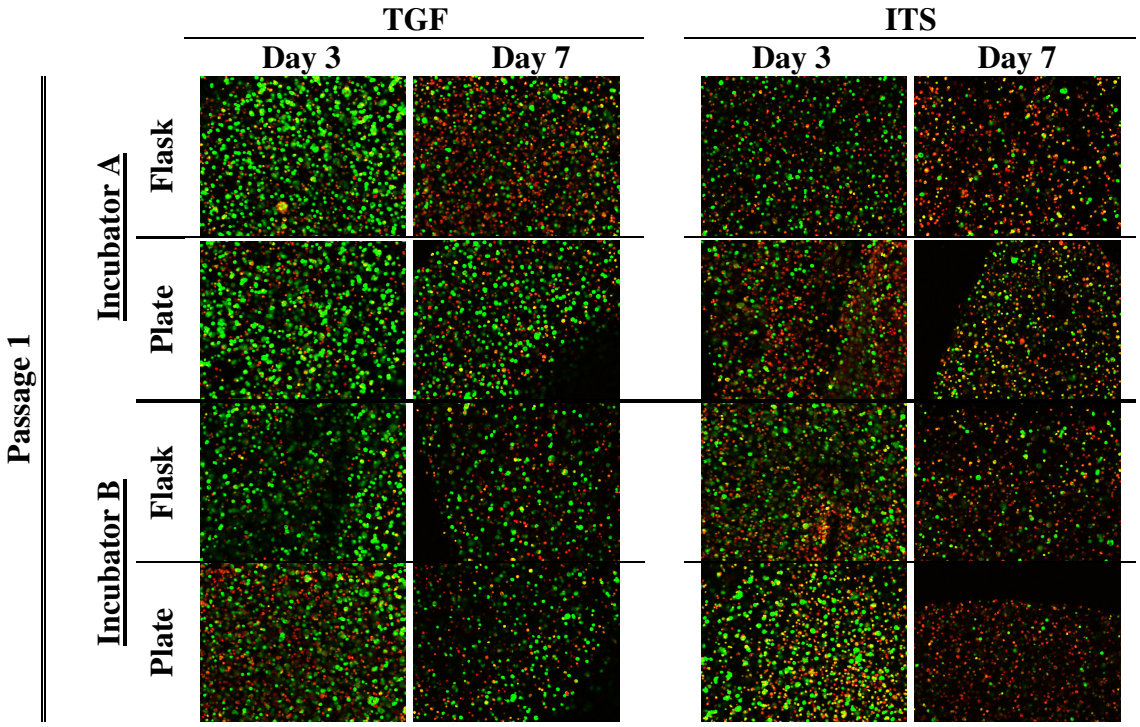

Figure D.2. Viability of P1 male BMSCs encapsulated in alginate gels under various culture conditions over time.

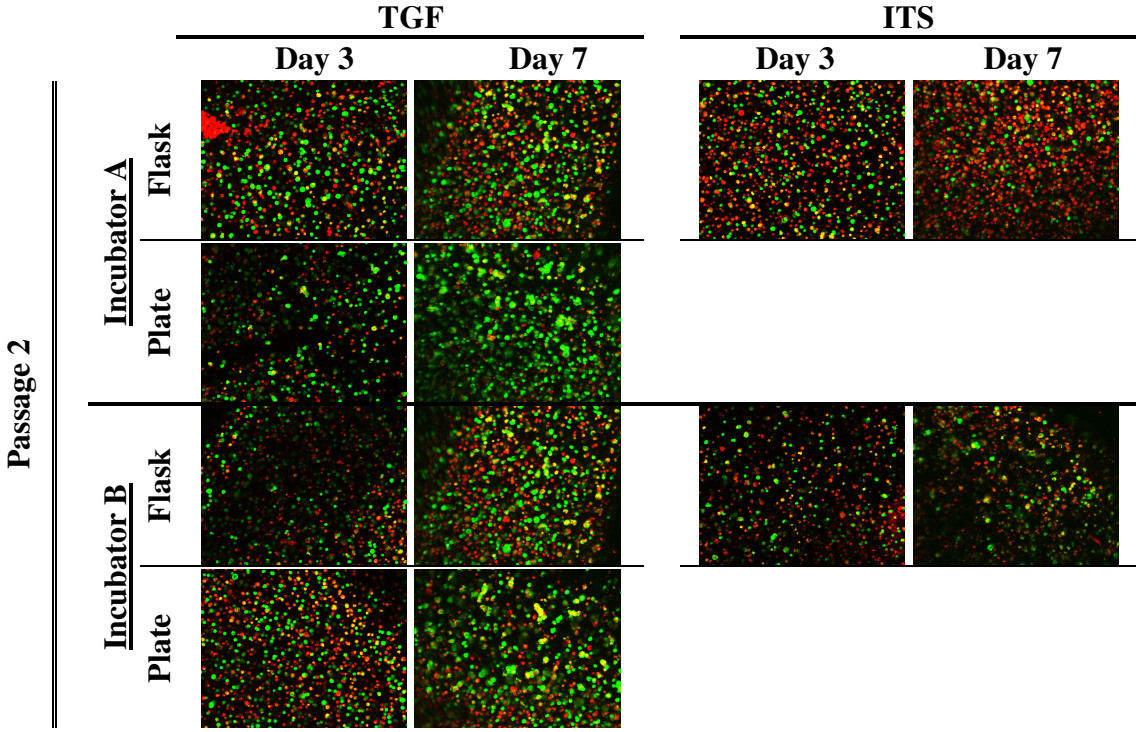

Figure D.5. Viability of P2 male BMSCs encapsulated in alginate gels under various culture conditions over time.

D.3. Effect of FGF-2 and *in situ* gelling SeaKem® agarose culture on the viability of male BMSCs

1. Purpose to verify that male BMSCs remain viable in 0.5% SeaKem® agarose for delivery into growth plate defects.
2. Methods
   a. Frozen P0 cells were plated in T-185 NUNC plates at a density of $1x10^6$ cells/plate. All plates were cultured in standard passaging media (α-MEM, 10% FBS, antibiotic/antimycotic) with or without 1ng/ml FGF-2 during monolayer expansion. At P1 and P2, cells were seeded in 0.5% SeaKem® agarose at a density of $20x10^6$ cells/ml.
   b. Samples were harvested on days 0, 3, and 7 for live/dead analysis
3. Results (**Figures D.4**) - P1 cells seeded in agarose remained highly viable at all timepoints with or without FGF-2 supplementation. Cell death increase in P2 cells seeded in agarose over time.
4. Conclusion – P1 cells will be used *in vivo* for the repair of growth plate defects.

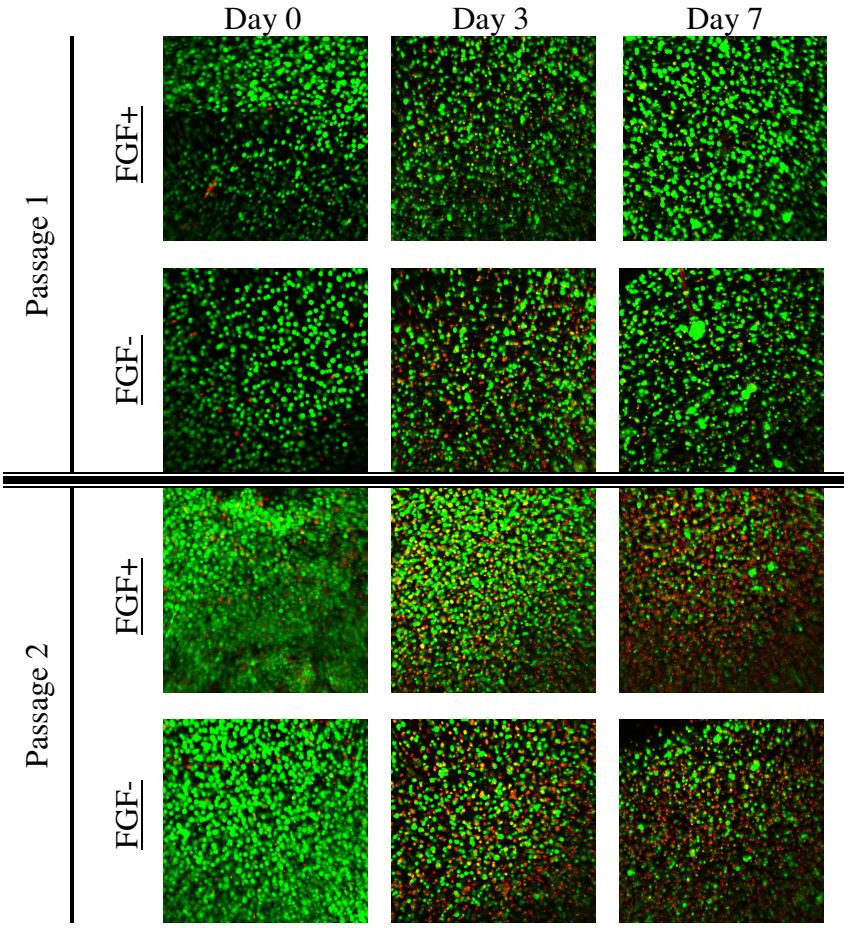

Figure D.4. Viability of male BMSCs passage with FGF-2 supplementation and culture in 0.5% SeaKem® agarose

APPENDIX E

E.1. Effect of Gelfoam® insertion into growth plate defects in Sprague Dawley rats on baseline healing

1. Purpose
   Previous studies indicated that bleeding from the marrow cavity was preventing agarose injected into the defect from fully conforming to the defect site due to mixing and/or back pressure from the marrow cavity. Hence antifibrolytic agents such as **aprotinin**, **ε-amino caproic acid**, and **tranexamic acid** were compared to **Gelfoam®** to determine which would clot the defect and allow for full conformal filling of the defect by injected agarose. Preliminary studies indicated that Gelfoam® was the most successful. In this study, the effects of Gelfoam® on the natural healing response of the defect model was examined.
2. Methods
   a. A defect was created in the distal femur of both legs in each rat (n=3) with the right leg receiving treatment a 2mm plug of Gelfoam®. The plug was pushed into place below the growth plate using a rod with a mechanical stop. The defect was then stuffed with dry cotton for 10 minutes. The defect in the left leg received no treatment.
   b. Both defects were left empty for 28 days. Baseline healing was defined as the final total and diaphyseal lengths of the bones receiving Gelfoam® versus the contralateral control.
3. Results
   a. No effect of the presence of Gelfoam® on the base healing response of growth plate defects after 28 days. However, the presence of Gelfoam® did decrease the BVF in the growth plate region by ~50% (paired t-test, $p<0.02$).
4. Conclusions
   Gelfoam® insertion decreases BVF within the defect while having no effect on limb length discrepancy over 28 days.

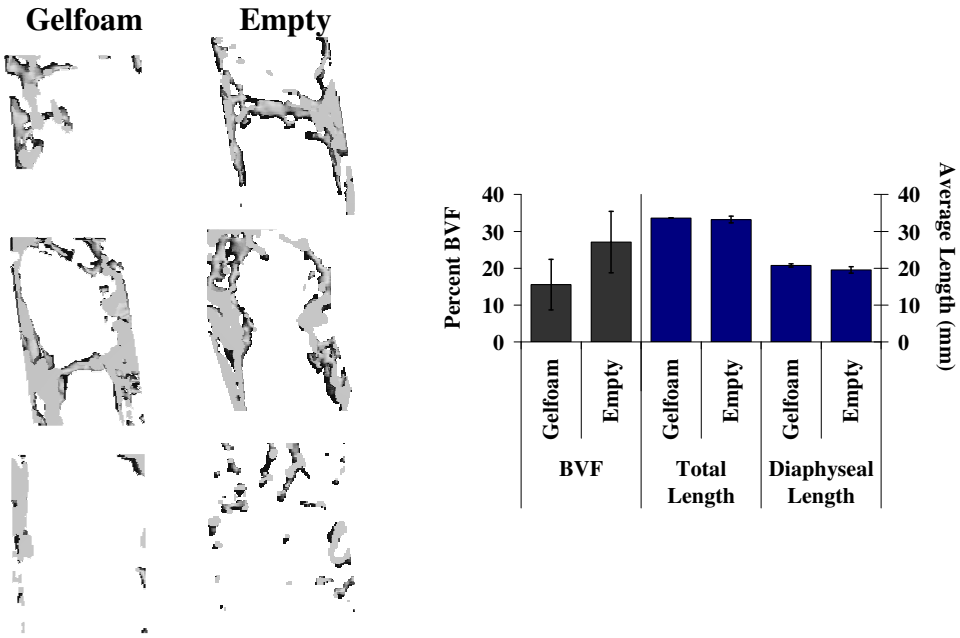

Figure E.1. Effect of Gelfoam® on defect BVF and limb length 28 days post surgery.

E.2. Comparison of 1% and 0.5% SeaKem agarose on growth plate defect healing in a model in Sprague Dawley rats

1. Purpose
   To determine whether or not the density of agarose injected into the defect had any effect on limb length shortening. A step toward specifying the gel composition in which cells will be introduced into the defect.
2. Method
   a. A defect was created in the distal femur of both legs in each rat (n=3) with the both legs receiving treatment with 100mg/ml tranexamic acid for 10 minutes to stop bleeding.
   b. Both defects were filled with 0.5% (right) or 1% agarose (left). Samples were harvested after 28 days.
3. Results
4. No differences in limb leg or BVF between defects filled with 0.5% agarose compared to those filled with 1%.

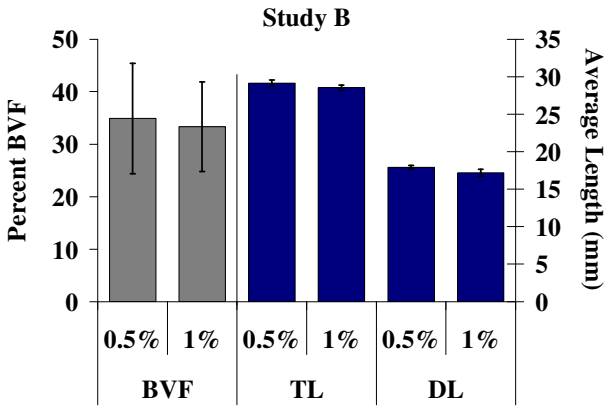

Figure E.26. Effect of agarose density on growth plate defect BVF and limb length 28 days post surgery.

5. Conclusions
   Agarose density did not influence the healing of growth plate defects

REFERENCES

[1] Hasler CC, Foster BK. Secondary tethers after physeal bar resection: a common source of failure? Clin Orthop 2002: 242-9.

[2] Wilsman NJ, Farnum CE, Leiferman EM, Fry M, Barreto C. Differential growth by growth plates as a function of multiple parameters of chondrocytic kinetics. J Orthop Res 1996;14: 927-36.

[3] Farnum CEaW, NJ. Converting a differentiation cascade into longitudinal growth: stereology and analysis of transgenic animals as tools for understanding growth plate function. Curr Opin Orthop 2001;12: 428-433.

[4] Ferguson C, Alpern E, Miclau T, Helms JA. Does adult fracture repair recapitulate embryonic skeletal formation? Mech Dev 1999;87: 57-66.

[5] Ballock RT, O'Keefe RJ. The biology of the growth plate. J Bone Joint Surg Am 2003;85-A: 715-26.

[6] Grimsrud CD, Romano PR, D'Souza M, Puzas JE, Reynolds PR, Rosier RN, O'Keefe RJ. BMP-6 is an autocrine stimulator of chondrocyte differentiation. J Bone Miner Res 1999;14: 475-82.

[7] Smink JJ, Koster JG, Gresnigt MG, Rooman R, Koedam JA, Van Buul-Offers SC. IGF and IGF-binding protein expression in the growth plate of normal, dexamethasone-treated and human IGF-II transgenic mice. J Endocrinol 2002;175: 143-53.

[8] Erickson DM, Harris SE, Dean DD, Harris MA, Wozney JM, Boyan BD, Schwartz Z. Recombinant bone morphogenetic protein (BMP)-2 regulates costochondral growth plate chondrocytes and induces expression of BMP-2 and BMP-4 in a cell maturation-dependent manner. J Orthop Res 1997;15: 371-80.

[9] Enomoto-Iwamoto M, Iwamoto M, Mukudai Y, Kawakami Y, Nohno T, Higuchi Y, Takemoto S, Ohuchi H, Noji S, Kurisu K. Bone morphogenetic protein signaling is required for maintenance of differentiated phenotype, control of proliferation, and hypertrophy in chondrocytes. J Cell Biol 1998;140: 409-18.

[10] Leboy PS, Sullivan TA, Nooreyazdan M, Venezian RA. Rapid chondrocyte maturation by serum-free culture with BMP-2 and ascorbic acid. J Cell Biochem 1997;66: 394-403.

[11] Schwartz Z, Sylvia VL, Liu Y, Dean DD, Boyan BD. Treatment of resting zone chondrocytes with bone morphogenetic protein-2 induces maturation into a phenotype characteristic of growth zone chondrocytes by downregulating responsiveness to

24,25(OH)2D3 and upregulating responsiveness to 1,25-(OH)2D3. Endocrine 1998;9: 273-80.

[12] Wilkins KE. Principles of fracture remodeling in children. Injury 2005;36 Suppl 1: A3-11.

[13] Caine D, DiFiori J, Maffulli N. Physeal injuries in children's and youth sports: reasons for concern? Br J Sports Med 2006;40: 749-60.

[14] Rogers LF, Poznanski AK. Imaging of epiphyseal injuries. Radiology 1994;191: 297-308.

[15] Rodriguez-Merchan EC. Pediatric skeletal trauma: a review and historical perspective. Clin Orthop Relat Res 2005: 8-13.

[16] Ecklund K, Jaramillo D. Imaging of growth disturbance in children. Radiol Clin North Am 2001;39: 823-41.

[17] Damron TA, Margulies BS, Strauss JA, O'Hara K, Spadaro JA, Farnum CE. Sequential histomorphometric analysis of the growth plate following irradiation with and without radioprotection. J Bone Joint Surg Am 2003;85-A: 1302-13.

[18] Segev Y, Landau D, Davidoff-Friedman S, Weinreb M, Phillip M. Involvement of the skeletal GH-IGF system in an experimental model of diabetes-induced growth retardation. Acta Diabetol 2002;39: 61-7.

[19] Takahi K, Hashimoto J, Hayashida K, Shi K, Takano H, Tsuboi H, Matsui Y, Nakase T, Tomita T, Ochi T, Yoshikawa H. Early closure of growth plate causes poor growth of long bones in collagen-induced arthritis rats. J Musculoskelet Neuronal Interact 2002;2: 344-51.

[20] Nyska M, Shabat S, Long PH, Howard C, Ezov N, Levin-Harrus T, Mittelman M, Redlich M, Yedgar S, Nyska A. Disseminated thrombosis-induced growth plate necrosis in rat: a unique model for growth plate arrest. J Pediatr Orthop 2005;25: 346-50.

[21] Xian CJ, Zhou FH, McCarty RC, Foster BK. Intramembranous ossification mechanism for bone bridge formation at the growth plate cartilage injury site. J Orthop Res 2004;22: 417-26.

[22] Ogden JA. Injury to the growth mechanisms of the immature skeleton. Skeletal Radiol 1981;6: 237-53.

[23] Peterson HA. Triplane fracture of the distal humeral epiphysis. J Pediatr Orthop 1983;3: 81-4.

[24] Bailey RW, Dubow HI. Evolution of the concept of an extensible nail accommodating to normal longitudinal bone growth: clinical considerations and implications. Clin Orthop Relat Res 1981: 157-70.

[25] Lee MA, Nissen TP, Otsuka NY. Utilization of a murine model to investigate the molecular process of transphyseal bone formation. J Pediatr Orthop 2000;20: 802-6.

[26] Young SJ, Barnett PL, Oakley EA. 11. Fractures and minor head injuries: minor injuries in children II. Med J Aust 2005;182: 644-8.

[27] Sailhan F, Chotel F, Guibal AL, Gollogly S, Adam P, Berard J, Guibaud L. Three-dimensional MR imaging in the assessment of physeal growth arrest. Eur Radiol 2004;14: 1600-8.

[28] Forriol F, Shapiro F. Bone development: interaction of molecular components and biophysical forces. Clin Orthop Relat Res 2005: 14-33.

[29] Craig JG, Cramer KE, Cody DD, Hearshen DO, Ceulemans RY, van Holsbeeck MT, Eyler WR. Premature partial closure and other deformities of the growth plate: MR imaging and three-dimensional modeling. Radiology 1999;210: 835-43.

[30] Craig JG, Cody DD, Van Holsbeeck M. The distal femoral and proximal tibial growth plates: MR imaging, three-dimensional modeling and estimation of area and volume. Skeletal Radiol 2004;33: 337-44.

[31] Guarino J, Tennyson S, Barrios Y, Shea K, Pfeiffer R, Sabick M. Modeling the growth plates in the pediatric knee: implications for anterior cruciate ligament reconstruction. Comput Med Imaging Graph 2004;28: 419-24.

[32] Buchmann RF, Jaramillo D. Imaging of articular disorders in children. Radiol Clin North Am 2004;42: 151-68, vii.

[33] Harcke HT, Synder M, Caro PA, Bowen JR. Growth plate of the normal knee: evaluation with MR imaging. Radiology 1992;183: 119-23.

[34] Chung T, Jaramillo D. Normal maturing distal tibia and fibula: changes with age at MR imaging. Radiology 1995;194: 227-32.

[35] Peskin B, Shupak A, Misselevich I, Zinman C, Levin D, Jacob Z, Reis DN, Boss JH. Transphyseal osseous bridges in experimental osteonecrosis of the femoral head of the rat. Histologic study of the bony bridges connecting the epiphyseal with the metaphyseal bony trabeculae through gaps in the physeal cartilage. J Pediatr Orthop B 2001;10: 214-8.

[36] Cutler L, Molloy A, Dhukuram V, Bass A. Do CT scans aid assessment of distal tibial physeal fractures? J Bone Joint Surg Br 2004;86: 239-43.

[37] Kordelle J, Richolt JA, Millis M, Jolesz FA, Kikinis R. Development of the acetabulum in patients with slipped capital femoral epiphysis: a three-dimensional analysis based on computed tomography. J Pediatr Orthop 2001;21: 174-8.

[38] Martiana K, Low CK, Tan SK, Pang MW. Comparison of various interpositional materials in the prevention of transphyseal bone bridge formation. Clin Orthop 1996: 218-24.

[39] Cady RB, Spadaro JA, Fitzgerald JA, Pinkes J, Albanese SA. The effects of fat interposition for central-physeal defects. A histologic study in rabbits. Clin Orthop 1992: 304-9.

[40] Jouve JL, Guillaume JM, Frayssinet P, Launay F, Viehweger E, Panuel M, Bollini G. Growth plate behavior after desepiphysiodesis: experimental study in rabbits. J Pediatr Orthop 2003;23: 774-9.

[41] Lennox DW, Goldner RD, Sussman MD. Cartilage as an interposition material to prevent transphyseal bone bridge formation: an experimental model. J Pediatr Orthop 1983;3: 207-10.

[42] Glickman AM, Yang JP, Stevens DG, Bowen CV. Epiphyseal plate transplantation between sites of different growth potential. J Pediatr Orthop 2000;20: 289-95.

[43] Teot L, Giovannini UM, Colonna MR. Use of free scapular crest flap in pediatric epiphyseal reconstructive procedures. Clin Orthop 1999: 211-20.

[44] Boyer MI, Bowen CV. Microvascular transplantation of epiphyseal plates: studies utilizing allograft donor material. Orthop Clin North Am 2007;38: 103-8, vii.

[45] Ad-El DD, Paizer A, Pidhortz C. Bipedicled vascularized fibula flap for proximal humerus defect in a child. Plast Reconstr Surg 2001;107: 155-7.

[46] Mayr JM, Pierer GR, Linhart WE. Reconstruction of part of the distal tibial growth plate with an autologous graft from the iliac crest. J Bone Joint Surg Br 2000;82: 558-60.

[47] Jaramillo D, Shapiro F, Hoffer FA, Winalski CS, Koskinen MF, Frasso R, Johnson A. Posttraumatic growth-plate abnormalities: MR imaging of bony-bridge formation in rabbits. Radiology 1990;175: 767-73.

[48] Jouve JL, Cottalorda J, Mottet V, Frayssinet P, Petit P, Bollini G. Reimplantation of growth plate chondrocyte cultures in central growth plate defects: Part II. Surgical experimentation in rabbits. J Pediatr Orthop B 1998;7: 174-8.

[49] Foster BK, Hansen AL, Gibson GJ, Hopwood JJ, Binns GF, Wiebkin OW. Reimplantation of growth plate chondrocytes into growth plate defects in sheep. J Orthop Res 1990;8: 555-64.

[50] Zhou Y, Lu S, Wang J, Zhang Y, Huang J. [The treatment of premature arrest of growth plate with a novel engineered growth plate: experimental studies]. Zhonghua Wai Ke Za Zhi 2000;38: 742-4, 42.

[51] Hui JH, Li L, Teo YH, Ouyang HW, Lee EH. Comparative study of the ability of mesenchymal stem cells derived from bone marrow, periosteum, and adipose tissue in treatment of partial growth arrest in rabbit. Tissue Eng 2005;11: 904-12.

[52] Chen F, Hui JH, Chan WK, Lee EH. Cultured mesenchymal stem cell transfers in the treatment of partial growth arrest. J Pediatr Orthop 2003;23: 425-9.

[53] Li L, Hui JH, Goh JC, Chen F, Lee EH. Chitin as a scaffold for mesenchymal stem cells transfers in the treatment of partial growth arrest. J Pediatr Orthop 2004;24: 205-10.

[54] Garces GL, Mugica-Garay I, Lopez-Gonzalez Coviella N, Guerado E. Growth-plate modifications after drilling. J Pediatr Orthop 1994;14: 225-8.

[55] Zhou FH, Foster BK, Sander G, Xian CJ. Expression of proinflammatory cytokines and growth factors at the injured growth plate cartilage in young rats. Bone 2004;35: 1307-15.

[56] Arasapam G, Scherer M, Cool JC, Foster BK, Xian CJ. Roles of COX-2 and iNOS in the bony repair of the injured growth plate cartilage. J Cell Biochem 2006;99: 450-61.

[57] Ngo TQ, Scherer MA, Zhou FH, Foster BK, Xian CJ. Expression of bone morphogenic proteins and receptors at the injured growth plate cartilage in young rats. J Histochem Cytochem 2006;54: 945-54.

[58] Shefelbine SJ, Augat P, Claes L, Beck A. Intact fibula improves fracture healing in a rat tibia osteotomy model. J Orthop Res 2005;23: 489-93.

[59] Wang JW, Li W, Xu SW, Yang DS, Wang Y, Lin M, Zhao GF. Osteoporosis influences the middle and late periods of fracture healing in a rat osteoporotic model. Chin J Traumatol 2005;8: 111-6.

[60] Hayashi K, Fotovati A, Ali SA, Oda K, Oida H, Naito M. Prostaglandin EP4 receptor agonist augments fixation of hydroxyapatite-coated implants in a rat model of osteoporosis. J Bone Joint Surg Br 2005;87: 1150-6.

[61] Damron TA, Mathur S, Horton JA, Strauss J, Margulies B, Grant W, Farnum CE, Spadaro JA. Temporal changes in PTHrP, Bcl-2, Bax, caspase, TGF-beta, and FGF-2

expression following growth plate irradiation with or without radioprotectant. J Histochem Cytochem 2004;52: 157-67.

[62] Garimella R, Bi X, Camacho N, Sipe JB, Anderson HC. Primary culture of rat growth plate chondrocytes: an in vitro model of growth plate histotype, matrix vesicle biogenesis and mineralization. Bone 2004;34: 961-70.

[63] Benya PD, Shaffer JD. Dedifferentiated chondrocytes reexpress the differentiated collagen phenotype when cultured in agarose gels. Cell 1982;30: 215-24.

[64] Bonaventure J, Kadhom N, Cohen-Solal L, Ng KH, Bourguignon J, Lasselin C, Freisinger P. Reexpression of cartilage-specific genes by dedifferentiated human articular chondrocytes cultured in alginate beads. Exp Cell Res 1994;212: 97-104.

[65] Imabayashi H, Mori T, Gojo S, Kiyono T, Sugiyama T, Irie R, Isogai T, Hata J, Toyama Y, Umezawa A. Redifferentiation of dedifferentiated chondrocytes and chondrogenesis of human bone marrow stromal cells via chondrosphere formation with expression profiling by large-scale cDNA analysis. Exp Cell Res 2003;288: 35-50.

[66] Raghunath J, Rollo J, Sales KM, Butler PE, Seifalian AM. Biomaterials and scaffold design: key to tissue-engineering cartilage. Biotechnol Appl Biochem 2007;46: 73-84.

[67] Lin Z, Willers C, Xu J, Zheng MH. The chondrocyte: biology and clinical application. Tissue Eng 2006;12: 1971-84.

[68] Frenkel SR, Di Cesare PE. Scaffolds for articular cartilage repair. Ann Biomed Eng 2004;32: 26-34.

[69] Sharma B, Elisseeff JH. Engineering structurally organized cartilage and bone tissues. Ann Biomed Eng 2004;32: 148-59.

[70] Rahaman MN, Mao JJ. Stem cell-based composite tissue constructs for regenerative medicine. Biotechnol Bioeng 2005;91: 261-84.

[71] Chen HC, Hu YC. Bioreactors for tissue engineering. Biotechnol Lett 2006;28: 1415-23.

[72] Abousleiman RI, Sikavitsas VI. Bioreactors for tissues of the musculoskeletal system. Adv Exp Med Biol 2006;585: 243-59.

[73] Ragan PM, Badger AM, Cook M, Chin VI, Gowen M, Grodzinsky AJ, Lark MW. Down-regulation of chondrocyte aggrecan and type-II collagen gene expression correlates with increases in static compression magnitude and duration. J Orthop Res 1999;17: 836-42.

[74] Ragan PM, Chin VI, Hung HH, Masuda K, Thonar EJ, Arner EC, Grodzinsky AJ, Sandy JD. Chondrocyte extracellular matrix synthesis and turnover are influenced by static compression in a new alginate disk culture system. Arch Biochem Biophys 2000;383: 256-64.

[75] Wong M, Siegrist M, Gaschen V, Park Y, Graber W, Studer D. Collagen Fibrillogenesis by Chondrocytes in Alginate. Tissue Eng 2002;8: 979-987.

[76] Giannoni P, Siegrist M, Hunziker EB, Wong M. The mechanosensitivity of cartilage oligomeric matrix protein (COMP). Biorheology 2003;40: 101-9.

[77] Hung CT, Lima EG, Mauck RL, Taki E, LeRoux MA, Lu HH, Stark RG, Guo XE, Ateshian GA. Anatomically shaped osteochondral constructs for articular cartilage repair. J Biomech 2003;36: 1853-64.

[78] Toyoda T, Seedhom BB, Kirkham J, Bonass WA. Upregulation of aggrecan and type II collagen mRNA expression in bovine chondrocytes by the application of hydrostatic pressure. Biorheology 2003;40: 79-85.

[79] Chowdhury TT, Bader DL, Lee DA. Dynamic compression counteracts IL-1 beta-induced release of nitric oxide and PGE2 by superficial zone chondrocytes cultured in agarose constructs. Osteoarthritis Cartilage 2003;11: 688-96.

[80] Homicz MR, Chia SH, Schumacher BL, Masuda K, Thonar EJ, Sah RL, Watson D. Human septal chondrocyte redifferentiation in alginate, polyglycolic acid scaffold, and monolayer culture. Laryngoscope 2003;113: 25-32.

[81] Shin H, Temenoff JS, Mikos AG. In vitro cytotoxicity of unsaturated oligo[poly(ethylene glycol) fumarate] macromers and their cross-linked hydrogels. Biomacromolecules 2003;4: 552-60.

[82] Temenoff JS, Mikos AG. Review: tissue engineering for regeneration of articular cartilage. Biomaterials 2000;21: 431-40.

[83] Raghunath J, Salacinski HJ, Sales KM, Butler PE, Seifalian AM. Advancing cartilage tissue engineering: the application of stem cell technology. Curr Opin Biotechnol 2005;16: 503-9.

[84] Gao J, Dennis JE, Solchaga LA, Goldberg VM, Caplan AI. Repair of osteochondral defect with tissue-engineered two-phase composite material of injectable calcium phosphate and hyaluronan sponge. Tissue Eng 2002;8: 827-37.

[85] Solchaga LA, Gao J, Dennis JE, Awadallah A, Lundberg M, Caplan AI, Goldberg VM. Treatment of osteochondral defects with autologous bone marrow in a hyaluronan-based delivery vehicle. Tissue Eng 2002;8: 333-47.

[86] Marcacci M, Zaffagnini S, Kon E, Visani A, Iacono F, Loreti I. Arthroscopic autologous chondrocyte transplantation: technical note. Knee Surg Sports Traumatol Arthrosc 2002;10: 154-9.

[87] Hwang NS, Varghese S, Zhang Z, Elisseeff J. Chondrogenic differentiation of human embryonic stem cell-derived cells in arginine-glycine-aspartate-modified hydrogels. Tissue Eng 2006;12: 2695-706.

[88] Schmidt O, Mizrahi J, Elisseeff J, Seliktar D. Immobilized fibrinogen in PEG hydrogels does not improve chondrocyte-mediated matrix deposition in response to mechanical stimulation. Biotechnol Bioeng 2006;95: 1061-9.

[89] Bryant SJ, Durand KL, Anseth KS. Manipulations in hydrogel chemistry control photoencapsulated chondrocyte behavior and their extracellular matrix production. J Biomed Mater Res A 2003;67: 1430-6.

[90] Bryant SJ, Anseth KS, Lee DA, Bader DL. Crosslinking density influences the morphology of chondrocytes photoencapsulated in PEG hydrogels during the application of compressive strain. J Orthop Res 2004;22: 1143-9.

[91] Bryant SJ, Bender RJ, Durand KL, Anseth KS. Encapsulating chondrocytes in degrading PEG hydrogels with high modulus: engineering gel structural changes to facilitate cartilaginous tissue production. Biotechnol Bioeng 2004;86: 747-55.

[92] Bryant SJ, Chowdhury TT, Lee DA, Bader DL, Anseth KS. Crosslinking density influences chondrocyte metabolism in dynamically loaded photocrosslinked poly(ethylene glycol) hydrogels. Ann Biomed Eng 2004;32: 407-17.

[93] Anseth KS, Metters AT, Bryant SJ, Martens PJ, Elisseeff JH, Bowman CN. In situ forming degradable networks and their application in tissue engineering and drug delivery. J Control Release 2002;78: 199-209.

[94] Wang DA, Varghese S, Sharma B, Strehin I, Fermanian S, Gorham J, Fairbrother DH, Cascio B, Elisseeff JH. Multifunctional chondroitin sulphate for cartilage tissue-biomaterial integration. Nat Mater 2007;6: 385-92.

[95] Park H, Temenoff JS, Tabata Y, Caplan AI, Mikos AG. Injectable biodegradable hydrogel composites for rabbit marrow mesenchymal stem cell and growth factor delivery for cartilage tissue engineering. Biomaterials 2007;28: 3217-27.

[96] Sharma B, Williams CG, Khan M, Manson P, Elisseeff JH. In vivo chondrogenesis of mesenchymal stem cells in a photopolymerized hydrogel. Plast Reconstr Surg 2007;119: 112-20.

[97] Alford JW, Cole BJ. Cartilage restoration, part 2: techniques, outcomes, and future directions. Am J Sports Med 2005;33: 443-60.

[98] Alford JW, Cole BJ. Cartilage restoration, part 1: basic science, historical perspective, patient evaluation, and treatment options. Am J Sports Med 2005;33: 295-306.

[99] Hanada K, Solchaga LA, Caplan AI, Hering TM, Goldberg VM, Yoo JU, Johnstone B. BMP-2 induction and TGF-beta 1 modulation of rat periosteal cell chondrogenesis. J Cell Biochem 2001;81: 284-94.

[100] Mardones RM, Reinholz GG, Fitzsimmons JS, Zobitz ME, An KN, Lewallen DG, Yaszemski MJ, O'Driscoll SW. Development of a biologic prosthetic composite for cartilage repair. Tissue Eng 2005;11: 1368-78.

[101] Fitzsimmons JS, Sanyal A, Gonzalez C, Fukumoto T, Clemens VR, O'Driscoll SW, Reinholz GG. Serum-free media for periosteal chondrogenesis in vitro. J Orthop Res 2004;22: 716-25.

[102] O'Driscoll SW. Technical considerations in periosteal grafting for osteochondral injuries. Clin Sports Med 2001;20: 379-402, vii.

[103] Ballock RT, O'Keefe RJ. Physiology and pathophysiology of the growth plate. Birth Defects Res Part C Embryo Today 2003;69: 123-43.

[104] Sylvia VL, Schwartz Z, Dean DD, Boyan BD. Transforming growth factor-beta1 regulation of resting zone chondrocytes is mediated by two separate but interacting pathways. Biochim Biophys Acta 2000;1496: 311-24.

[105] Nasatzky E, Grinfeld D, Boyan BD, Dean DD, Ornoy A, Schwartz Z. Transforming growth factor-beta1 modulates chondrocyte responsiveness to 17beta-estradiol. Endocrine 1999;11: 241-9.

[106] Nasatzky E, Azran E, Dean DD, Boyan BD, Schwartz Z. Parathyroid hormone and transforming growth factor-beta1 coregulate chondrocyte differentiation in vitro. Endocrine 2000;13: 305-13.

[107] Rosado E, Schwartz Z, Sylvia VL, Dean DD, Boyan BD. Transforming growth factor-beta1 regulation of growth zone chondrocytes is mediated by multiple interacting pathways. Biochim Biophys Acta 2002;1590: 1-15.

[108] Smink JJ, Koedam JA, Koster JG, van Buul-Offers SC. Dexamethasone-induced growth inhibition of porcine growth plate chondrocytes is accompanied by changes in levels of IGF axis components. J Endocrinol 2002;174: 343-52.

[109] Mushtaq T, Farquharson C, Seawright E, Ahmed SF. Glucocorticoid effects on chondrogenesis, differentiation and apoptosis in the murine ATDC5 chondrocyte cell line. J Endocrinol 2002;175: 705-13.

[110] Siebler T, Robson H, Shalet SM, Williams GR. Dexamethasone inhibits and thyroid hormone promotes differentiation of mouse chondrogenic ATDC5 cells. Bone 2002;31: 457-64.

[111] Schwartz Z, Gates PA, Nasatzky E, Sylvia VL, Mendez J, Dean DD, Boyan BD. Effect of 17 beta-estradiol on chondrocyte membrane fluidity and phospholipid metabolism is membrane-specific, sex-specific, and cell maturation-dependent. Biochim Biophys Acta 1996;1282: 1-10.

[112] Schwartz Z, Ehland H, Sylvia VL, Larsson D, Hardin RR, Bingham V, Lopez D, Dean DD, Boyan BD. 1alpha,25-dihydroxyvitamin D(3) and 24R,25-dihydroxyvitamin D(3) modulate growth plate chondrocyte physiology via protein kinase C-dependent phosphorylation of extracellular signal-regulated kinase 1/2 mitogen-activated protein kinase. Endocrinology 2002;143: 2775-86.

[113] Qi WN, Scully SP. Type II collagen modulates the composition of extracellular matrix synthesized by articular chondrocytes. J Orthop Res 2003;21: 282-9.

[114] Ballock RT, Heydemann A, Wakefield LM, Flanders KC, Roberts AB, Sporn MB. TGF-beta 1 prevents hypertrophy of epiphyseal chondrocytes: regulation of gene expression for cartilage matrix proteins and metalloproteases. Dev Biol 1993;158: 414-29.

[115] Giannoni P, Cancedda R. Articular chondrocyte culturing for cell-based cartilage repair: needs and perspectives. Cells Tissues Organs 2006;184: 1-15.

[116] Kawashima-Ohya Y, Satakeda H, Kuruta Y, Kawamoto T, Yan W, Akagawa Y, Hayakawa T, Noshiro M, Okada Y, Nakamura S, Kato Y. Effects of parathyroid hormone (PTH) and PTH-related peptide on expressions of matrix metalloproteinase-2, -3, and -9 in growth plate chondrocyte cultures. Endocrinology 1998;139: 2120-7.

[117] Yoshida E, Noshiro M, Kawamoto T, Tsutsumi S, Kuruta Y, Kato Y. Direct inhibition of Indian hedgehog expression by parathyroid hormone (PTH)/PTH-related peptide and up-regulation by retinoic acid in growth plate chondrocyte cultures. Exp Cell Res 2001;265: 64-72.

[118] Weisser J, Riemer S, Schmidl M, Suva LJ, Poschl E, Brauer R, von der Mark K. Four distinct chondrocyte populations in the fetal bovine growth plate: highest expression levels of PTH/PTHrP receptor, Indian hedgehog, and MMP-13 in hypertrophic chondrocytes and their suppression by PTH (1-34) and PTHrP (1-40). Exp Cell Res 2002;279: 1-13.

[119] Schwartz Z, Dean DD, Walton JK, Brooks BP, Boyan BD. Treatment of resting zone chondrocytes with 24,25-dihydroxyvitamin D3 [24,25-(OH)2D3] induces

differentiation into a 1,25-(OH)2D3-responsive phenotype characteristic of growth zone chondrocytes. Endocrinology 1995;136: 402-11.

[120] Boyan BD, Schwartz Z, Swain LD. Cell maturation-specific autocrine/paracrine regulation of matrix vesicles. Bone Miner 1992;17: 263-8.

[121] Boyan BD, Sylvia VL, Dean DD, Del Toro F, Schwartz Z. Differential regulation of growth plate chondrocytes by 1alpha,25-(OH)2D3 and 24R,25-(OH)2D3 involves cell-maturation-specific membrane-receptor-activated phospholipid metabolism. Crit Rev Oral Biol Med 2002;13: 143-54.

[122] Bentley G, Greer RB, 3rd. Homotransplantation of isolated epiphyseal and articular cartilage chondrocytes into joint surfaces of rabbits. Nature 1971;230: 385-8.

[123] Xu JW, Zaporojan V, Peretti GM, Roses RE, Morse KB, Roy AK, Mesa JM, Randolph MA, Bonassar LJ, Yaremchuk MJ. Injectable tissue-engineered cartilage with different chondrocyte sources. Plast Reconstr Surg 2004;113: 1361-71.

[124] Lee EH, Chen F, Chan J, Bose K. Treatment of growth arrest by transfer of cultured chondrocytes into physeal defects. J Pediatr Orthop 1998;18: 155-60.

[125] Olin A, Creasman C, Shapiro F. Free physeal transplantation in the rabbit. An experimental approach to focal lesions. J Bone Joint Surg Am 1984;66: 7-20.

[126] Abad V, Uyeda JA, Temple HT, De Luca F, Baron J. Determinants of spatial polarity in the growth plate. Endocrinology 1999;140: 958-62.

[127] Lee KM, Cheng AS, Cheung WH, Lui PP, Ooi V, Fung KP, Leung PC, Leung KS. Bioengineering and characterization of physeal transplant with physeal reconstruction potential. Tissue Eng 2003;9: 703-11.

[128] Park JS, Ahn JI, Oh DI. Chondrocyte allograft transplantation for damaged growth plate reconstruction. Yonsei Med J 1994;35: 378-87.

[129] Benya PD, Brown PD, Padilla SR. Microfilament modification by dihydrocytochalasin B causes retinoic acid-modulated chondrocytes to reexpress the differentiated collagen phenotype without a change in shape. J Cell Biol 1988;106: 161-70.

[130] Mahmoudifar N, Doran PM. Tissue engineering of human cartilage and osteochondral composites using recirculation bioreactors. Biomaterials 2005;26: 7012-24.

[131] Tobita M, Ochi M, Uchio Y, Mori R, Iwasa J, Katsube K, Motomura T. Treatment of growth plate injury with autogenous chondrocytes: a study in rabbits. Acta Orthop Scand 2002;73: 352-8.

[132] Tuli R, Seghatoleslami MR, Tuli S, Wang ML, Hozack WJ, Manner PA, Danielson KG, Tuan RS. A simple, high-yield method for obtaining multipotential mesenchymal progenitor cells from trabecular bone. Mol Biotechnol 2003;23: 37-49.

[133] Tuli R, Tuli S, Nandi S, Wang ML, Alexander PG, Haleem-Smith H, Hozack WJ, Manner PA, Danielson KG, Tuan RS. Characterization of multipotential mesenchymal progenitor cells derived from human trabecular bone. Stem Cells 2003;21: 681-93.

[134] Noth U, Osyczka AM, Tuli R, Hickok NJ, Danielson KG, Tuan RS. Multilineage mesenchymal differentiation potential of human trabecular bone-derived cells. J Orthop Res 2002;20: 1060-9.

[135] Miura M, Miura Y, Sonoyama W, Yamaza T, Gronthos S, Shi S. Bone marrow-derived mesenchymal stem cells for regenerative medicine in craniofacial region. Oral Dis 2006;12: 514-22.

[136] Caplan AI. Review: mesenchymal stem cells: cell-based reconstructive therapy in orthopedics. Tissue Eng 2005;11: 1198-211.

[137] Sinanan AC, Buxton PG, Lewis MP. Muscling in on stem cells. Biol Cell 2006;98: 203-14.

[138] Dragoo JL, Carlson G, McCormick F, Khan-Farooqi H, Zhu M, Zuk PA, Benhaim P. Healing Full-Thickness Cartilage Defects Using Adipose-Derived Stem Cells. Tissue Eng 2007.

[139] Wall ME, Bernacki SH, Loboa EG. Effects of Serial Passaging on the Adipogenic and Osteogenic Differentiation Potential of Adipose-Derived Human Mesenchymal Stem Cells. Tissue Eng 2007.

[140] Gimble JM, Katz AJ, Bunnell BA. Adipose-derived stem cells for regenerative medicine. Circ Res 2007;100: 1249-60.

[141] Kurth T, Hedbom E, Shintani N, Sugimoto M, Chen FH, Haspl M, Martinovic S, Hunziker EB. Chondrogenic potential of human synovial mesenchymal stem cells in alginate. Osteoarthritis Cartilage 2007.

[142] Koga H, Muneta T, Ju YJ, Nagase T, Nimura A, Mochizuki T, Ichinose S, von der Mark K, Sekiya I. Synovial stem cells are regionally specified according to local microenvironments after implantation for cartilage regeneration. Stem Cells 2007;25: 689-96.

[143] Yoshimura H, Muneta T, Nimura A, Yokoyama A, Koga H, Sekiya I. Comparison of rat mesenchymal stem cells derived from bone marrow, synovium, periosteum, adipose tissue, and muscle. Cell Tissue Res 2007;327: 449-62.

[144] Giordano A, Galderisi U, Marino IR. From the laboratory bench to the patient's bedside: an update on clinical trials with mesenchymal stem cells. J Cell Physiol 2007;211: 27-35.

[145] Liu TM, Martina M, Hutmacher DW, Hui JH, Lee EH, Lim B. Identification of common pathways mediating differentiation of bone marrow- and adipose tissue-derived human mesenchymal stem cells into three mesenchymal lineages. Stem Cells 2007;25: 750-60.

[146] Becker AJ, Mc CE, Till JE. Cytological demonstration of the clonal nature of spleen colonies derived from transplanted mouse marrow cells. Nature 1963;197: 452-4.

[147] Friedenstein AJ, Piatetzky S, II, Petrakova KV. Osteogenesis in transplants of bone marrow cells. J Embryol Exp Morphol 1966;16: 381-90.

[148] Tsutsumi S, Shimazu A, Miyazaki K, Pan H, Koike C, Yoshida E, Takagishi K, Kato Y. Retention of multilineage differentiation potential of mesenchymal cells during proliferation in response to FGF. Biochem Biophys Res Commun 2001;288: 413-9.

[149] Neuhuber B, Gallo G, Howard L, Kostura L, Mackay A, Fischer I. Reevaluation of in vitro differentiation protocols for bone marrow stromal cells: disruption of actin cytoskeleton induces rapid morphological changes and mimics neuronal phenotype. J Neurosci Res 2004;77: 192-204.

[150] Alhadlaq A, Mao JJ. Mesenchymal stem cells: isolation and therapeutics. Stem Cells Dev 2004;13: 436-48.

[151] Martin I, Shastri VP, Padera RF, Yang J, Mackay AJ, Langer R, Vunjak-Novakovic G, Freed LE. Selective differentiation of mammalian bone marrow stromal cells cultured on three-dimensional polymer foams. J Biomed Mater Res 2001;55: 229-35.

[152] Mackay AM, Beck SC, Murphy JM, Barry FP, Chichester CO, Pittenger MF. Chondrogenic differentiation of cultured human mesenchymal stem cells from marrow. Tissue Eng 1998;4: 415-28.

[153] Kadiyala S, Young RG, Thiede MA, Bruder SP. Culture expanded canine mesenchymal stem cells possess osteochondrogenic potential in vivo and in vitro. Cell Transplant 1997;6: 125-34.

[154] Kavalkovich KW, Boynton RE, Murphy JM, Barry F. Chondrogenic differentiation of human mesenchymal stem cells within an alginate layer culture system. In Vitro Cell Dev Biol Anim 2002;38: 457-66.

[155] Angele P, Kujat R, Nerlich M, Yoo J, Goldberg V, Johnstone B. Engineering of osteochondral tissue with bone marrow mesenchymal progenitor cells in a derivatized hyaluronan-gelatin composite sponge. Tissue Eng 1999;5: 545-54.

[156] Masuda K, Pfister BE, Sah RL, Thonar EJ. Osteogenic protein-1 promotes the formation of tissue-engineered cartilage using the alginate-recovered-chondrocyte method. Osteoarthritis Cartilage 2006;14: 384-91.

[157] Johnstone B, Hering TM, Caplan AI, Goldberg VM, Yoo JU. In vitro chondrogenesis of bone marrow-derived mesenchymal progenitor cells. Exp Cell Res 1998;238: 265-72.

[158] Barry F, Boynton RE, Liu B, Murphy JM. Chondrogenic differentiation of mesenchymal stem cells from bone marrow: differentiation-dependent gene expression of matrix components. Exp Cell Res 2001;268: 189-200.

[159] Hanada K, Dennis JE, Caplan AI. Stimulatory effects of basic fibroblast growth factor and bone morphogenetic protein-2 on osteogenic differentiation of rat bone marrow-derived mesenchymal stem cells. J Bone Miner Res 1997;12: 1606-14.

[160] Madry H, Emkey G, Zurakowski D, Trippel SB. Overexpression of human fibroblast growth factor 2 stimulates cell proliferation in an ex vivo model of articular chondrocyte transplantation. J Gene Med 2004;6: 238-45.

[161] Stevens MM, Marini RP, Martin I, Langer R, Prasad Shastri V. FGF-2 enhances TGF-beta1-induced periosteal chondrogenesis. J Orthop Res 2004;22: 1114-9.

[162] Mandl EW, Jahr H, Koevoet JL, van Leeuwen JP, Weinans H, Verhaar JA, van Osch GJ. Fibroblast growth factor-2 in serum-free medium is a potent mitogen and reduces dedifferentiation of human ear chondrocytes in monolayer culture. Matrix Biol 2004;23: 231-41.

[163] Cheon JE, Kim IO, Kim CJ, Kim WS, Yoo WJ, Choi IH, Yeon KM. Imaging findings after fat graft interposition in an injured growth plate: an experimental study in rabbits. Invest Radiol 2003;38: 695-703.

[164] Xian CJ, Howarth GS, Cool JC, Foster BK. Effects of acute 5-fluorouracil chemotherapy and insulin-like growth factor-I pretreatment on growth plate cartilage and metaphyseal bone in rats. Bone 2004;35: 739-49.

[165] Cornelia E. Farnum NJW. Growth Plate Cellular Function. In: Joseph A. Buckwalter M, Michael G. Ehrlich, MD, Linda J. Sandell, PhD, Stephen B. Trippel, MD, editor. Skeletal growth and Development: Clinical Issues and Basic Science Advances. 1st ed. Rosemont: American Academy of Orthopaedic Surgeons; 1998, p. 203-223.

[166] Martin EA, Ritman EL, Turner RT. Time course of epiphyseal growth plate fusion in rat tibiae. Bone 2003;32: 261-7.

[167] Haines RW. The histology of epiphyseal union in mammals. J Anat 1975;120: 1-25.

[168] Thomas BJ, Byers S, Johnstone EW, Foster BK. The effect of recombinant human osteogenic protein-1 on growth plate repair in a sheep model. J Orthop Res 2005;23: 1336-44.

[169] Phieffer LS, Meyer RA, Jr., Gruber HE, Easley M, Wattenbarger JM. Effect of interposed periosteum in an animal physeal fracture model. Clin Orthop 2000: 15-25.

[170] Cheon JE, Kim IO, Choi IH, Kim CJ, Cho TJ, Kim WS, Yoo WJ, Yeon KM. Magnetic resonance imaging of remaining physis in partial physeal resection with graft interposition in a rabbit model: a comparison with physeal resection alone. Invest Radiol 2005;40: 235-42.

[171] Johnstone B, Yoo JU. Autologous mesenchymal progenitor cells in articular cartilage repair. Clin Orthop 1999: S156-62.

[172] Caterson EJ, Li WJ, Nesti LJ, Albert T, Danielson K, Tuan RS. Polymer/alginate amalgam for cartilage-tissue engineering. Ann N Y Acad Sci 2002;961: 134-8.

[173] Majumdar MK, Wang E, Morris EA. BMP-2 and BMP-9 promotes chondrogenic differentiation of human multipotential mesenchymal cells and overcomes the inhibitory effect of IL-1. J Cell Physiol 2001;189: 275-84.

[174] Awad HA, Halvorsen YD, Gimble JM, Guilak F. Effects of transforming growth factor beta1 and dexamethasone on the growth and chondrogenic differentiation of adipose-derived stromal cells. Tissue Eng 2003;9: 1301-12.

[175] Martin I, Padera RF, Vunjak-Novakovic G, Freed LE. In vitro differentiation of chick embryo bone marrow stromal cells into cartilaginous and bone-like tissues. J Orthop Res 1998;16: 181-9.

[176] Shin H, Quinten Ruhe P, Mikos AG, Jansen JA. In vivo bone and soft tissue response to injectable, biodegradable oligo(poly(ethylene glycol) fumarate) hydrogels. Biomaterials 2003;24: 3201-11.

[177] Balakrishnan B, Jayakrishnan A. Self-cross-linking biopolymers as injectable in situ forming biodegradable scaffolds. Biomaterials 2005;26: 3941-51.

[178] Toyoda T, Seedhom BB, Yao JQ, Kirkham J, Brookes S, Bonass WA. Hydrostatic pressure modulates proteoglycan metabolism in chondrocytes seeded in agarose. Arthritis Rheum 2003;48: 2865-72.

[179] Chowdhury TT, Bader DL, Shelton JC, Lee DA. Temporal regulation of chondrocyte metabolism in agarose constructs subjected to dynamic compression. Arch Biochem Biophys 2003;417: 105-11.

[180] Mouw JK, Case ND, Guldberg RE, Plaas AH, Levenston ME. Variations in matrix composition and GAG fine structure among scaffolds for cartilage tissue engineering. Osteoarthritis Cartilage 2005;13: 828-36.

[181] Galois L, Hutasse S, Cortial D, Rousseau CF, Grossin L, Ronziere MC, Herbage D, Freyria AM. Bovine chondrocyte behaviour in three-dimensional type I collagen gel in terms of gel contraction, proliferation and gene expression. Biomaterials 2006;27: 79-90.

[182] Cohen SB, Meirisch CM, Wilson HA, Diduch DR. The use of absorbable co-polymer pads with alginate and cells for articular cartilage repair in rabbits. Biomaterials 2003;24: 2653-60.

[183] Awad HA, Wickham MQ, Leddy HA, Gimble JM, Guilak F. Chondrogenic differentiation of adipose-derived adult stem cells in agarose, alginate, and gelatin scaffolds. Biomaterials 2004;25: 3211-22.

[184] Gruber HE, Leslie K, Ingram J, Norton HJ, Hanley EN. Cell-based tissue engineering for the intervertebral disc: in vitro studies of human disc cell gene expression and matrix production within selected cell carriers. Spine J 2004;4: 44-55.

[185] Xu XL, Lou J, Tang T, Ng KW, Zhang J, Yu C, Dai K. Evaluation of different scaffolds for BMP-2 genetic orthopedic tissue engineering. J Biomed Mater Res B Appl Biomater 2005;75: 289-303.

[186] Martin I, Vunjak-Novakovic G, Yang J, Langer R, Freed LE. Mammalian chondrocytes expanded in the presence of fibroblast growth factor 2 maintain the ability to differentiate and regenerate three-dimensional cartilaginous tissue. Exp Cell Res 1999;253: 681-8.

[187] Mastrogiacomo M, Cancedda R, Quarto R. Effect of different growth factors on the chondrogenic potential of human bone marrow stromal cells. Osteoarthritis Cartilage 2001;9 Suppl A: S36-40.

[188] Kotev-Emeth S, Savion N, Pri-chen S, Pitaru S. Effect of maturation on the osteogenic response of cultured stromal bone marrow cells to basic fibroblast growth factor. Bone 2000;27: 777-83.

[189] Derfoul A, Perkins GL, Hall DJ, Tuan RS. Glucocorticoids promote chondrogenic differentiation of adult human mesenchymal stem cells by enhancing expression of cartilage extracellular matrix genes. Stem Cells 2006;24: 1487-95.

[190] Grigoriadis AE, Heersche JN, Aubin JE. Differentiation of muscle, fat, cartilage, and bone from progenitor cells present in a bone-derived clonal cell population: effect of dexamethasone. J Cell Biol 1988;106: 2139-51.

[191] Alhadlaq A, Mao JJ. Tissue-engineered neogenesis of human-shaped mandibular condyle from rat mesenchymal stem cells. J Dent Res 2003;82: 951-6.

[192] Martin I, Muraglia A, Campanile G, Cancedda R, Quarto R. Fibroblast growth factor-2 supports ex vivo expansion and maintenance of osteogenic precursors from human bone marrow. Endocrinology 1997;138: 4456-62.

[193] Cartmell SH, Porter BD, Garcia AJ, Guldberg RE. Effects of medium perfusion rate on cell-seeded three-dimensional bone constructs in vitro. Tissue Eng 2003;9: 1197-203.

[194] Farndale RW, Buttle DJ, Barrett AJ. Improved quantitation and discrimination of sulphated glycosaminoglycans by use of dimethylmethylene blue. Biochim Biophys Acta 1986;883: 173-7.

[195] Enobakhare BO, Bader DL, Lee DA. Quantification of sulfated glycosaminoglycans in chondrocyte/alginate cultures, by use of 1,9-dimethylmethylene blue. Anal Biochem 1996;243: 189-91.

[196] Kim YJ, Sah RL, Doong JY, Grodzinsky AJ. Fluorometric assay of DNA in cartilage explants using Hoechst 33258. Anal Biochem 1988;174: 168-76.

[197] Ma HL, Hung SC, Lin SY, Chen YL, Lo WH. Chondrogenesis of human mesenchymal stem cells encapsulated in alginate beads. J Biomed Mater Res 2003;64A: 273-81.

[198] Uludag H, De Vos P, Tresco PA. Technology of mammalian cell encapsulation. Adv Drug Deliv Rev 2000;42: 29-64.

[199] Leddy HA, Awad HA, Guilak F. Molecular diffusion in tissue-engineered cartilage constructs: effects of scaffold material, time, and culture conditions. J Biomed Mater Res 2004;70B: 397-406.

[200] Wee S, Gombotz WR. Protein release from alginate matrices. Adv Drug Deliv Rev 1998;31: 267-285.

[201] Brodkin KR, Garcia AJ, Levenston ME. Chondrocyte phenotypes on different extracellular matrix monolayers. Biomaterials 2004;25: 5929-38.

[202] Lawson MA, Barralet JE, Wang L, Shelton RM, Triffitt JT. Adhesion and growth of bone marrow stromal cells on modified alginate hydrogels. Tissue Eng 2004;10: 1480-91.

[203] Clancy RM, Rediske J, Tang X, Nijher N, Frenkel S, Philips M, Abramson SB. Outside-in signaling in the chondrocyte. Nitric oxide disrupts fibronectin-induced assembly of a subplasmalemmal actin/rho A/focal adhesion kinase signaling complex. J Clin Invest 1997;100: 1789-96.

[204] Martin JA, Buckwalter JA. Effects of fibronectin on articular cartilage chondrocyte proteoglycan synthesis and response to insulin-like growth factor-I. J Orthop Res 1998;16: 752-7.

[205] Dennis JE, Konstantakos EK, Arm D, Caplan AI. In vivo osteogenesis assay: a rapid method for quantitative analysis. Biomaterials 1998;19: 1323-8.

[206] Taira M, Toyosawa S, Ijyuin N, Takahashi J, Araki Y. Studies on osteogenic differentiation of rat bone marrow stromal cells cultured in type I collagen gel by RT-PCR analysis. J Oral Rehabil 2003;30: 802-7.

[207] Schecroun N, Delloye C. Bone-like nodules formed by human bone marrow stromal cells: comparative study and characterization. Bone 2003;32: 252-60.

[208] Mitchell JB, McIntosh K, Zvonic S, Garrett S, Floyd ZE, Kloster A, Halvorsen YD, Storms RW, Goh B, Kilroy G, Wu X, Gimble JM. The immunophenotype of human adipose derived cells: Temporal changes in stromal- and stem cell-associated markers. Stem Cells 2005.

[209] Walsh S, Jefferiss C, Stewart K, Jordan GR, Screen J, Beresford JN. Expression of the developmental markers STRO-1 and alkaline phosphatase in cultures of human marrow stromal cells: regulation by fibroblast growth factor (FGF)-2 and relationship to the expression of FGF receptors 1-4. Bone 2000;27: 185-95.

[210] Kato Y, Gospodarowicz D. Sulfated proteoglycan synthesis by confluent cultures of rabbit costal chondrocytes grown in the presence of fibroblast growth factor. J Cell Biol 1985;100: 477-85.

[211] Kato Y, Iwamoto M. Fibroblast growth factor is an inhibitor of chondrocyte terminal differentiation. J Biol Chem 1990;265: 5903-9.

[212] Sekiya I, Koopman P, Tsuji K, Mertin S, Harley V, Yamada Y, Shinomiya K, Nifuji A, Noda M. Dexamethasone enhances SOX9 expression in chondrocytes. J Endocrinol 2001;169: 573-9.

[213] Chrysis D, Zaman F, Chagin AS, M T, Savendahl L. DEXAMETHASONE INDUCES APOPTOSIS IN PROLIFERATIVE CHONDROCYTES THROUGH ACTIVATION OF CASPASES AND SUPPRESSION OF THE Akt-(PI3K) SIGNALING PATHWAY. Endocrinology 2004.

[214] Lalonde KA, Letts M. Traumatic growth arrest of the distal tibia: a clinical and radiographic review. Can J Surg 2005;48: 143-7.

[215] Cannata G, De Maio F, Mancini F, Ippolito E. Physeal fractures of the distal radius and ulna: long-term prognosis. J Orthop Trauma 2003;17: 172-9; discussion 179-80.

[216] Houshian S, Holst AK, Larsen MS, Torfing T. Remodeling of Salter-Harris type II epiphyseal plate injury of the distal radius. J Pediatr Orthop 2004;24: 472-6.

[217] Coleman RM, Case ND, Guldberg RE. Hydrogel effects on bone marrow stromal cell response to chondrogenic growth factors. Biomaterials 2007;28: 2077-86.

[218] Deasy BM, Lu A, Tebbets JC, Feduska JM, Schugar RC, Pollett JB, Sun B, Urish KL, Gharaibeh BM, Cao B, Rubin RT, Huard J. A role for cell sex in stem cell-mediated skeletal muscle regeneration: female cells have higher muscle regeneration efficiency. J Cell Biol 2007;177: 73-86.

[219] Worster AA, Brower-Toland BD, Fortier LA, Bent SJ, Williams J, Nixon AJ. Chondrocytic differentiation of mesenchymal stem cells sequentially exposed to transforming growth factor-beta1 in monolayer and insulin-like growth factor-I in a three-dimensional matrix. J Orthop Res 2001;19: 738-49.

[220] Masuda K, Sah RL, Hejna MJ, Thonar EJ. A novel two-step method for the formation of tissue-engineered cartilage by mature bovine chondrocytes: the alginate-recovered-chondrocyte (ARC) method. J Orthop Res 2003;21: 139-48.

[221] Hochberg Z. Clinical physiology and pathology of the growth plate. Best Pract Res Clin Endocrinol Metab 2002;16: 399-419.

[222] Palmer AW, Guldberg RE, Levenston ME. Analysis of cartilage matrix fixed charge density and three-dimensional morphology via contrast-enhanced microcomputed tomography. Proc Natl Acad Sci U S A 2006;103: 19255-60.

[223] Gosain AK, Recinos RF, Agresti M, Khanna AK. TGF-beta1, FGF-2, and receptor mRNA expression in suture mesenchyme and dura versus underlying brain in fusing and nonfusing mouse cranial sutures. Plast Reconstr Surg 2004;113: 1675-84.

[224] Opperman LA, Galanis V, Williams AR, Adab K. Transforming growth factor-beta3 (Tgf-beta3) down-regulates Tgf-beta3 receptor type I (Tbetar-I) during rescue of cranial sutures from osseous obliteration. Orthod Craniofac Res 2002;5: 5-16.

[225] Opperman LA, Moursi AM, Sayne JR, Wintergerst AM. Transforming growth factor-beta 3(Tgf-beta3) in a collagen gel delays fusion of the rat posterior interfrontal suture in vivo. Anat Rec 2002;267: 120-30.

[226] Opperman LA, Fernandez CR, So S, Rawlins JT. Erk1/2 signaling is required for Tgf-beta 2-induced suture closure. Dev Dyn 2006;235: 1292-9.

[227] Longaker MT. Role of TGF-beta signaling in the regulation of programmed cranial suture fusion. J Craniofac Surg 2001;12: 389-90.

[228] Adab K, Sayne JR, Carlson DS, Opperman LA. Tgf-beta1, Tgf-beta2, Tgf-beta3 and Msx2 expression is elevated during frontonasal suture morphogenesis and during active postnatal facial growth. Orthod Craniofac Res 2002;5: 227-37.

[229] Fagenholz PJ, Warren SM, Greenwald JA, Bouletreau PJ, Spector JA, Crisera FE, Longaker MT. Osteoblast gene expression is differentially regulated by TGF-beta isoforms. J Craniofac Surg 2001;12: 183-90.

[230] Mehlhorn AT, Schmal H, Kaiser S, Lepski G, Finkenzeller G, Stark GB, Sudkamp NP. Mesenchymal stem cells maintain TGF-beta-mediated chondrogenic phenotype in alginate bead culture. Tissue Eng 2006;12: 1393-403.

[231] Segev O, Chumakov I, Nevo Z, Givol D, Madar-Shapiro L, Sheinin Y, Weinreb M, Yayon A. Restrained chondrocyte proliferation and maturation with abnormal growth plate vascularization and ossification in human FGFR-3(G380R) transgenic mice. Hum Mol Genet 2000;9: 249-58.

[232] Sannasgala SS, Johnson DR. Kinetic parameters in the growth plate of normal and achondroplastic (cn/cn) mice. J Anat 1990;172: 245-58.

[233] Chen J, Coleman, RM, Bell, BF, Yoon, J, Yao, H, Schwartz, Z, , Guldberg R, and Boyan, BD. Rickets is Associated with Failure to Form Bone Tethers at the Osteochondral Junction. 2007.